ABSTRACT

Title of Document: CATALYTIC FEATURES OF THE IODINE SALVAGING ENZYME IODOTYROSINE DEIODINASE.

Patrick Michael McTamney, II
Doctor of Philosophy, 2009

Directed By: Professor Steven Rokita
Department of Chemistry and Biochemistry

The need for iodide in biology is almost exclusively limited to its role in thyroid hormones, yet the recycling of thyroidal iodide is still critical for human health. The flavoprotein iodotyrosine deiodinase (IYD) salvages iodide from byproducts (mono- and diiodotyrosine, MIT and DIT) of thyroid hormone biosynthesis. The original proposal for the deiodination mechanism of IYD included a nucleophilic attack on the iodo group by an active site cysteine. Although this proposal had strong precedence, site-directed mutagenesis has now proven this wrong. Further investigation of the IYD mechanism required large scale protein expression and isolation. This was stymied by the lack of a convenient isolation system until a truncated and soluble version of wild-type IYD could be expressed in yeast and insect cells.

Large scale isolation of this soluble enzyme derivative provided the necessary material for crystallographic studies that in turn resulted in a structure of IYD at 2.0 Å

resolution. The structure verified IYD's assignment in the NAD(P)H oxidase/flavin reductase superfamily and showed that no cysteine residues were in the active site. Structures of IYD with bound MIT and DIT were also obtained and indicated that these substrates are sequestered within the active site by inducing helical structure in two otherwise disordered regions of the enzyme to form an active site lid. This lid confers substrate specificity and is critical in positioning substrate such that it stacks on the isoalloxazine of the flavin mononucleotide (FMN) cofactor. Further investigation identified 3-bromo and 3-chlorotyrosine as substrates for IYD, while 3-fluorotyrosine was not dehalogenated by IYD. These new substrates illustrate IYD's activity as a general dehalogenase and IYD's strong dehalogenating power. Mechanistic studies utilizing 5-deazaFMN, which is incapable of performing 1 electron processes, indicated that IYD dehalogenation occurs via two sequential 1 electron transfers from reduced FMN to substrate. Anaerobic single turnover assays and mechanistic precedence have led to a likely mechanism of dehalogenation for IYD involving substrate tautomerization followed by injection of an electron into the carbonyl of the keto intermediate which then facilitates dehalogenation.

CATALYTIC FEATURES OF THE IODINE SALVAGING ENZYME IODOTYROSINE DEIODINASE.

By

Patrick Michael McTamney, II

Dissertation submitted to the Faculty of the Graduate School of the
University of Maryland, College Park, in partial fulfillment
of the requirements for the degree of
Doctor of Philosophy
2009

Advisory Committee:
Professor Steven Rokita, Chair
Professor Dorothy Beckett
Professor Ian Mather
Assistant Professor Ashton Cropp
Assistant Professor Barbara Gerratana

Dedication

To my family, thank you for your continued support.

Acknowledgements

The list of people have who have contributed to my success during graduate school is quite extensive, and this is simply an attempt to acknowledge everyone.

I must first start by thanking Dr. Steven Rokita. I have learned so much from you. You have made me a better scientist, writer, presenter, and independent thinker. You have made me realize my strengths and weaknesses in science-some things stand out more than others. I, like everyone who works in your laboratory, appreciate your dedication to your research and to your students. You truly are an exceptional mentor and person.

Thank you to my committee, Professors Gerratana, Beckett, Cropp, and Mather. You have taught me beyond what is in a textbook. Your expertise has made my time at Maryland much easier. Thank you for encouraging me to think! A special thanks to Dr. Barbara Gerratana for all of your help with my independent proposal.

Numerous experiments and data in this dissertation were made possible due to the contributions other laboratories both on and off the University of Maryland campus. Dr. LaRonde-LeBlanc and Seth Thomas crystallized and solved the structure of iodotyrosine deiodinase. Your work has provided understanding for decades of experiments on this enzyme. Most of the work in this dissertation would not be possible without the expertise of Chi-wei Hung and the entire Bentley Lab. Thank you for teaching me how to take care of my Sf9 cells. Thank you to Dr. Hamza'slab, especially Caitlin Hall, for all of the help with mammalian cell culture. Thank you to Min Jai from Dr. Blough's lab for helping design the set up for the

anaerobic assay for monitoring single turnover. Your time and expertise is greatly appreciated. Thank you to Maria del Mar Ingaramo for help fitting fluorescence binding data. The EPR measurements of IYD were performed by Dr. Veronika Szalai (the University of Maryland, Baltimore County). Dr. Szalai, thank you for your time and assistance. Thank you for taking the time to solve my problem. Thank you to Dr. Dave Ballou and Dr. Bruce Palfey (the University of Michigan) for the deazaflavin analogues. I would not have been able to finish my story without them.

I have been fortunate to receive financial support during my graduate time from two sources. First, I am forever indebted to Dr. Herman Kraybill. Receiving your fellowship has made an impact on my personal and professional life. You are an example of science's best. Thank you for giving back. Ann G. Wylie, the dissertation fellowship given by the Graduate School in your name has allowed me to focus my time and efforts towards completing this dissertation.

To all of my Rokita lab friends, past and present, thank you for all of you help along the way. Jim Watson and Emily Weinert, you are my namesake; although I am sure I do not live up to it. That is probably a good thing. Thanks for teaching me the ropes. Jen Adler, I truly appreciate you being there every day. You have helped me solve most of my problems. Neil Campbell, thank you for helping me solve the rest of them. I have never met another person with such an immense gift for nicknames. Amy Finch, thank you for being the voice of reason in the lab. Although I never met you, I owe you a drink Jessica Friedman. Yishan Zhou, keep the positive attitude, it will work! Mike McCrane, thank you for all the HPLC and NMR help. Chengyun,

Petrina, and AB, thanks for everything and good luck. To everyone else in the lab, I appreciate all of your help. Look me up if ever need anything.

A special thanks to the Julin lab. I knew little biochemistry prior to graduate school. Matt Servinsky, Will Shadrick, and Steve Polansky, you taught me practical biochemistry. The good and the bad, all of it! Remember, if your experiment doesn't work, it is probably transformalase, and you will have to (re)search, again. To all the Kahn members, there are too many to list individually, thank you for being the support group next door. Thank you to the Cropp lab for all of your help, whether it be with PCR, yeast, or laptop batteries. Bryan, I wish you would stay in the area, but enjoy moving away, you'll be better off. Thank you to all the other labs in the department

In addition, I would to thank several people who preceded my studies at the University of Maryland. My undergraduate professors Dr. David Schedler, Dr. Clyde Stanton, and Dr. Duane Pontius, thank you for inspiring me to pursue science. I cannot thank you enough. Coach Dobbs, anytime I begin to slow down, I always think of you and the V.

Finally, the support of my family has been so important to me. Thank you Pat and Diane for all of the life lessons and for all of your prayers. You have given me everything I will ever need to succeed in life. I hope that I can someday repay you. Kelly, thank you for being "my little sister." I promise no more rooster feathers, ever. Most importantly, one person has been with me every step of this process over the past four years. For that, I am eternally grateful Mandy.

Table of Contents

List of Tables

Chapter 1

None

Chapter 2

Chapter 3

Chapter 4

Chapter 5

Chapter 6

None

List of Figures

Chapter 1

Chapter 2

Chapter 3

Chapter 4

Chapter 5

Chapter 6

None

List of Abbreviations

ε_{280}	extinction coefficient at 280 nm
λ_{em}	fluorescence emission wavelength
λ_{ex}	fluorescence excitation wavelength
BCA	bicinchoninic acid
CHO	Chinese hamster ovary
Cys	cysteine
DIT	3,5-diiodotyrosine
$D^{125}IT$	diiodotyrosine labeled with ^{125}I iodine
DMEM	Dulbecco's modified Eagle's medium
DPBS	Dulbecco's phosphate buffered saline
EPR	electron paramagnetic resonance
FAD	flavin adenine dinucleotide
FCS	fetal calf serum
FMN	flavin mononucleotide
FMN_{ox}	flavin mononucleotide oxidized species
FMN_{red}	flavin mononucleotide reduced species
FMN_{semi}	flavin mononucleotide semiquinone species
GdnHCl	guanidinium hydrochloride
HEK293	human embryonic kidney 293
ID	iodothyroine deiodinase
IPTG	isopropyl β-D-1-thiogalactopyranoside
IYD	iodotyrosine deiodinase

IYD(Δ2-32)His_6	transmembrane domain deleted IYD variant with *C*-term histidine tag
k_{cat}	catalytic rate
K_D	dissociation constant
kDa	kilodalton
K_M	Michaelis-Menten constant
MGYH	minimal glycerol medium plus histidine
MBT	3-monobromotyrosine
MCT	3-monochlorotyrosine
Me-Tyr	3-methyltyrosine
MFT	3-monofluorotyrosine
MIT	3-monoiodotyrosine
MNT	3-mononitrotyrosine
MMH	minimal methanol medium plus histidine
MOI	multiplicity of infection
Mut	methanol utilizing phenotype of Pichia pastoris
NADPH	nicotinamide adenine dinucleotide phosphate
NIS	Na^+/I^- symporter
NOX/FRase	NAD(P)H oxidase/flavin reductase
OD_{600}	optical density at 600 nm
optIYD(ΔTM)His_6	synthetic *Mus musculus* IYD gene for *Pichia pastoris* expression
PCP	pentachlorophenol

pfu	plaque forming units
PSG	penicillin-streptomycinglutamine
redox	reduction-oxidation
SDS-PAGE	sodium dodecyl sulfate-polyacrylamide gel electrophoresis
Se-Cys	selenocysteine
SNAr	nucleophilic aromatic substitution
SRN1	free radical aromatic substitution
TCE	tetrachloroethene
TCHQ	tetrachlorohydroquinone
TG	thyroglobulin
TRX	thioredoxin
Tyr	tyrosine

Chapter 1: Introduction to iodotyrosine deiodinase

1.1 Iodine is a precious element in thyroxine biosynthesis

The element iodine is primarily found in seawater; however, it plays a critical role in physiology. The element's association with human physiology was recognized only nine years after its first discovery (*1*). This occurred in 1820 when Coindet announced that iodine treatment could reduce the size of goiters in patients (*1*). Almost a century later, iodine's biological role was finally ascribed to its incorporation into the thyroid hormone thyroxine or T_4 (Figure 1-1) (*2*). T_4 is essential in regulating intermediary metabolism in nearly all tissues (*3-5*). It is considered a prohormone with its regulatory action occurring via deiodination to its active form T_3 followed by subsequent deiodination to the inactive hormone T_2 by

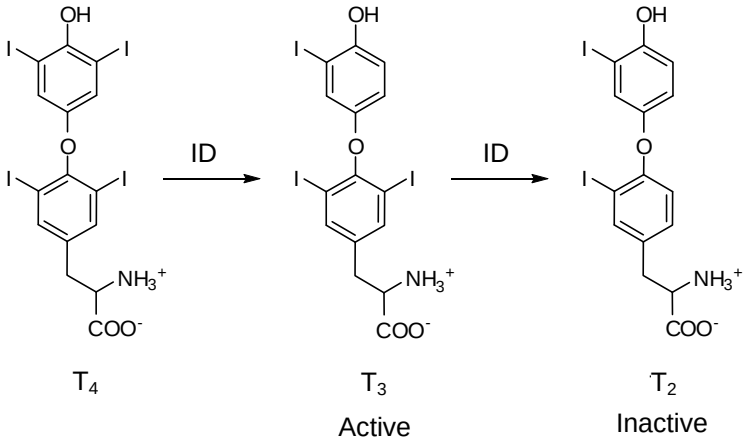

Figure 1-1. Activation and inactivation of thyroid hormone by ID.

iodothyronine deiodinase (ID) (*5-7*). T_4 and its derivatives affect a number of physiological processes including protein synthesis, fat and carbohydrate metabolism, obligatory heat production, as well as growth and development (*3, 8*).

Biosynthesis of T_4 occurs over several steps (Figure 1-2) (*4, 9, 10*) and is promoted by thyroid stimulating hormone (*11*). First, iodide is procured from the blood stream across the basal cell membrane of thyroid follicular cells by the Na^+/I^- symporter (NIS) (*12*). Once internalized, iodide is concentrated to the basal

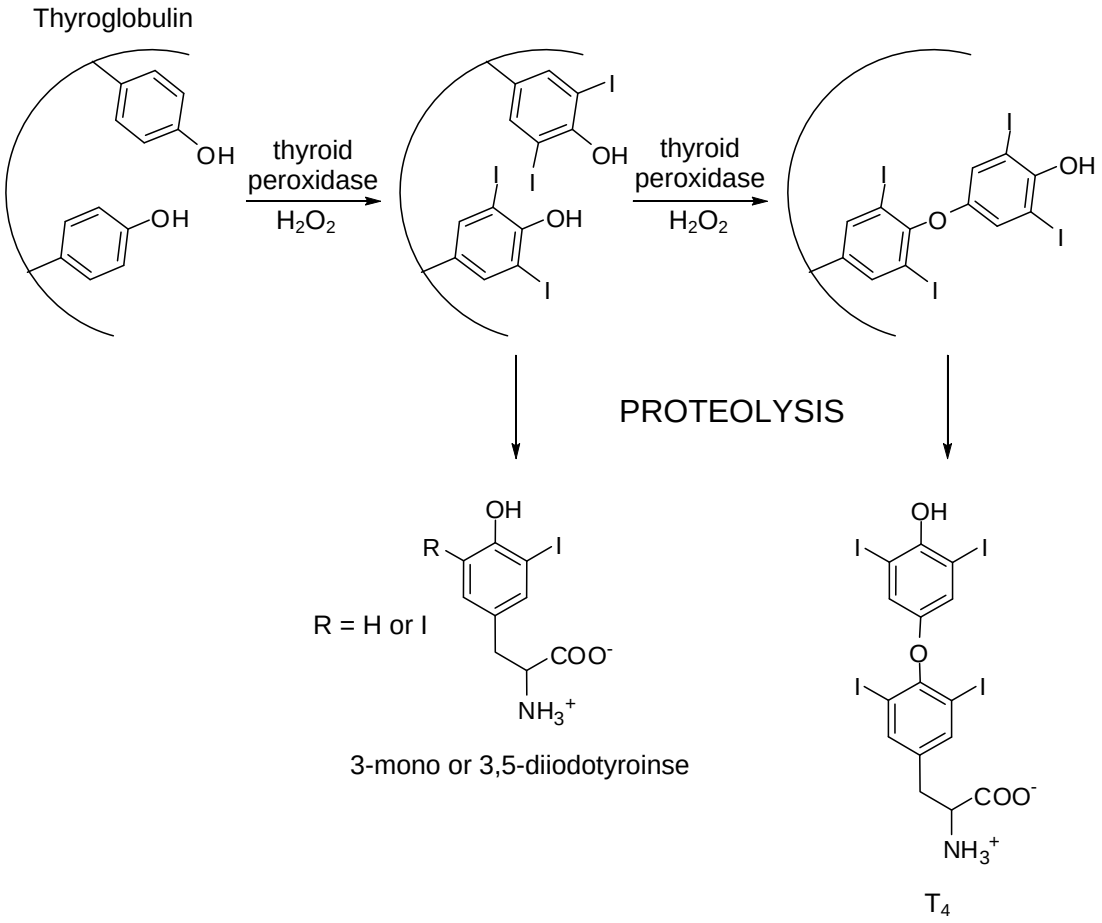

Figure 1-2. T_4 biosynthesis.

membrane by NIS (*13*). This pool of iodide is then incorporated at the 3- and/or 5-position of specific tyrosine (Tyr) residues of the thyroidal protein thyroglobulin (TG) (*14, 15*). Thyroid peroxidase is responsible for this iodination as well as the next step in biosynthesis for which the 3-monoiodinated and/or 3,5-diiodinated tyrosine side chains of TG are coupled to form the basis of T_4 or T_3 (*16*). The now mature TG is stored in the extracellular colloid until needed. In order to secrete T4, mature TG is taken up in the follicular cells by endocytosis into small microsome vesicles where it is then proteolyzed. This releases free T_4 and T_3, as well as significant amounts of the uncoupled iodinated tyrosines 3-mono- and 3,5-diiodotyrosines (MIT and DIT, respectively) which are byproducts of T_4 biosynthesis. Lastly, T_4 and T_3 are transported from the thyroid cell into the bloodstream where they circulate and act on cells distant from the thyroid (*17, 18*).

Iodide is scarce in the environment, especially in landlocked areas which lack accessibility to the sea. Insufficient levels of the micronutrient iodide limit T_4 biosynthesis which can subsequently result in diseases like hypothyroidism and goiter, while more severe developmental problems including cretinism can occur (*19, 20*). Iodide deficiency is not limited to these landlocked regions (*8*). In fact, it is a global health problem that plagues even developed countries with as many as 2 billion people affected worldwide in 2007 according to the World Health Organization (*21*). Interestingly, only 100-200 μg of daily dietary intake of the precious micronutrient is required for proper thyroid function (*22*).

The thyroid has evolved two distinct mechanisms for accumulating and salvaging iodide in order to maintain its necessary homeostasis. The first involves the

aforementioned NIS (*12*, *13*). This enzyme not only sequesters iodide into follicular cells to levels 20 to 50 times that of normal thyroid plasma (<1 μg/mL). The second mechanism involves iodide salvage from the MIT and DIT uncoupled byproducts of T_4 biosynthesis. The enzyme iodotyrosine deiodinase (IYD) recycles iodide from these byproducts by reductively dehalogenating both MIT and DIT (Figure 1-3) (*23*) but not thyroid hormones (*24*). Thus, IYD allows both the liberated iodide and tyrosine to be reused for thyroid hormone production. IYD activity is critical since MIT and DIT comprise greater than 70 % of the iodinated residues of proteolyzed TG (T_4 or T_3 comprise the other 30 %) (*7*, *19*), and these byproducts would otherwise be excreted from the body along with their iodine equivalents (*25*). The significance of IYD's ability to recycle thyroidal iodide is well illustrated in patients first identified in 1956 (*25-27*), as well as the those reported quite recently (*28*, *29*) who's congenital goiter and/or cretinism was attributed to deiodinase deficiency.

1.2 Iodotyrosine deiodinase is a novel flavoprotein

The presence of an enzyme responsible for deiodinating the free iodotyrosines released upon proteolysis of TG was first postulated in 1952 (*30*). This hypothesis

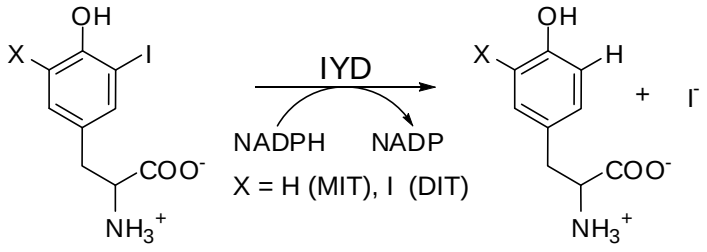

Figure 1-3. IYD catalyzes dehalogenation of MIT and DIT.

was confirmed several years later when the absence of IYD activity was documented in patients with goiter and IYD activity was observed with thyroid homogenates (*25-27*). Almost two decades passed before IYD was first purified from thyroid homogenates and partially characterized. The enzyme was found associated with microsomes existing as a 42 kilodalton (kDa) homodimer with a single flavin mononucleotide (FMN) cofactor (*31, 32*).

Because IYD catalyzes a reductive process, turnover requires that the enzyme's bound FMN cofactor be reduced. Nicotinamide adenine dinucleotide phosphate (NADPH) (-317 mV (*33*)) has been identified as the electron donor utilized in IYD's physiological reduction (*23, 34*). However, solubilization of IYD from its native membrane resulted in loss of NADPH-responsive activity, while strong reducing agents like dithionite (-660 mV) which are capable of reducing IYD *in vitro* maintained deiodinase activity following enzyme solubilization (*35*). This loss of NADPH-responsive activity upon solubilization in conjunction with the unusually low reduction-oxidation (redox) potential obtained for IYD (-412 mV) (*32*) resulted in the proposal that a yet unidentified reductase mediates the physiological reduction of IYD (*36*). Moreover, the idea of a yet unidentified reductase recently garnered increased support when IYD displayed NADPH-responsive and dithionite activity in presence of human embryonic kidney 293 (HEK 293) cell lysates and only dithionite activity in the presence of Chinese hamster ovary (CHO) cell lysates (*37, 38*). This signified that the yet unidentified reductase or an equivalent is expressed in HEK293 cells, but not in CHO cells.

Further studies of IYD languished for several decades until the gene encoding IYD was identified just a few years ago (*37*) by serial analysis of gene expression of novel thyroid genes (*39*). The encoded IYD protein possessed deiodinase activity when recombinantly expressed in mammalian cells (*37*). Simultaneously, the Rokita lab affirmed the gene identification through protein sequencing of a porcine thyroid isolate exhibiting deiodinase activity (*40*). IYD was predicted at the time to comprise an *N*-terminal membrane domain (residues 1-24), an intermediate domain of unknown structure and function (residues 25-81), and a catalytic domain (residues 82-285) through sequence analysis (Figure 1-4) (*40*).

The catalytic domain of IYD displays homology to the NAD(P)H oxidase/flavin reductase (NOX/FRase) superfamily of flavoproteins (*40*) which catalyze reduction of nitroaromatics and reduction of flavin substrates by an obligate 2 electron process (*41-44*). Because the catalysis of the superfamily proteins is so distinctive from IYD's, they cannot be considered for precedence of IYD's mechanism. In fact, precedence for IYD's catalysis is very limited since IYD is unique in that it uses a flavin to catalyze reductive dehalogenation and unusual in that reductive processes are generally associated with anaerobic organisms (*45*).

Figure 1-4. IYD consists of a membrane anchor (residues 1-23), an intermediate domain (residues 24-81), and a NOX/FRase domain (residues 82-285).

1.3 Mechanistic precedence for IYD catalysis

Flavin cofactors (FMN and flavin adenine dinucleotide (FAD)) are versatile catalysts well known for their ability to catalyze both 1 (2 x 1 e^-) and 2 electron (1 x 2 subsequent transfers of a single electron or a single transfer of two electrons from

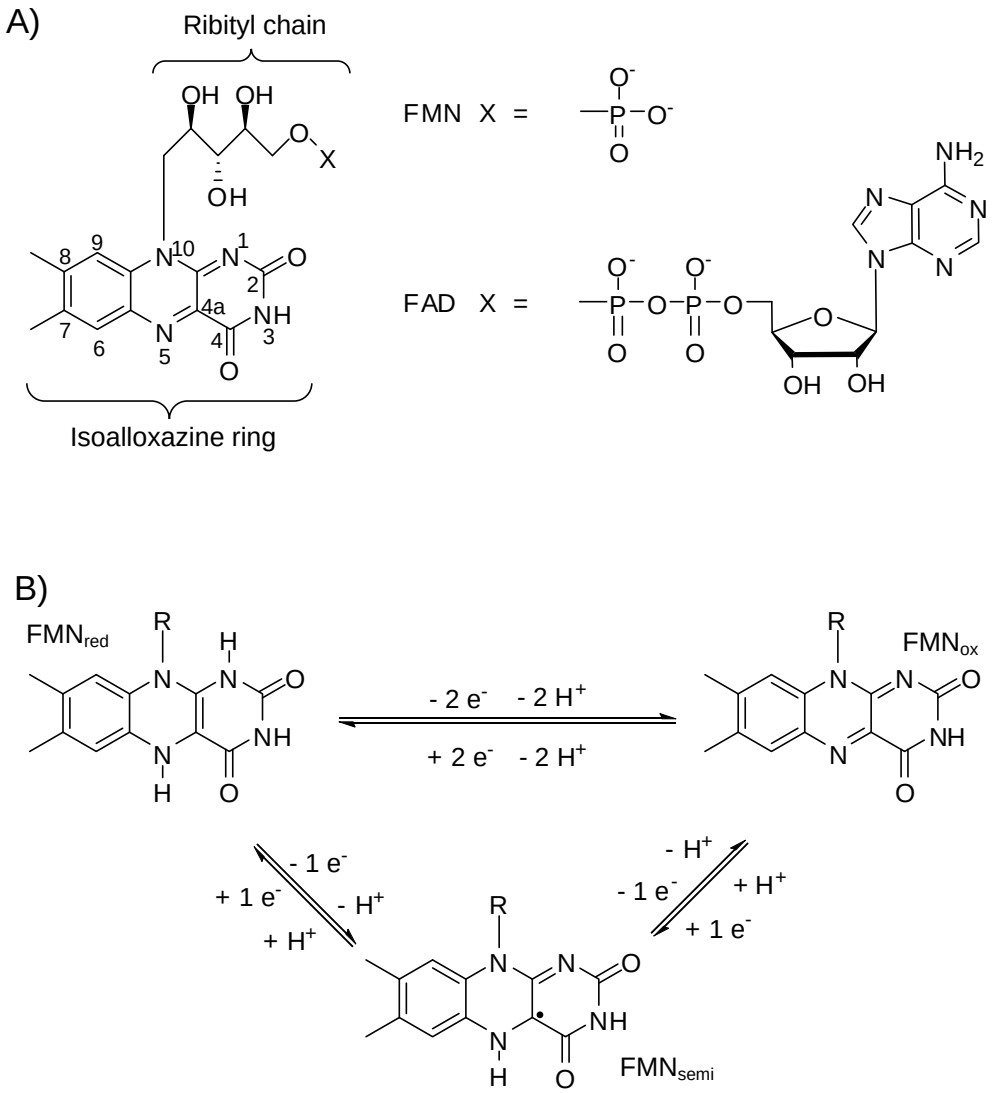

Figure 1-5. Flavin cofactors. A) Flavin cofactors are commonly flavin mononucleotide (FMN) and flavin adenine dinucleotide (FAD). They are composed of an isoalloxazine ring, a ribityl chain and an additional moiety attached to the ribityl chain. B) Reduced FMN (FMN_{red}) can be oxidized (FMN_{ox}) by a single 2 electron oxidation or by 2 sequential 1 electron oxidation which proceed through an FMN semiquinone radical (FMN_{semi}).

fully reduced flavin, respectively. The incorporation of flavin into proteins determines the cofactor's reactivity, as residue interactions to the isoalloxazine influence flavin's catalytic properties (*47, 48*). This allows flavins to promote a wide range of reactions and are involved in a number of diverse biological processes including bioluminescence (*49*), photosynthesis (*50*), apoptosis (*51*), and even DNA repair (*52*).

Despite flavin's vast range of enzyme classes with which flavins are associated (reductases, oxygenases, electron transferases, dehydogenases, etc. (*46*)), flavoprotein precedence for reductive dehalogenation is nonexistent. The few characterized flavoproteins, other than IYD, that catalyze dehalogenation are all monoxygenases (*53-55*). These other flavin dehalogenases cannot serve as catalytic precedence for IYD since none perform dehalogenation in a reductive fashion. Additionally, only two other flavoproteins have been proposed to catalyze reductive dehalogenation, and minimal information is available for these enzymes (*56, 57*). Only a flavin has been implicated in their overall reaction and the net process appears to be reductive in nature. Since flavin chemistry provides no precedence for IYD's catalysis, precedence was sought from other catalytic processes.

1.4 Mechanistic precedence for 2 electron reductive dehalogenation

Reductive dehalogenation is one of the three main categories of dehalogenases which include hydrolytic, oxygen dependent, and reductive processes (Figure 1-6) (*45, 58, 59*). Considerable effort has been directed in utilizing these different dehalogenase enzymes for bioremediation of halogenated compounds and solvents

(*45, 58, 59*). This has led to many dehalogenases, including reductive dehalogenases, being well characterized.

The best characterized reductive dehalogenase from an aerobic organism is tetrachlorohydroquinone (TCHQ) dehalogenase from *Sphingobium chlorophenolicum* (*60-62*). TCHQ is involved in the third and fourth steps of the pentachlorophenol (PCP) catabolic pathway which recently evolved to degrade the PCP pesticide. Catalysis by TCHQ dehalogenase relies on oxidation of glutathione for dehalogenation (Figure 1-7) (*60*). Upon binding, the substrate is deprotonated and subsequently converted to a keto tautomer. Glutathione then performs nucleophilic attack, which generates free chloride. The covalent attachment of glutathione to the

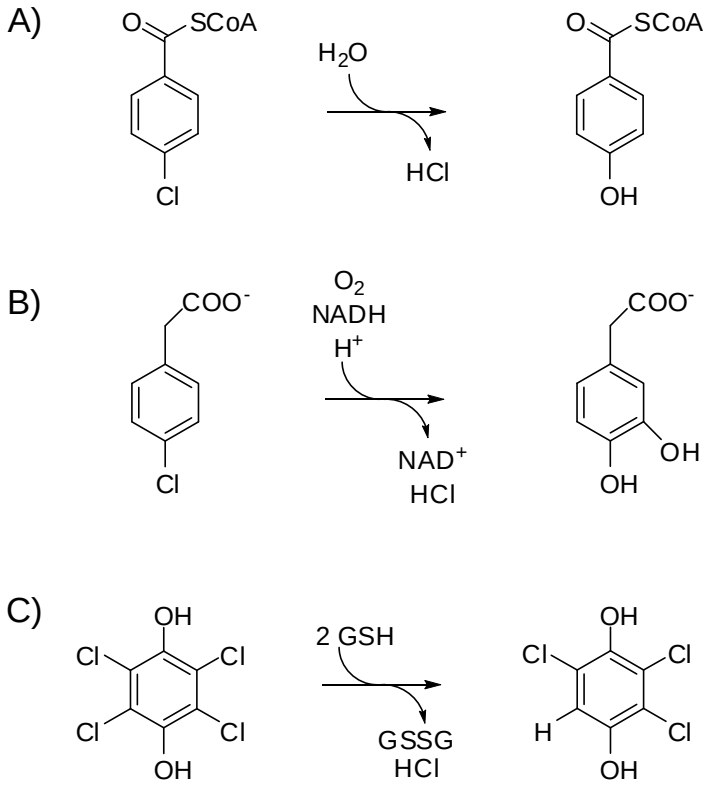

Figure 1-6. Dehalogenation by bacterial enzymes depend on either A) hydrolytic, B) oxygen dependent, or C) reductive catalysis. Figure modified from Copley (*59*).

substrate is next broken by cysteine (Cys) 13 attack. This releases the reduced product, and finally, active enzyme is regenerated by sulfide exchange with a second glutathione.

Another well studied reductive dehalogenase, but not for bioremediation purposes, is the previously mentioned ID that catalyzes the physiological deiodination of thyroid hormones. ID and IYD are the only reductive dehalogenases in mammals and catalyze almost equivalent reactions. The proposed mechanism of ID (Figure 1-8) (*63, 64*) initially involves the deprotonation of the substrate's phenolic hydrogen, allowing tautomerization of substrate. The selenide of an active site selenocysteine is responsible for dehalogenation (*65, 66*) through nucleophilic attack of the iodine. Lastly, the covalent Se-I bond is reduced by an unidentified cofactor *in vivo* although thiols can be used *in vitro*.

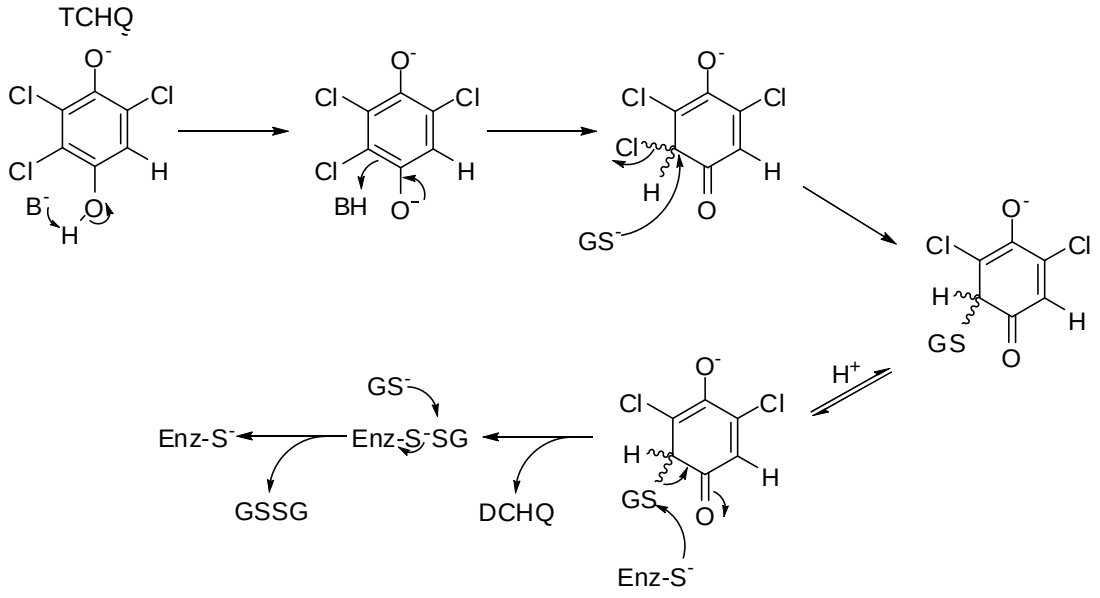

Figure 1-7. Proposed mechanism of TCHQ dehalogenase catalysis (*60*).

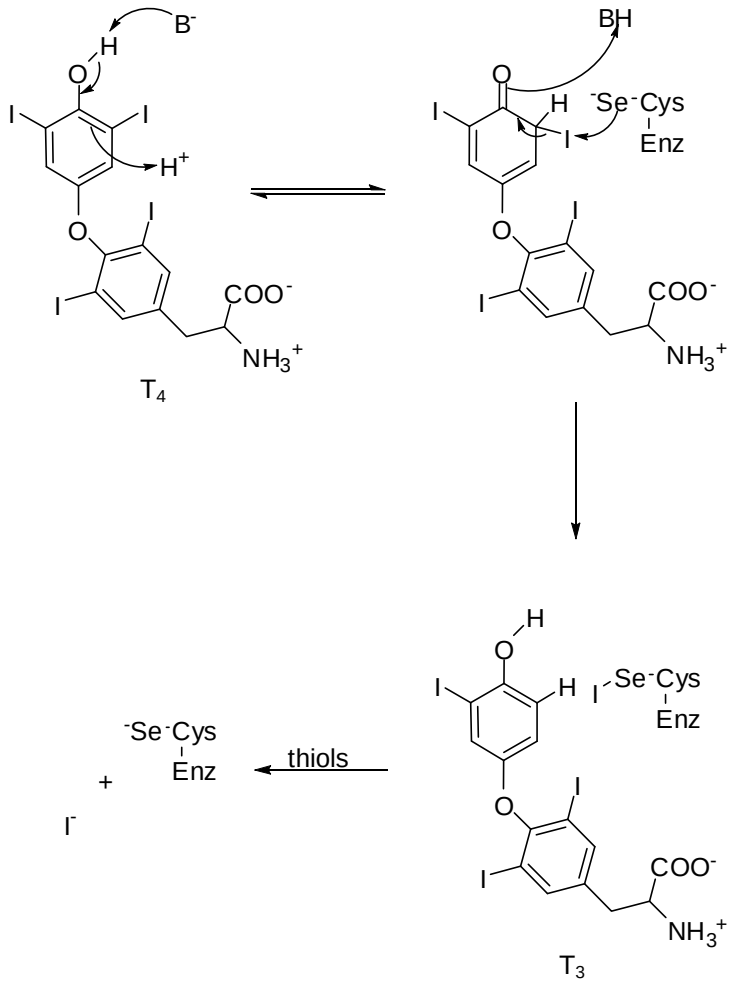

Figure 1-8. Proposed mechanism of ID catalysis (*63, 64*).

1.5 IYD mechanism closest to precedence

The mechanisms described in the previous section can serve as precedence for the mechanism of deiodination by IYD despite their lack of flavin since they all couple dehalogenation through an analogous reducing step. Although IYD is a flavoprotein and both 1 and 2 electron transfer mechanisms should be considered, a 2 electron mechanism is closest to the existing precedent. A tautomeric mimic of substrate displayed strong deiodinase inhibition (*67*), indicating that IYD preferably

binds and stabilizes a nonaromatic intermediate similar to both TCHQ dehalogenase and ID. Additionally, IYD contains 3 highly conserved Cys residues which could act as nucleophiles similarly to the selenide of selenocysteine in the ID mechanism (*40*).

Therefore, a logical proposal for IYD's mechanism involves a 2 electron transfer ultimately resulting in deiodination of substrate (Figure 1-9). This can be envisioned with an initial deprotonation of the phenolic hydrogen of substrate which leads to tautomerization. The sulfur of an active site Cys would then perform nucleophilic attack on the iodine of the intermediate. This would break the substrate iodine bond, generating tyrosine and a covalent sulfenyl iodine bond. A two electron reduction of this C-I bond by reduced FMN would then release free iodide, as well as create a covalent flavin-enzyme adduct. Complete oxidation of the FMN would release the nucleophilic Cys and reduction of FMN by NADPH would subsequently regenerate catalytic IYD.

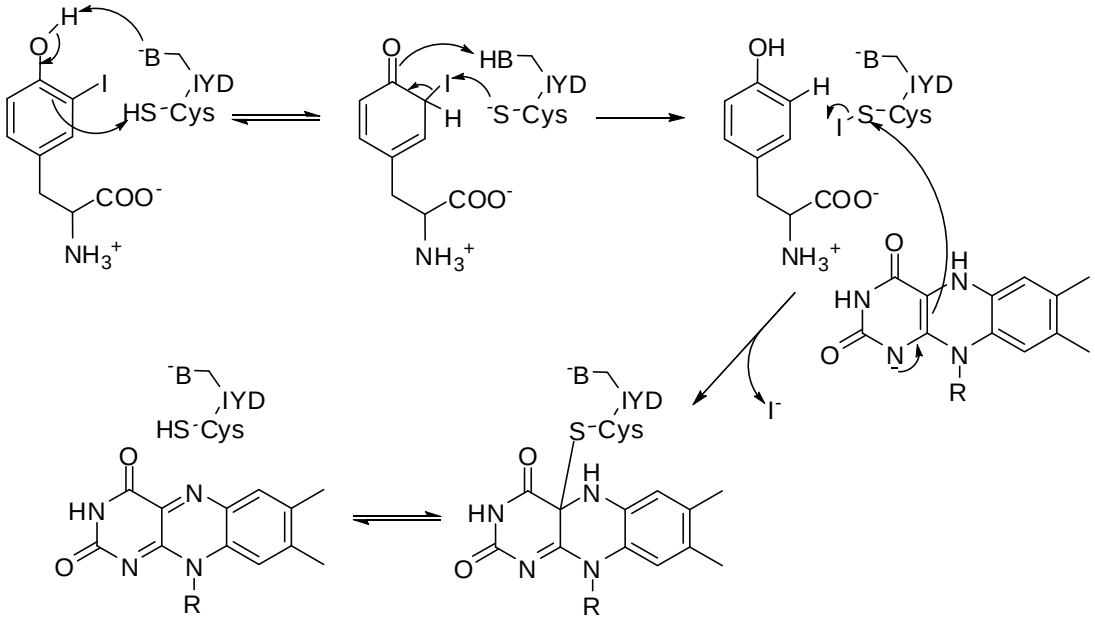

Figure 1-9. IYD mechanism closest to TCHQ dehalogenase and ID precedence.

1.6 Mechanistic precedence for 1 electron reductive dehalogenation

Although the IYD deiodination mechanism closest to precedence is a 2 electron process, 1 electron pathways must also be considered for precedence because IYD is a flavoprotein. There are few examples of reductive dehalogenation where a radical mechanism is suggested, and they all involve a corrinoid cofactor (*68, 69*). Of these, evidence for a radical mechanism has only been shown for tetrachloroethene (TCE) reductive dehalogenase (*70*). Its proposed mechanism for dechlorination of 2,3-dichloropropene (Figure 1-10) involves the reduction of substrate to a radical anion. This occurs though a dissociative 1 electron transfer from a superreduced corrinoid cob(I)alamin. This then facilitates chloride release and formation of a neutral radical which reacts with the Co^{II} of the corrinoid to generate a covalent intermediate. Protonation of this intermediate releases the 2-chloropropene product and the corrinoid is reduced to its resting state by iron sulfur clusters.

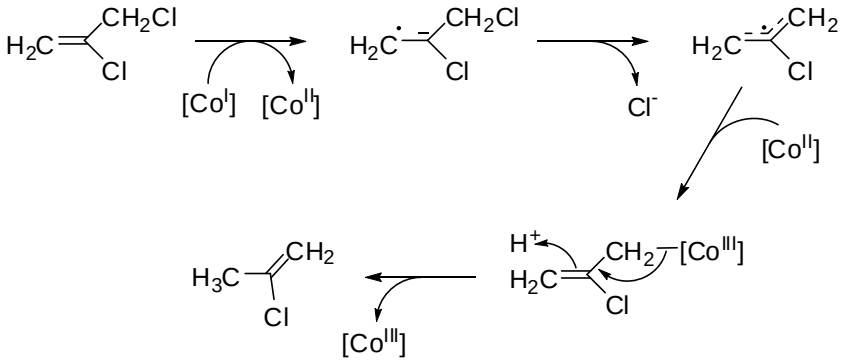

Figure 1-10. Proposed mechanism of TCE reductive dehalogenase (*70*).

1.7 Specific aims

IYD is an enzyme that plays a critical role in physiology, yet it remained poorly characterized for approximately 50 years. Recent reports have provided a platform for significant advances in our understanding of IYD catalysis and reductive dehalogenation (*37, 40*). The goal of my research was to gain an understanding of IYD's catalysis at the molecular level. Specifically, this dissertation addresses the following:

1) The mechanism closest to precedence for IYD catalysis suggests the redox involvement of an active site Cys residue. The requirement of Cys for IYD catalysis was investigated through site-directed-mutagenesis to determine if IYD catalysis does indeed involve Cys nucleophilic attack.

2) Isolation of IYD in large scale had never been achieved but was essential for overcoming the protein folding limitations of *E. coli* and the cost/time restrictions associated with mammalian cell expression. Thus, both yeast and insect expression of IYD were evaluated as sources for large scale isolation of IYD.

3) Substituents at the 3-position of tyrosine were previously suggested to influence IYD substrate recognition (*71, 72*). With purified enzyme, the role of substituents at the 3-position were directly investigated with assays for binding by fluorescence quenching and anaerobic single turnover.

4) IYD could catalyze deiodination via a 1 or 2 electron transfer mechanism. These two possible mechanisms were distinguished by monitoring catalysis of IYD reconstituted with 5 and 1-deazaflavin analogues.

Chapter 2: Dependence of cysteine for IYD catalyzed deiodination

2.1 Introduction

The mechanism closest to precedent for dehalogenation by IYD shares three processes with the two reductive dehalogenases TCHQ dehalogenase and ID discussed in detail in Chapter 1 (Figure 2-1): 1) tautomerization of substrate, 2) nucleophilic attack of substrate by the sulfur of cysteine or the selium of selenocyteine, and 3) reduction of the covalent bond formed by nucleophilic attack. Both TCHQ dehalogenase and ID are thought to tautomerize their respective substrates to nonaromatic intermediates, but the two differ in their means of dehalogenation (*60, 73*). TCHQ dehalogenase catalyzes dehalogenation of the TCHQ intermediate through nucleophilic attack on the chlorine bearing carbon by the sulfur of glutathione (*60*). ID, on the other hand, performs nucleophilic attack on the iodine by the selenium of a selenocysteine (Se-Cys) (*73*). Finally, both reductive dehalogenases reduce the covalent enzyme complex to regenerate catalytically active enzyme.

The Rokita lab previously proposed a mechanism of deiodination for IYD based on TCHQ dehalogenase and ID mechanistic precedence (Figure 2-2) (*67*). The initial step in the proposed mechanism of IYD catalysis involves the tautomerization of substrate to its keto form. This results in the formation of an iodine bearing carbon which is now sp^3 hybridized following abstraction of the phenolic hydrogen. This

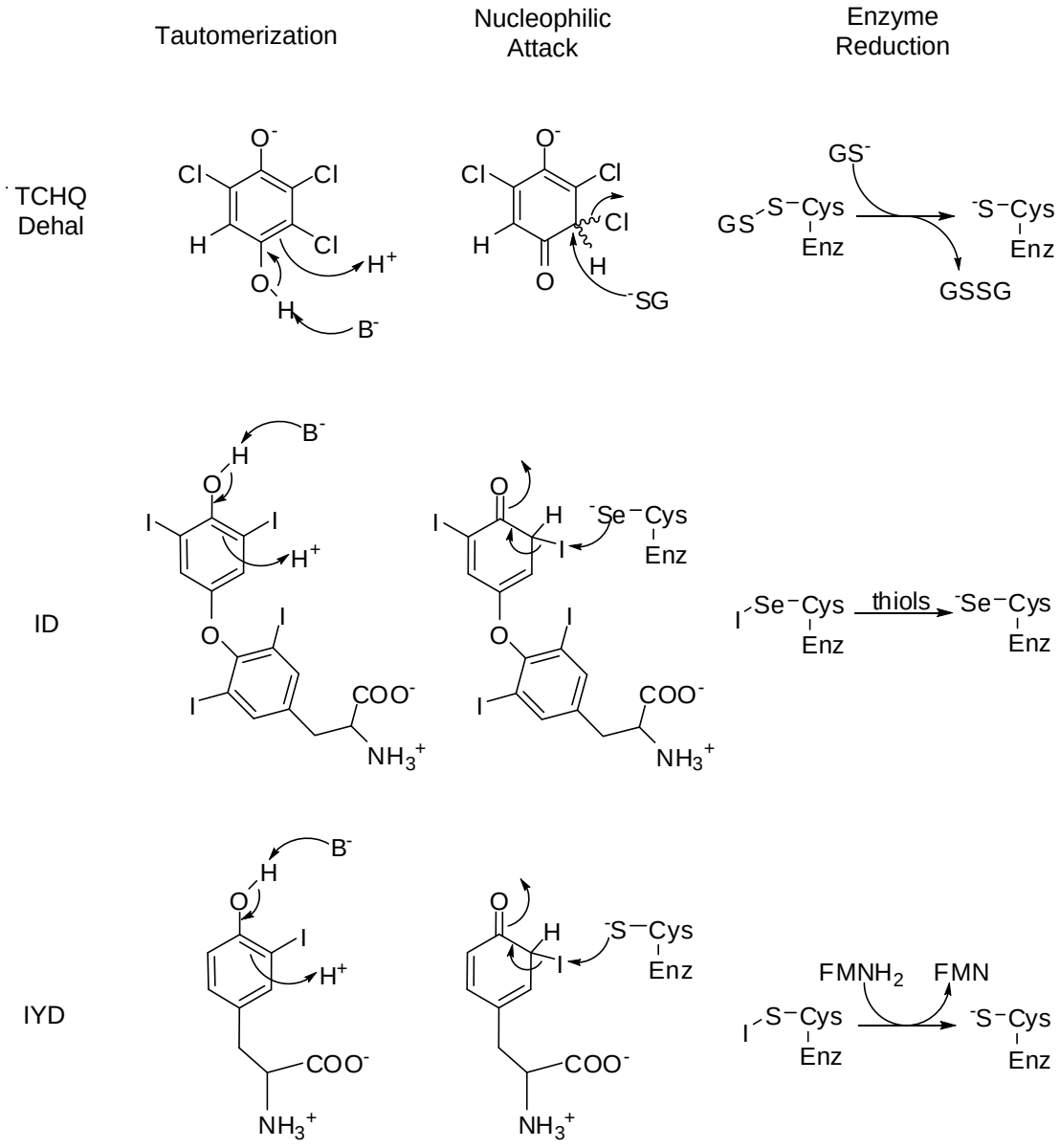

Figure 2-1. Mechanistic similarities in dehalogenation by TCHQ dehalogenase and ID as precedence for the proposed mechanism of IYD.

step in the proposed mechanism was bolstered by inhibition of IYD activity with a series of *N*-pyridonal compounds that mimic the proposed nonaromatic intermediate (*N*-methyl derivative K_I is 24 ± 8 nM) (Figure 2-3). These derivatives displayed strong inhibition of deiodinase activity, which is associated with tight binding. This indicates that IYD binds and stabilizes a nonaromatic keto tautomer (*67*).

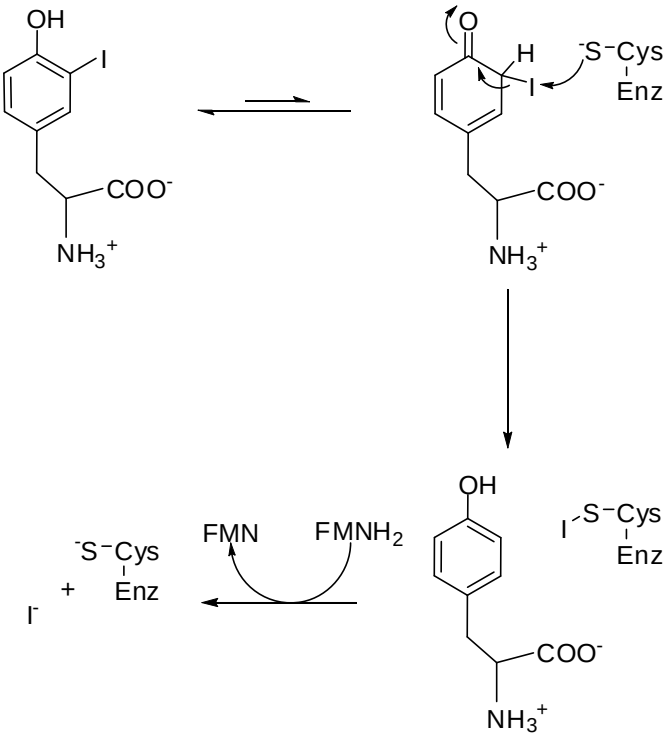

Figure 2-2. Proposed mechanism of IYD deiodination. Figure modified from Kunishima et al. (*67*).

Following tautomerization, the proposed mechanism of IYD relies on nucleophilic attack of the substrate's iodine substituent by a Cys residue. The nucleophilic attack of iodine by IYD is equivalent to ID catalysis although IYD was proposed to utilize the sulfur of an active site Cys in place of the selenium of an ID

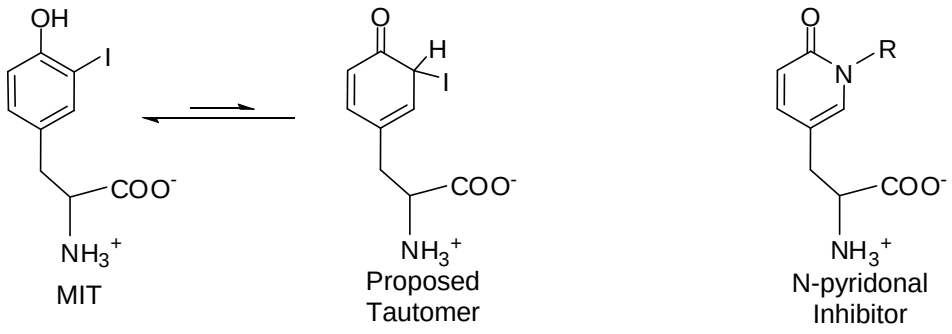

Figure 2-3. *N*-Pyridonal inhibitors mimic the proposed tautomeric intermediate.

Se-Cys. This nucleophilic attack generates reduced tyrosine as well as an S-I covalent bond between a Cys residue and iodine. As for experimental precedence, the thiol of Cys has been shown capable of promoting deiodination of MIT in model studies (*74*). Additionally, deiodination of aryl iodides by thiols proceeds through a nucleophilic attack of iodide. Cleavage of the C-I bond by halophilic attack from Cys would be facilitated by a nonaromatic keto intermediate due to reduced bond strength: C-I aryl bond is 65 kcal/mol while C-I allyl bond in only 41 kcal/mol (*75*). Similar dehalogenation by halophilic attack has been proposed for model studies of *o*-bromophenol (*76*).

The hypothesis of an active site Cys involved in catalysis was strengthened once the sequence of the IYD gene was identified and expressed recombinantly in HEK293 cells (*37, 40*). Three highly conserved Cys residues were identified by BLAST sequence analysis of several mammals (Figure 2-4) (*40*). One Cys, C13 (*Mus musculus*), is located in the predicted membrane domain of IYD and not involved in catalysis (*40*). This was confirmed as activity was retained in the truncated IYD variant (Δ2-32) which was present in the soluble fraction of cell lysates (*38*). The remaining two Cys residues, C217 and C239, were located within the predicted catalytic domain of IYD. Upon structural modeling with enzymes in the NOX/FRase superfamily, C217 and C239 (*Mus musculus*) were predicted to be in close proximity to the isoalloxazine portion of the FMN cofactor, with the sulfur of C239 within 5 Å (Figure 2-5) (*40*). Notably, among organisms that utilize thyroxine, all homologous proteins contain a Cys pair analogous to C217 and C239 (*77*). This is

in contrast to the rest of the NOX/FRase superfamily, which lack these Cys residues and the ability to perform reductive dehalogenation.

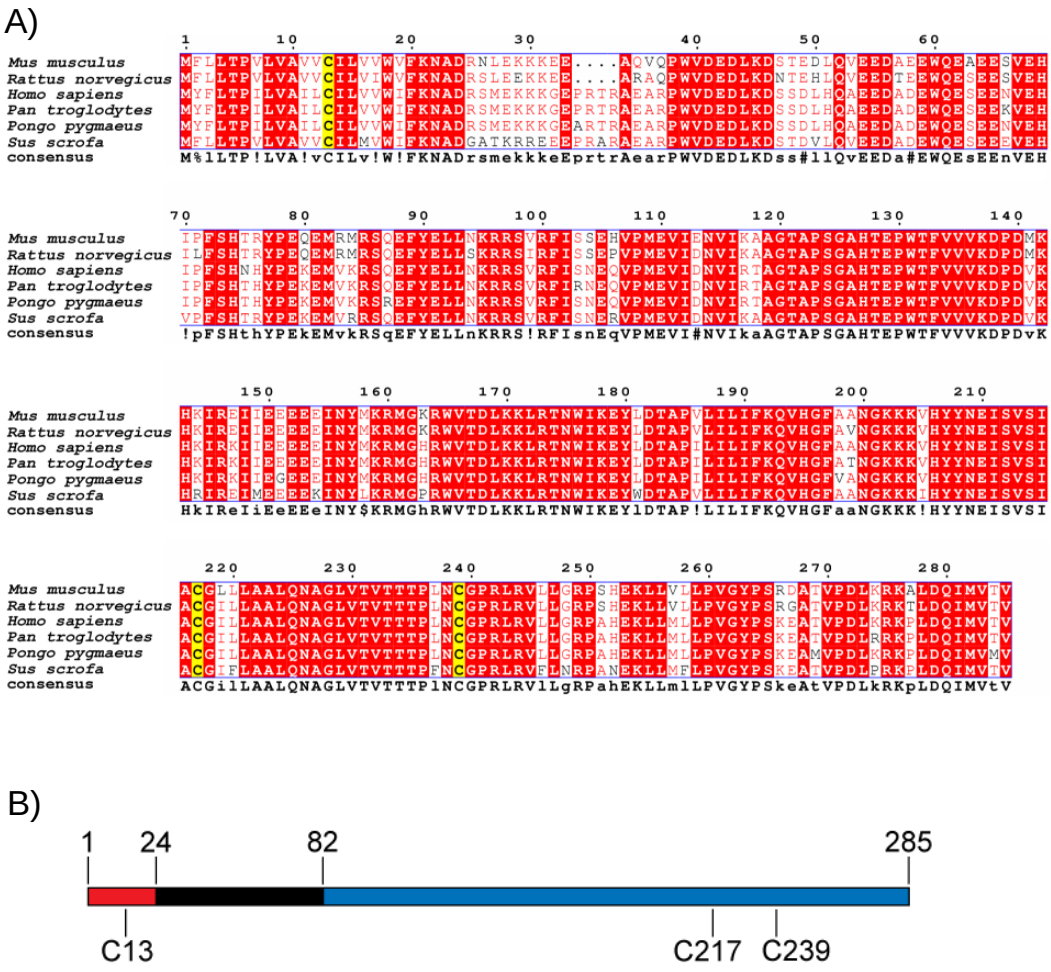

Figure 2-4. The amino acid sequence of *Mus musculus* IYD contains three conserved cysteines. A) Sequence alignment of multiple mammalian IYD proteins according to Clustal W 1.83. Sequence gaps are indicated by (.) and the consensus sequence is shown below the alignment. Conserved residues are shown in red, but conserved Cys are shown in yellow. Figure modified from Friedman et al. (*40*). B) The conserved Cys in *Mus musculus* IYD (C13, C217, and C239) map to the transmembrane domain (1-24) and the NOX/FRase domain (83-285). Figure modified from Watson et al. (*38*).

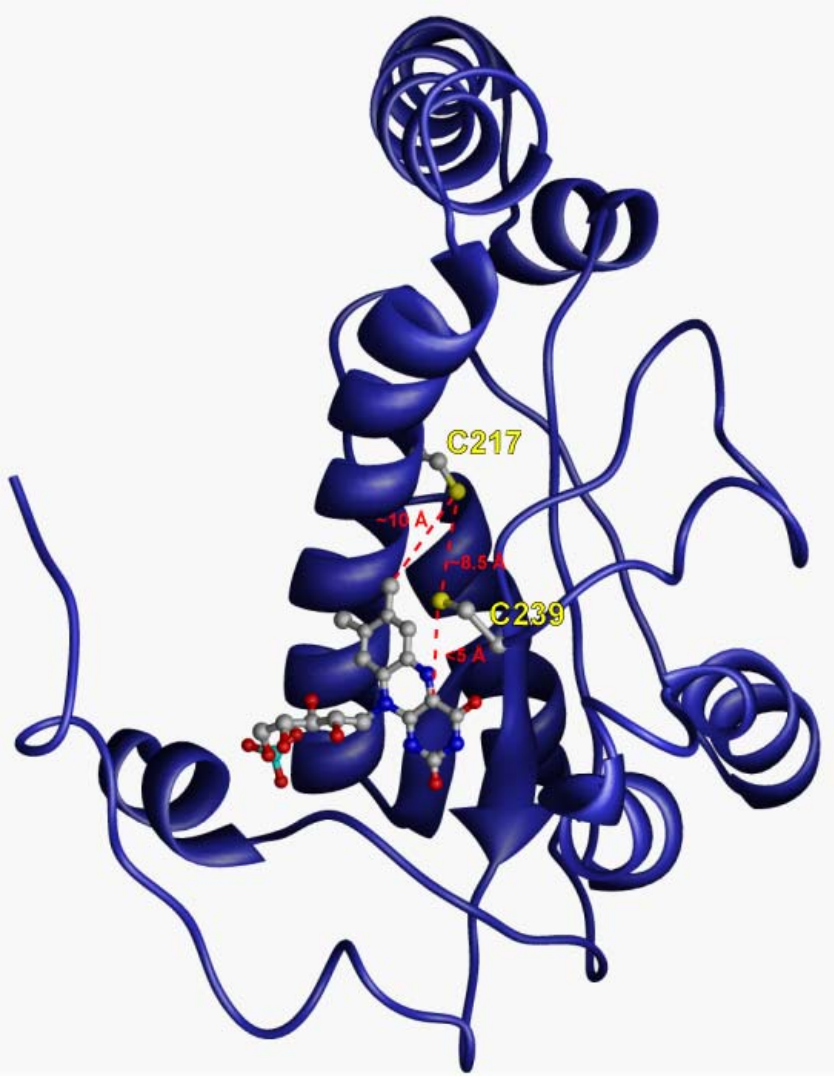

Figure 2-5. Model structure of the NOX/FRase domain of *Mus musculus* IYD. Residues 88-285 of IYD were modeled using MODWEB following threading through NfsB-NfnB (PDB code 1ICR). C217 and C239 are colored yellow and in close proximity to the FMN. Figure modified from Friedman et al. (*40*).

Cys was predicted to play a vital role in the mechanism of IYD and either C217 or C239 may function as the nucleophilic residue in deiodination. The ability to express IYD in HEK293 cells provided the first possibility to selectively probe these two Cys residues. Through site directed mutagenesis of IYD, C217 and C239 were determined to be nonessential for IYD catalysis.

2.2 Experimental Procedures

Materials. Oligodeoxynucleotide primers were obtained from Integrated DNA Technology (Coralville, IA). All enzymes were purchased from New England Biolabs (Ipswich, MA). $Na^{125}I$ used for radiolabeling of DIT was obtained from Perkin Elmer (Waltham, MA) (*78*). All other reagents were obtained at the highest grade available and used without further purification.

General methods. DNA isolation was performed using either Qiagen Qiaprep Mini, Midi, and Maxiprep Kits or Fermentas GeneJet Plasmid Miniprep Kit. PCR reactions were performed using an Eppendorf Mastercycler. All horizontal DNA agarose gel electrophoresis was performed at 125 V using the appropriate percentage of agarose with Fermentas Mass Mix DNA Ladder (*79*). *E. coli* transformations utilized an Eppendorf Electroporator 2510 (1700 V, 1 mm gap cuvette) and were plated on antibiotic selective LB plates (*79*). All DNA sequencing was performed by Geneway Research (Hayward, CA). Protein concentrations were determined using the Pierce bicinchoninic acid (BCA) assay. Vertical protein electrophoresis was performed at 200 V using the Bio-Rad Mini Protean 3 gel electrophoresis system. Denaturing discontinuous sodium dodecyl sulfate-polyacrylamide gel electrohphoresis (SDS-PAGE) gels (12 % acrylamide resolving and 5 % stacking) and 1X Laemmli running buffer were prepared according to standard protocols (*79, 80*). Protein gels were stained with Coomassie Brilliant Blue. All ligations and dephosphorylations were performed under standard conditions using T4 ligase, and Antarctic phosphatase, respectively.

Mutagenesis of IYD. Mutagenesis of IYD mammalian expression vector pcDNA3.1(+)-IYD (Dr. Jim Watson, University of Maryland) (*40*) containing full length IYD cDNA was performed according to the Stratagene Quickchange Kit. The C217A mutation variant was generated with oligonucleotides 5'-CAGTGTGTCCAT CGCC**GC*A***GGCCCCTGCTGGC-3' and 5'-GCCAGCAGG*AGGCCT***GC**GGCGAT GGACACACTG-3'. The C239A mutation variant was generated with oligonucleotides 5'-CACTACCACTCCCCTCAAC**GC**TGGTC*CTAGACTGA*GGGT GCTCC-3' and 5'-GGAGCACCC*TCAGTCTAG*GACCA**GC**GTTGAGGGGAGTGG TAGTG-3' (mutations in bold and introduced/removed restriction sites in italics). The C217A/C239A double mutation variant was generated by sequential mutagenesis with the sets of oligonucleotides above. Quickchange reactions were digested with *Dpn* I and then transformed into One Shot Top10 *E. coli* (Invitrogen, Carlsbad, CA). DNA from colonies resistant to ampicillin was isolated by miniprep and screened for the C217A and C239A mutations by restriction analysis for the addition of a *Stu* I site and changes to the banding pattern by *Bfa* I and *Hpy*181 I, respectively, before the genes were submitted for sequencing.

Expression of IYD in HEK293 cells. HEK293 mammalian cells were maintained in Dulbecco's modified Eagle's medium (DMEM, Invitrogen) supplemented with 10% fetal calf serum (FCS, Atlanta Biologicals) and 1% penicillin-streptomycinglutamine PSG (Invitrogen). Individual constructs of IYD plasmids (12 μg) were incubated for 20 min with 30 μL of Lipofectamine 2000 in Opti-MEM (Invitrogen) and then added to cells (~90 % confluent) in 10 cm dishes. The liquid medium was exchanged to DMEM, 10 % FCS and 1 % PSG after 6 hrs.

The cells were washed twice with 10 mL Dulbecco's phosphate buffered saline (DPBS, Invitrogen) 48 hrs after transfection and finally resuspended in DPBS again. Cells were harvested by centrifugation (300 x g for 5 min at 4 °C). Cell pellets were resuspended in 50 mM sodium phosphate pH 7.2 (1 mL/plate of harvested cells) supplemented with 0.25 M sucrose and 0.1 mM dithiothreitol. The cells were lysed by three freezing (liquid N_2) and thawing (37 °C) cycles followed by three passages through a 20 gauge needle.

Deiodinase activity. Enzymatic activity was measured using a standard assay described previously (*40, 78*). Assays were typically performed by addition of protein preparations (100 µL) to 300 µL of Solution 2 (1.66 mM methimazole, 0.1 mM FAD, 666 mM KCl, 333 mM potassium phosphate pH 7.4, and 166 mM 2-mercaptoethanol), 100 µL DIT (0-50 µM), 300 µL deionized water, and 100 µL [^{125}I]-diiodotyrosine ($D^{125}IT$) (~50 µCi/µmol). Reactions were initiated by addition of 100 µL of 10 % dithionite (w/v) in 5 % sodium bicarbonate (w/v). Samples were incubated under ambient temperature for 30 min and quenched by addition of 100 µL of 0.1 % DIT (w/v) in 0.1 N NaOH. A 250 µL aliquot (S) of the 1.1 mL final assay volume was removed and transferred to a vial containing 10 % acetic acid (4.75 mL) in order to determine the total radioactivity for each reaction sample. The remaining mixture (850 µL) was then passed through a cation exchange column (3.5 mL, AG 50W-X8 resin), washed an initial time with 10 % acetic acid (4.15 mL), and the eluent collected (A). The column was then washed a second time with 10 % acetic acid (5.00 mL), and the eluent was again collected (B). Each sample (S, A, and B) were diluted with 15 mL of Fisher Scientific Scintisafe plus 50 % scintillation fluid

and the amount of [^{125}I]-iodide present in each sample was quantified using a Packard 1600 TR liquid scintillation analyzer.

The percent of iodide released from each reaction (F) was calculated using Equation 2-1. The rate of iodide release (nmol/hr) was then calculated using Equation 2-2. Reactions were corrected for the fraction of background radioactivity obtained in the absence of protein (F_0), multiplied by a factor of 2 to convert the incubation time into hours, and then multiplied by the amount of initial substrate present in the assay (e. g. 10 nmol). This number was then multiplied by a factor of 2 because either of the iodide sites of DIT can be deiodinated, but statistically, only one is labeled with ^{125}I. Values were then normalized for the amount of IYD (μg) added to each reaction. The concentration of IYD in cell lysates was estimated by performing densitometry measurements (ImageQuant) of crude isolates following electrophoretic separation and subsequent Coomassie staining (See Appendix A for a representative gel). IYD turnover and kinetic constants were then calculated with data from multiple independent assay trials and were fit to Michaelis-Menten kinetics using Origin 7.0. k_{cat} values were obtained from the V_{max} and the respective molar concentration of the IYD protein.

Equation 2-1.

$$F = \frac{\frac{\text{dpm A} + \text{dpm B}}{0.85}}{\frac{\text{dpm S}}{0.25}}$$

Equation 2-2.

$$F - F_0 \times \frac{60 \text{ min/hr}}{30 \text{ min}} \times 10 \text{ nmol} \times 2$$

2.3 Results and Discussion

Investigation of cysteine involvement in IYD catalysis. Mutation of at least one of the Cys residues to Ala was expected to result in inactivated enzyme. Two single IYD mutation variants (C217A and C239A) and a double mutation variant (C217/239A) were generated in the full length *Mus musculus* IYD gene. These variants were expressed in HEK293 cells and assayed for deiodinase activity (Table 2-1). The C217A variant, which was suggested to be the more distal of the Cys pair with respect to the flavin and active site, displayed kinetics similar to those of the wild-type enzyme. Mutation of C239 resulted in a marked increase in both the Michaelis-Menten constant (K_M) and catalytic rate (k_{cat}) values although the k_{cat}/K_M decreased approximately 2.5 fold when compared to wild-type. Lastly, the double mutation variant retained activity with parameters intermediate between the two single Cys mutation variants (*38*). Thus, IYD catalysis is not dependent on the presence of Cys. This may not be entirely surprising since IYD and ID belong to two dissimilar structural superfamilies. What is surprising is that nature has developed two distinct mechanisms for catalyzing the dehalogenation of two almost identical substrates.

Table 2-1. Kinetics for wild-type and IYD mutation variants.[a, b]

IYD	$K_{M,}$ DIT (μM)	k_{cat} (min^{-1})	k_{cat}/K_M (min^{-1} μM^{-1})
Wt	8 ± 3[c]	7.1 ± 0.9	0.89
C217A	13 ± 4	8.3 ± 0.6	0.64
C239A	79 ± 7	28 ± 2	0.35
C217A C239A	42 ± 7	15 ± 2	0.36

[a]Values were included in Watson et al. (*38*)

[b]Kinetic values were obtained from fitting more than 3 kinetic trials to the Michaelis-Menten equation using Origin 7.0 (See Appendix B). K_M, V_{max}, and error values were obtained directly from fitting. The k_{cat} was obtained from the V_{max} and the respective molar concentration of the IYD protein.

[c]Substrate inhibition is responsible for a portion of the large uncertainty.

If Cys residues are not involved in catalysis, what role could they possess? The Cys mutation variants were shown not to affect the NADPH activity of IYD which relies on a yet unidentified reductase (*38*). This shows that the Cys residues are not critical for physiological catalysis as they are not required for dehalogenation of substrate or flavin reduction. Aside from catalysis, the Cys residues could be structurally important and aid protein stability. If so, they could exist as a disulfide bond if they truly are proximal to one another. Even though the roles of these Cys are still unclear, they are certainly not involved directly in catalysis, and IYD therefore does not follow the precedence of dehalogenation of ID and TCHQ dehalogenase. The repertoire of flavin catalysis has now been expanded to include reductive dehalogenation in the absence of redox-active thiols. Additional mechanisms of deiodination must then be investigated.

Possible mechanisms of IYD catalysis. Because IYD is a flavoprotein, both 1 and 2 electron transfer mechanisms should be reexamined. A mechanism similar to that already proposed would utilize a single 2 electron transfer from the reduced FMN (FMN_{red}) cofactor (Figure 2-6). This would again rely on a residue acting as a nucleophile and a reducing agent for deiodination. Nucleophilic residues other than the most obvious Cys should be considered. In particular, His and Lys residues could participate in catalysis since amines were recently shown to promote reductive dehalogenation in a model system (*81*). Also, the intermediate which would be expected in the case of Lys, Lys-εNH-X, has recently been proposed for the reverse process involving flavin dependent chlorination (*82*). Identifying residues that could participate as nucleophiles in IYD catalysis is problematic because the IYD gene is well conserved (80 % identity among mammals). An X-ray structure of the enzyme would likely be required in order to identify possible residues.

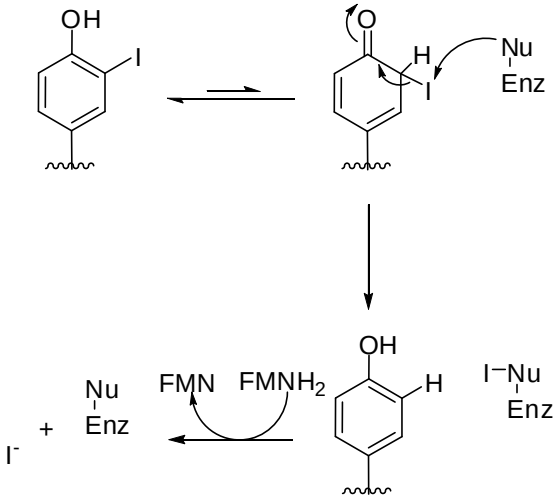

Figure 2-6. Possible S_NAr deiodination mechanism involving an unknown nucleophile.

Alternative to the involvement from a nucleophilic residue, a two electron mechanism could proceed through hydride transfer to substrate (Figure 2-7). Direct transfer of hydride from FMN_{red} by a nucleophilic aromatic substitution (S_NAr) mechanism is unlikely although it does provide a means of dehalogenation. The electron density of the phenyl ring of the substrate makes this reaction unlikely. Inclusion of electron withdrawing groups like nitro substituents similar to Sanger's reagent would be required for this mechanism to be considered. However, this electron density problem may be overcome by tautomerization of substrate. Nucleophilic attack by hydride to an sp^3 hybridized C but not an sp^2 hybridized C could facilitate an S_N2 like reaction and result in deiodination. Subsequent proton abstraction would then generate tyrosine product.

Alternative 1 electron mechanisms of IYD catalysis similar to that discussed

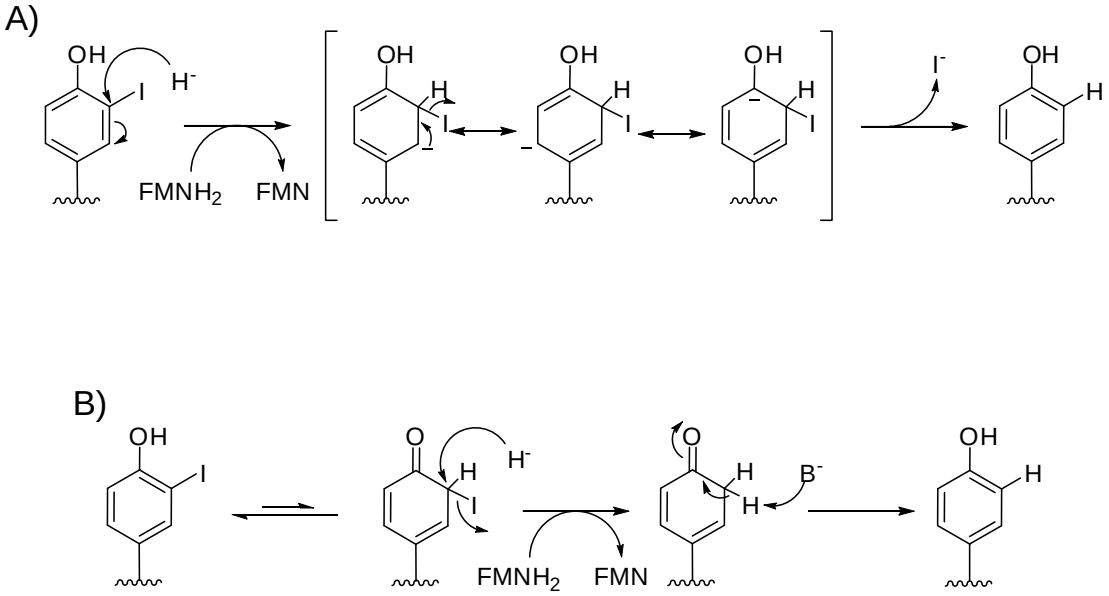

Figure 2-7. Possible 2 electron deiodination mechanisms involving hydride transfer directly from FMN_{red} A) to substrate and B) to substrate tautomer.

in Chapter 1 are fundamentally different from 2 electron mechanisms because they involve an initial single electron transfer to substrate from FMN_{red} to facilitate dehalogenation followed by an additional electron transfer from the generated flavin semiquione (FMN_{semi}). There are two 1 electron mechanistic routes to consider (Figure 2-8). The first possible route involves a free radical aromatic substitution ($S_{RN}1$) mechanism with an initial injection of an electron into the π system of the substrate. This results in a π anion radical which then facilitates deiodination, ultimately yielding the radical in place of the iodine. A second addition of an electron and a proton would complete catalysis as tyrosine product and oxidized FMN (FMN_{ox} would be formed. In contrast, the second route involves substrate tautomerization. It requires an initial step involving deprotonation of the substrate phenolic hydrogen and protonation of the iodine bearing carbon, leading to the keto form of the substrate. Addition of an electron into this system would facilitate deiodination and form a tyrosyl radical. Of note, the tyrosyl radical would be capable of resonance stabilization due to the initial tautomerization of the substrate. The addition of a second electron from the flavin semiquinone as well as reprotonation to the enol form of the phenol would complete catalysis by generating Tyr product.

In order to distinguish between a 1 or 2 electron mechanism for IYD catalysis, the flavin derivative 5-deazaFMN can be utilized (*73, 83-86*). This is due to the 5-deazaflavin's inability to stabilize a semiquinone radical (*87, 88*). Thus, incorporation of 5-deazaflavin derivatives into enzymes which follow a 1 electron process results in loss of activity, while those which follow a 2 electron process retain activity. In order to further probe the mechanism by reconstituting IYD with 5-

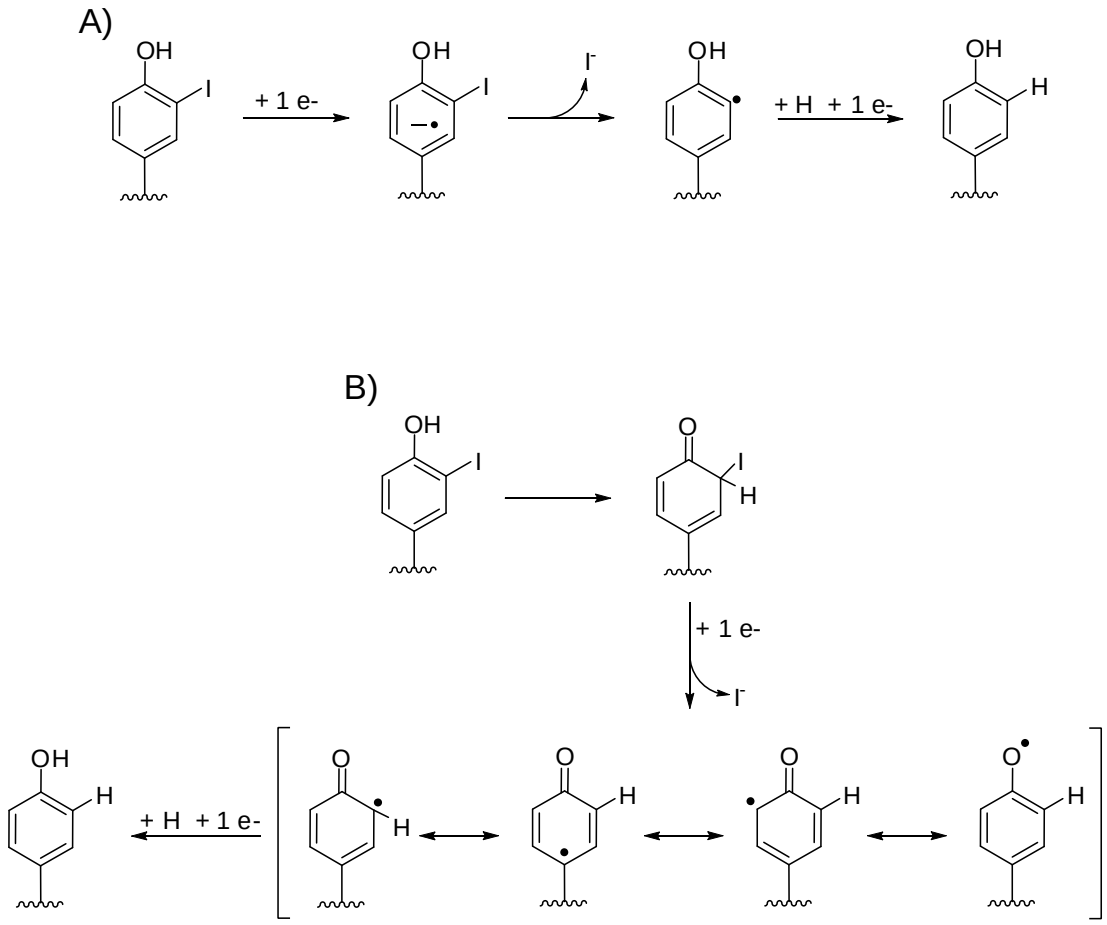

Figure 2-8. Possible 1 electron deiodination mechanisms involving radical transfer directly A) to substrate and B) to substrate tautomer.

deazaFMN, large scale isolation of recombinant IYD is required. These topics will be discussed in the remaining chapters.

Chapter 3: Large scale expression and isolation of IYD

3.1 Introduction

IYD was initially characterized (*31, 32*) almost a decade after it was first isolated in low yield from bovine thyroid homogenates (*35*). The purification procedure required solubilization of the protein by the following steps: 1) preparation of microsomes from thyroid tissues, 2) solubilization with steapsin, 3) fractionation by ammonium sulfate precipitation, and 4) sequential isolation using diethylaminoethyl-cellulose, hydroxylapatite, and gel filtration chromatography. This lengthy purification resulted in a homogenous IYD protein which was characterized by molecular weight (42 kDa) (*31*), cofactor incorporation (FMN) (*31*), and reduction potential (-420 mV) (*32*). A more thorough characterization of IYD, however, requires large scale isolation. Purification from thyroid homogenates doesn't provide a convenient method to accomplish this. Thus, an alternative source for isolating IYD is essential.

The gene encoding IYD was only recently identified and expressed (*37, 40*). The native IYD protein encoded by the gene was determined to be composed of three domains: an *N*-terminal membrane domain (1-24), an intermediate domain (25-82), and a catalytic NOX/FRase domain (83-295) (Figure 3-1) (*40*). Despite the ease of native IYD expression in HEK293 cells, isolation would be aided by expression of a soluble protein. Constructing a soluble IYD variant was stymied until the *N*-terminal

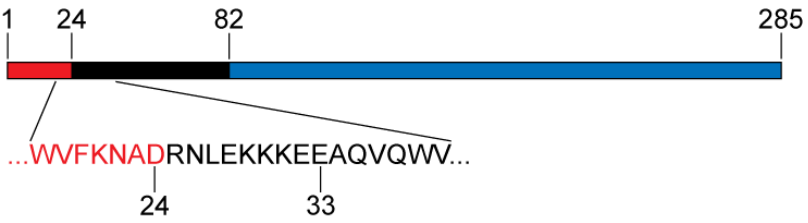

Figure 3-1. Engineering a soluble IYD. An *N*-terminal truncation of residues 2-32 removes the protein's membrane association, resulting in a soluble derivative of the enzyme.

truncation variant IYD(ΔTM)His_6 was expressed (*89*). This variant lacked amino acids predicted to anchor IYD in the membrane and contained an additional *C*-terminal polyhistidine for purification. This allowed recombinant expression of a now soluble and stable version of IYD. Interestingly, further truncation of IYD to only its NOX/FRase domain resulted in expression of insoluble and inactive protein (*89*). This indicated that a portion of the intermediate domain is required for proper protein folding despite all bacterial proteins in the superfamily lacking this domain. IYD(ΔTM)His_6 was never isolated from HEK293 cells due to the time and cost limitations associated with mammalian expression. Nonetheless, mammalian expression allowed identification of this construct for future large scale isolation in other systems.

Initially, large scale expression and isolation of IYD(ΔTM)His_6 was attempted in *E. coli* by the Rokita lab. At first, no induced protein was observed for expression in the BL21(DE3)pLysS *E. coli* strain (*90*). This was attributed to codon bias since IYD is a mammalian protein and contains numerous codons that are infrequently used in *E. coli* genes (Codon Usage Database, Kazusa DNA Research Institute) (*91*).

Rossetta 2(DE3) *E. coli* circumvented this problem because it supplements rare *E. coli* codons. Unfortunately, the protein expressed in this strain was in the form of inclusion bodies (*92*). Expression of insoluble protein seemed counterintuitive as other proteins within the NOX/FRase superfamily are bacterial and easily expressed by *E. coli* in large scale (*41-44*). Attempts to aid solubilization by altering expression conditions (isopropyl β-D-1-thiogalactopyranoside (IPTG) 20-100 μM and 18-37 ºC) did not affect the expression outcome (*92*). Additionally, several fusion proteins (glutathione-*S*-transferase, thioredoxin (TRX), and NusA) used to increase solubility did not render IYD(ΔTM)His_6 soluble although the TRX fusion appeared to increase solubility slightly (*90*). Even refolding studies with the TRX fusion protein failed to result in soluble protein (*93*).

With bacterial expression failing to yield soluble protein, yeast and insect expression remained the most viable alternatives for large scale isolation of IYD(ΔTM)His_6. The yeast strain *Pichia pastoris* has garnered significant attention as a heterologous protein expression system over the past 15 years due to several attractive properties. Namely, it provides the benefits of a eukaryotic expression system, it utilizes methanol for induction, and it grows to high cell densities (*94*). Expression in insect cells using baculovirus provides the most similar expression to mammalian cells. This system is eukaryotic like yeast, but it has advantages in protein folding with machinery more similar to mammalian, protein localization (*95*), and post-translational modifications (*96*).

Expression in *Pichia* and Sf9 insect cells were investigated simultaneously and provided systems for obtaining large scale expression and isolation of

IYD(ΔTM)His_6. Expression in *Pichia* was hindered until a synthetic gene with codon usage optimized for *Pichia* was utilized. Of the two expression systems, Sf9 cells provide protein with greater yields and purity. This allowed further characterization of IYD(ΔTM)His_6 as well as crystallographic studies which resulted in a 3-D structure at 2.0 Å resolution (*97*).

3.2 Experimental Procedures

Materials. Oligodeoxynucleotide primers were obtained from Integrated DNA Technology (Coralville, IA). Both EasySelect *Pichia* Expression and Bac-to-Bac Baculovirus Expression Kits were obtained from Invitrogen Corporation (Carlsbad, CA). All enzymes were purchased from New England Biolabs (Ipswich, MA). The plasmid pcDNA3.1(+)-IYD was obtained from Dr. Jim Watson (University of Maryland) (*40*). A synthetic variant of the *Mus musculus* gene flanked by *Eco*R I and *Not* I sites and inserted in pUCminusMCS was obtained from Blue Heron Biotechnology, Inc. (Bothell, WA). All cell lines were purchased from Invitrogen. $Na^{125}I$ used for radiolabeling of DIT was obtained from Perkin Elmer (Waltham, MA) (*78*). Antibodies for Western blotting were obtained from Novagen-EMD Biosciences (Madison, WI). All other reagents were obtained at the highest grade available and used without further purification.

General methods. DNA isolation was performed using either Qiagen (Hilden, Germany) Qiaprep Mini Kit or Fermentas (Burlington, Canada) GeneJet Plasmid Miniprep Kit. PCR reactions were performed using an Eppendorf (Hamburg, Germany) Mastercycler. All horizontal DNA agarose gel electrophoresis

was performed at 125 V using the appropriate percentage of agarose with Fermentas Mass Mix DNA Ladder (*79*). All ligations and dephosphorylations were performed under standard conditions using T4 ligase, and Antarctic phosphatase, respectively. *E. coli* transformations utilized an Eppendorf Electroporator 2510 (1700 V, 1 mm gap cuvette) and were plated on antibiotic selective LB plates (*79*). All DNA sequencing was performed by Geneway Research (Hayward, CA). *Pichia pastoris* and baculovirus procedures were performed according to Invitrogen's EasySelect *Pichia* Expression and Bac-to-Bac Baculovirus Expression Kits, respectively, unless otherwise noted. Vertical protein electrophoresis was performed at 200 V using a Bio-Rad (Hercules, CA) Mini Protean 3 gel electrophoresis system. Denaturing discontinuous SDS-PAGE gels (12 % acrylamide resolving and 5 % stacking) and 1X Laemmli running buffer were prepared according to standard protocols (*79, 98*). Protein gels were stained by Coomassie Brilliant Blue or used for Western Blotting. Electrophoretic transfer of proteins to polyvinylidene fluoride membranes (Invitrogen) for Western blotting was performed with the Bio-Rad Mini Trans-Blot Cell according to the manufacturer's directions. Polyhistidine tagged proteins were recognized using His•Tag Monoclonal Antibody and Goat Anti-Mouse IgG Alkaline Phosphatase Conjugate (*79*). Fluorescence from ECF (GE Healthcare Bio-sciences Corp.-Waukesha, WI) was detected using a Storm 860 (GE Healthcare Bio-sciences Corp.). UV measurements were made with a Hewlett-Packard 8453 spectrophotometer (Palo Alto, CA) while fluorescence measurements were made with a Hitachi F-4500 fluorescence spectrophotometer (Tokyo, Japan). Deiodinase activity was measured according to the procedure described in Chapter 2.

Subcloning of IYD(ΔTM)His_6 for expression in *Pichia pastoris*. Plasmids containing IYD(ΔTM)His_6 were constructed for recombination into *Pichia*. pPICZA-IYD(ΔTM)His_6 was generated from the *Mus musculus* IYD gene by PCR amplification of pcDNA3.1(+)-IYD (*40*) with primers 5'–CGGTACCTCGAGAATA ATGTTTGCTCAAGTTCAGCCCTGG-3' and 5'-CTCGAGGCGGCCGCCTAATG GTGATGGTGATGGTGTACTGTCACCATGAT-3'. PCR product was digested with *Not* I and *Xho* I and then ligated into pPICZA. pPICZA-optIYD(ΔTM)His_6 was assembled by inserting the synthetic variant of the *Mus musculus* IYD gene into pPICZA after *Eco*R I and *Not* I digests. Ligated plasmids were transformed into One Shot Top10 cells. Clones for both pPICZA-IYD(ΔTM)His_6 and pPICZA-optIYD(ΔTM)His_6 were identified by sequencing the DNA of colonies demonstrating resistance to the appropriate antibiotic.

IYD(ΔTM)His_6 recombinant *Pichia* clones were generated for both pPICZA-IYD(ΔTM)His_6 and pPICZa-optIYD(ΔTM)His_6. Plasmids pPICZA-IYD(ΔTM)His_6 and pPICZa-optIYD(ΔTM)His_6 were linearized with *Bst*X I prior to transformation into electrocompetent histidine deficient GS115 *Pichia pastoris* cells (*99*). *Pichia* colonies exhibiting zeocin resistance were analyzed for the presence of the IYD gene using the Easy Select Kit protocol modified to allow PCR to be performed directly using *Pichia* colonies. These modifications entailed suspending colonies in water to an optical density at 600 nm (OD_{600}) of 20, heating this by microwave on high for 1 minute, and then directly performing PCR on the mixture in the presence of 20 μM primer supplied by the manufacturer. PCR products corresponding to IYD recombination were gel purified and sequenced. Transformants confirmed to contain

the gene for IYD were analyzed for their methanol utilizing (Mut) phenotype on minimal methanol medium plus histidine (MMH) plates.

Subcloning of IYD(ΔTM)His_6 for expression in Sf9 insect cells. pFASTBAC1 plasmid containing IYD(ΔTM)His_6 was constructed for bacmid generation. The *Mus musculus* IYD gene was amplified from pcDNA3.1(+)-IYD (*40*) with primers 5'-AAGCTTAAGCTTGGATCCGCCACCATGTTTCTCCTCAC CCCA-3' and 5'-CTCGAGCTCGAGCTAATGGTGATGGTGATGGTGTACTGTC ACCATGATC-3' to generate the plasmid pFASTBAC1-IYD(ΔTM)His_6. The PCR product and pFASTBAC1 were digested with *Bam*H I and *Xho* I. The gene insert was ligated into the plasmid and transformed into One Shot Top10 cells. DNA isolated from resistant colonies was sequenced to verify plasmid construction.

Bacmid containing IYD(ΔTM)His_6 was constructed through transposition of pFASTBAC1-IYD(ΔTM)His_6 into the baculovirus shuttle vector, bMON14272 (Invitrogen). This was accomplished by transforming pFASTBAC1-IYD(ΔTM)His_6 into MAX Efficiency DH10Bac *E. coli*. Colonies resistant to gentamycin, kanamycin, and tetracycline were then plated on bluo-gal/IPTG selective plates to screen for colonies containing the desired recombinant bacmid. PCR was performed using DNA isolated from several white colonies to verify pFASTBAC1-IYD(ΔTM)His_6 recombination into the bacmid. The desired bacmid was confirmed by sequencing PCR products.

Recombinant baculovirus was generated with bacmid containing IYD(ΔTM)His_6. Serum-free adapted Sf9 cells maintained in SF-900 II SFM (Invitrogen) were transfected with pFASTBAC1-IYD(ΔTM)His_6 recombinant

bacmid DNA and Celfectin Reagent (Invitrogen). The IYD recombinant baculovirus was collected from the growth medium 72 hrs after bacmid transfection. Virus concentrations were determined by an end point dilution virus titer (*100*). Virus was amplified with a multiplicity of infection (MOI) of 0.05 (plaque forming units (pfu)/cell) and the growth medium from subsequent virus propagations was saved as IYD recombinant baculovirus stock.

Enzyme expression in *Pichia pastoris*. Clones containing IYD(ΔTM)His_6 with a positive Mut phenotype were grown overnight in a minimal glycerol medium plus histidine (MGYH) to an OD_{600} between 2 and 6 (30 °C). These cells were centrifuged (5 min at 5,000 x g) and resuspended in MMH medium for induction to an OD_{600} of 1. Cells were then induced 48 hrs (30 °C), pelleted by centrifugation, and resuspended in a solution appropriate for subsequent affinity purification (500 mM NaCl, 50 mM sodium phosphate buffer, 10 mM imidazole, 150 μM FMN, pH 8.0). Cells were lysed by 3 passages through a French press at approximately 10,000 psi. Lysates were centrifuged at 12,000 x g for 10 min (4 °C) to remove cellular debris. Supernatants were centrifuged a second time at 20,000 x g for 1 hr (4 °C) and finally filtered (0.22 μm) to remove any additional particulates.

Enzyme expression in Sf9 insect cells. Sf9 cells were infected by pFASTBAC1-IYD(ΔTM)His_6 recombinant baculovirus stock in Sf9-900 II SFM with an MOI of 1 (pfu/cell). Cells were incubated at 27 °C for 72 hrs and then harvested by centrifugation at 500 x g for 5 min (RT). The cell pellet was resuspended in an appropriate solution for affinity chromatography and lysed by three freezing (liquid N_2) and thawing (37 °C) cycles followed by three passages through a 20 gauge

needle. Lysates were centrifuged at 20,000 x g for 1 hour (4 °C), and finally, supernatant was filtered through a 0.22 μm filter.

Purification of IYD(ΔTM)His$_6$. IYD(ΔTM)His$_6$ was purified from cell lysates using an AKTA FPLC (GE Healthcare Bio-sciences Corp.) with a 1 mL HisTrap HP column chelated with Ni^{2+}. Soluble lysates were applied to the affinity column, washed with 5 column volumes of wash buffer (500 mM NaCl, 50 mM sodium phosphate, 20 mM imidazole, pH 8.0) and eluted using a linear gradient of 20-300 mM imidazole over 20 mL. Fractions containing IYD(ΔTM)His$_6$, as identified by SDS-PAGE, were pooled and dialyzed overnight (4 °C) against 10 mM potassium phosphate, pH 7.4. The concentration of bound FMN cofactor was determined using an ε_{450} 12,500 M^{-1} cm^{-1} (*101*). The concentration of holoenzyme was calculated using an ε_{280} of 57,600 M^{-1} cm^{-1} determined using the Edelhoch method (*102*).

3.3 Results and Discussion

Expression and isolation of IYD(ΔTM)His$_6$. The soluble IYD(ΔTM)His$_6$ protein identified by expression in mammalian cells (*89*) was investigated simultaneously for expression and isolation in *Pichia* and in Sf9 cells. These two expression systems overcame the yield limitations of mammalian expression and the folding problems encountered in *E. coli*.

Expression and isolation of soluble IYD(ΔTM)His_6 was first accomplished in *Pichia* although recombinant clones encoding the *Mus musculus* gene for IYD(ΔTM)His_6 (Figure 3-2) failed to express the protein. Cell lysates lacked deiodinase activity and expression of the protein was undetectable by Coomassie

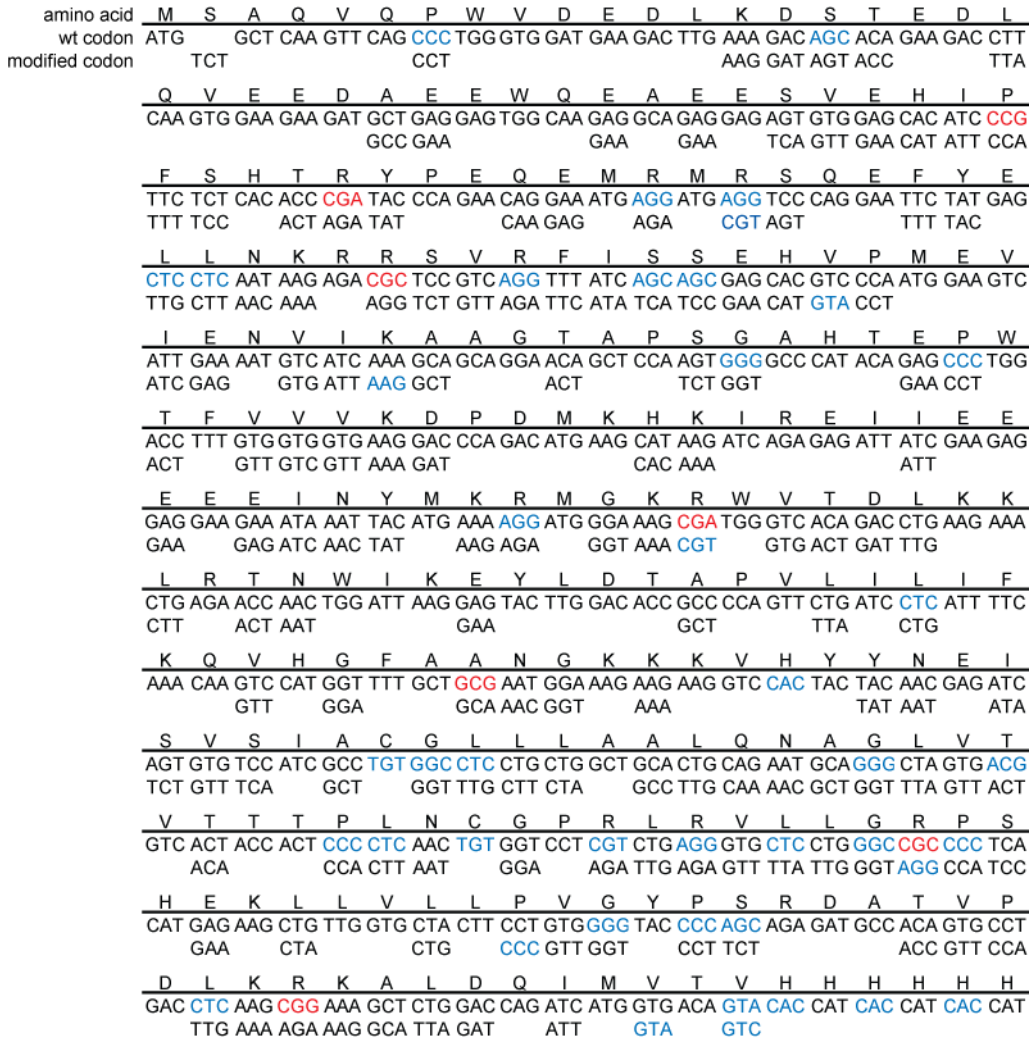

Figure 3-2. Nucleotide sequences used for expression of IYD(ΔTM)His_6. The wild-type *Mus musculus* gene shown below the amino acid sequence was used for expression in Sf9 cells, but failed to express in *Pichia*. The synthetic gene used for expression in *Pichia* contained numerous codon changes which are shown below the nucleotide sequence. Red and blue codons signify changes to bring *Pichia* usage from below 0.5 and 1 % to above 1 %, respectively.

staining or by Western blotting. Varied lengths of expression (24-96 hrs) and methanol induction concentrations (0.5 - 2.0 % v/v) were ineffective in stimulating IYD(ΔTM)His_6 expression. This absence of expression was not a result of problems in transformation. PCR and sequencing verified that the desired gene had recombined into the *Pichia* genome (Figure 3-3). It was hypothesized that the deficiency in expression was due to the differing codon usage between *Pichia* and *Mus musculus*. The gene contains a significant number of codons rarely utilized in *Pichia* (Codon Usage Database, Kazusa DNA Research Institute) (*91*).

To avoid these rarely used tRNAs, a synthetic gene was constructed (Figure 3-2). Rare codons with usage below 5 per thousand comprised 2 % of the *Mus musculus* gene. These codons were replaced in the synthetic gene with codons of high usage in *Pichia*. This gene was also designed to reduce the usage of less rare codons with

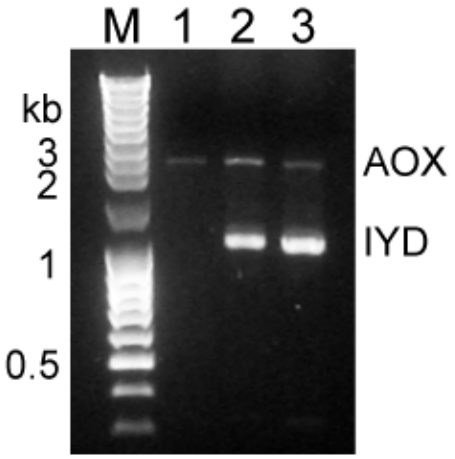

Figure 3-3. PCR verification of IYD recombination into *Pichia pastoris* (GS115) clones. Direct colony PCR was performed on a *Pichia* negative control which lacks IYD gene recombination (Lane 1), a pPICZA-IYD(ΔTM)His_6 *Pichia* clone (lane 2), and a pPICZA-optIYD(ΔTM)His_6 *Pichia* clone (lane 3). The AOX1 gene (2.2 kb) of GS115 *Pichia* is evident in each PCR sample, confirming each clone is Mut^+. PCR products were detected with ethidium staining following agarose (1%) gel electrophoresis.

frequencies between 5 and 10 per thousand from 13 % to 5 %. The synthetic gene also minimized repetitive usage of particular codons. For instance, GAG which encodes Glu is utilized 6 times in the span of 11 codons (amino acids 27-37) in the *Mus musculus* gene. This was reduced to two occurrences in that same span in the synthetic gene by substituting 4 of the GAG codons with GAA. Finally, additional codon substitutions reduced the predicted mRNA secondary structure of the native gene transcript by approximately 46 % according to mFold (*103*). Of note, a potential hairpin structure in the yeast consensus sequence (comparable to a Kozak sequence) which includes the start codon was removed. Removal of similar mRNA secondary structure in this region has been shown to increase translation in *E. coli* (*104*).

Pichia clones containing the synthetic gene now express IYD(ΔTM)His_6, although it is at a low level (approximately 2 % of the total protein) (Figure 3-4). This low expression still yields IYD(ΔTM)His_6 at mg quantities per L of culture (Table 3-1). This is primarily because of *Pichia's* ability to grow to high cell densities. Purification from expression lysates required only a single Ni^{2+} affinity chromatography step and resulted in protein of acceptable purity.

IYD(ΔTM)His_6 is also expressed very efficiently in Sf9 cells. Sf9 cells infected with recombinant baculovirus containing the truncated *Mus musculus* gene resulted in very high expression with IYD(ΔTM)His_6 comprising 10 % of the total protein (Figure 3-4). Isolation of IYD(ΔTM)His_6 from cell lysates again required only a single Ni^{2+} affinity chromatography step but yielded an approximate 20 fold increase in isolated protein per liter of culture in comparison to *Pichia*. Moreover, the

Table 3-1. Isolation yields of IYD(ΔTM)His_6.[a]

Expression System	IYD mg / g cell pellet	IYD mg / L culture	IYD Purity[b] (%)
P. pastoris	0.18 ± 0.03	2.2 ± 0.6	91 ± 5
Sf9	3.98 ± 0.03	43 ± 8	99 ± 0.1

aAll measurements were performed in triplicate.
[b]Purity was calculated by densitometry over the full land length and width using ImageQuant 5.2 (See Appendix C for a representative gel).

isolated protein was of exceptional purity (Table 3-1). These drastic differences in both yield and purity outweigh the fact that expression in insect cells is more costly than yeast and that generating virus for infection of Sf9 cells is lengthy. The Sf9 system was the source of most enzyme used for characterization because of its high purity.

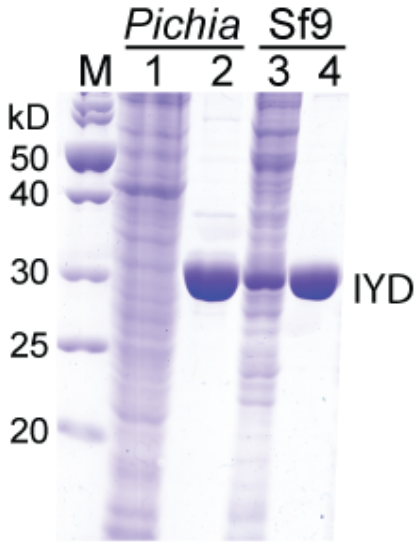

Figure 3-4. Denaturing PAGE analysis of IYD(ΔTM)His_6 expression and purification from *Pichia* and Sf9. Ni^{2+} affinity chromatography with expression lystates (*Pichia* and Sf9-lanes 1 and 3, respectively) yielded pure protein from *Pichia* (Lane 2) and Sf9 (Lane 4). Molecular weight standards are shown (lane M).

Characterization of isolated IYD(ΔTM)His$_6$. Isolated IYD(ΔTM)His$_6$ was initially analyzed spectrophotometrically (Figure 3-5). It had absorbance peaks of 274, 363, and 447 nm. The two higher wavelength peaks are representative of an oxidized flavin and are similar to those previously reported for IYD isolated from bovine thyroids (*31*). Additionally, the 363 and 447 nm peaks are blue shifted 9 and 3 nm, respectively, from unbound FMN. Excitation of the IYD(ΔTM)His$_6$ FMN at 447 nm results in a broad fluorescence peak with a maximum emission at 527 nm. The intensity of this peak is reduced approximately 1.5 fold compared to free FMN.

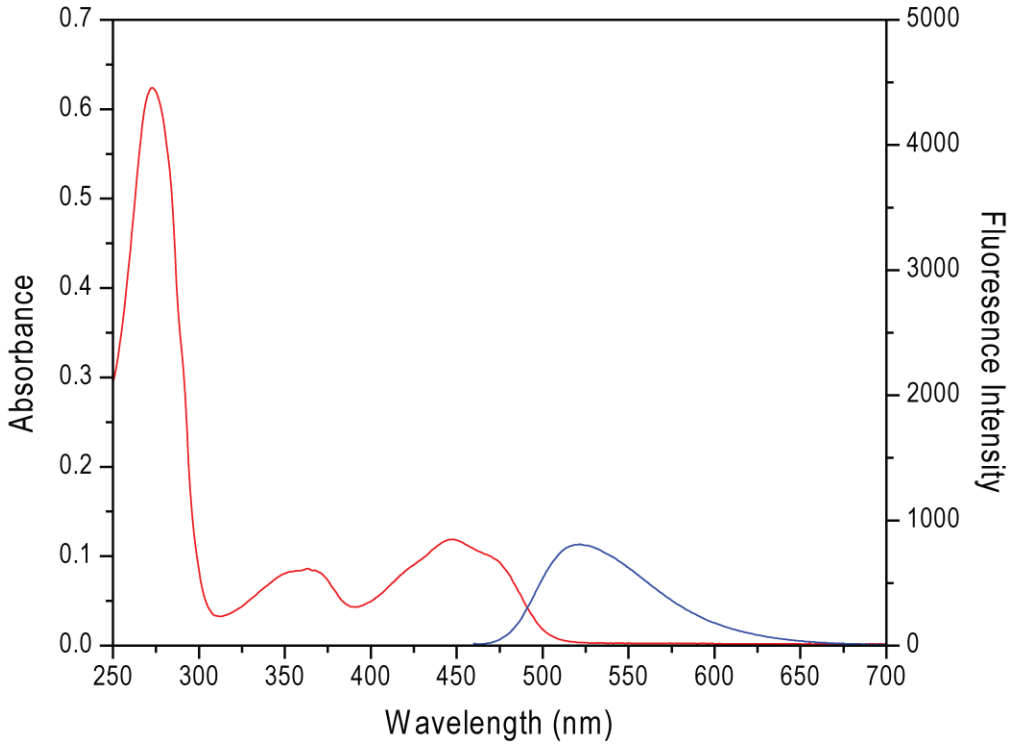

Figure 3-5. Spectroscopic analysis of IYD(ΔTM)His$_6$. Absorbance spectrum (10 μM) is shown in red and emission spectrum (15 μM) following excitation at 447 nm is shown in blue.

In order to determine the concentration of IYD(ΔTM)His_6 in solution, an extinction coefficient at 280 nm (ε_{280}) was determined by the Edelhoch method (*102*). This was calculated using the extinction coefficient values for Trp and Tyr in 6 M guanadinium hydrochloride (GdnHCl) and 8 M urea (*105*). The absorbance of IYD(ΔTM)His_6 denatured in 6 M GdnHCl and 8 M urea was corrected for FMN contribution at A_{280}. The remaining absorbance was attributed to the five Trp and seven Tyr residues of IYD(ΔTM)His_6. The ε_{280} for the IYD(ΔTM)His_6 holoenzyme was estimated to be 57,600 M^{-1} cm^{-1} and is almost identical to the predicted value of 57,555 M^{-1} cm^{-1} (*105*).

Based on the ε_{280} of IYD(ΔTM)His_6, the stoichiometry of FMN in the protein was determined to be 2.0 FMN molecules per IYD(ΔTM)His_6 dimer using the FMN ε_{450}. This ratio of FMN to protein dimer was obtained for protein isolated from both *Pichia* and Sf9 cells. Interestingly, this stoichiometry contrasts the IYD isolated by Rosenberg and Goswami (*31*). A single FMN molecule per IYD dimer was reported

Table 3-2. Kinetic parameters of IYD derivatives.[a,b]

Expression System	IYD	K_M (μM)	k_{cat} (min^{-1})	k_{cat}/K_M (min^{-1} μM^{-1})
HEK293[a]	IYD(ΔTM)	6 ± 2	5.8 ± 0.6	0.95
Pichia[b]	IYD(ΔTM)His_6	19 ± 3	6.9 ± 1.3	0.36
Sf9[b]	IYD(ΔTM)His_6	9 ± 1	4.5 ± 0.7	0.49

[a]Values are from Watson et. al using whole cell lysates of HEK293 (*38*).
[b]Kinetic values were obtained from deiodination data fit to Michaelis-Menten kinetics (See Appendix D).

with IYD isolated from bovine thyroids. The basis of this discrepancy is unclear, but it may due to the excess FMN added during the Ni^{2+} affinity chromatography step.

The kinetic constants for deiodination of IYD(ΔTM)His_6 isolated from *Pichia* and Sf9 was comparable and similar to those reported for the expression of soluble IYD(ΔTM) in HEK293 lysates (Table 3-2) (*38*). The Michaelis constant K_M was approximately three fold greater for the *Pichia* isolate than other proteins. The k_{cat} of all three proteins was indistinguishable since all agreed within error, while the overall k_{cat}/K_M was 2 fold lower for each of the isolated proteins than IYD(ΔTM) from HEK293 lysates.

Structure of IYD(ΔTM)His_6. The structure of IYD(ΔTM)His_6, as well as its costructures with substrates MIT and DIT were solved at 2.0, 2.45, and 2.6 Å (protein data bank codes 3GB5, 3GFD, and 3GH8), respectively, by Seth Thomas through collaboration with the LaRonde-LeBlanc lab (University of Maryland) (Figure 3-6) (*97*). The structure displays electron density beginning with residue S66 of the interdomain, with the *N*-terminal portion of the protein (residues 33-65) which immediately follow IYD's membrane anchor lacking density. Additionally, IYD's placement in the NOX/FRase structural superfamily was confirmed as it contains the α-β fold characteristic to all superfamily proteins. The IYD structure contains 2 FMN molecules per constitutive dimer with the active sites comprised of regions of each polypeptide, which is also common to the superfamily. Additionally, most flavin contacts to the isoalloxazine ring, ribityl tail, and phosphate are also conserved (Figure 3-7) (*41, 42, 44, 80, 106-109*).

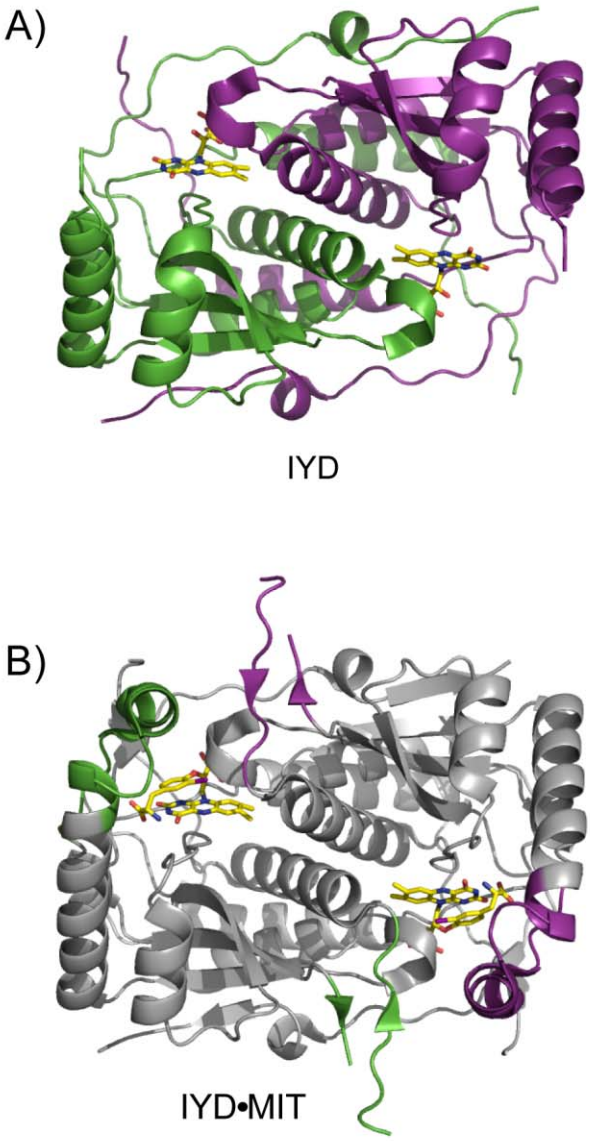

Figure 3-6. IYD structure. A) Native IYD homodimer structure crystallized in the absence of substrate. Monomer units are distinguished by color. Disordered regions are not shown and residues 156 - 177 and 195 – 208 connect the structure at nonterminal ends. B) Native IYD homodimer structure crystallized in the presence of MIT. The substrate induced structure is shown in color according to the respective monomers. Figure is modified from Thomas et al. (*97*).

Interestingly, substrate binding induces helix-loop and helix formation of two otherwise unstructured regions (Figure 3-8). The structure of this induced region is very similar to IYD's closest structural neighbor BluB. This is despite the low identity (19 %) between the two proteins and BluB's distinctive activity of cannibalizing its FMN cofactor (Figure 3-9) (*106*). This region of their structures

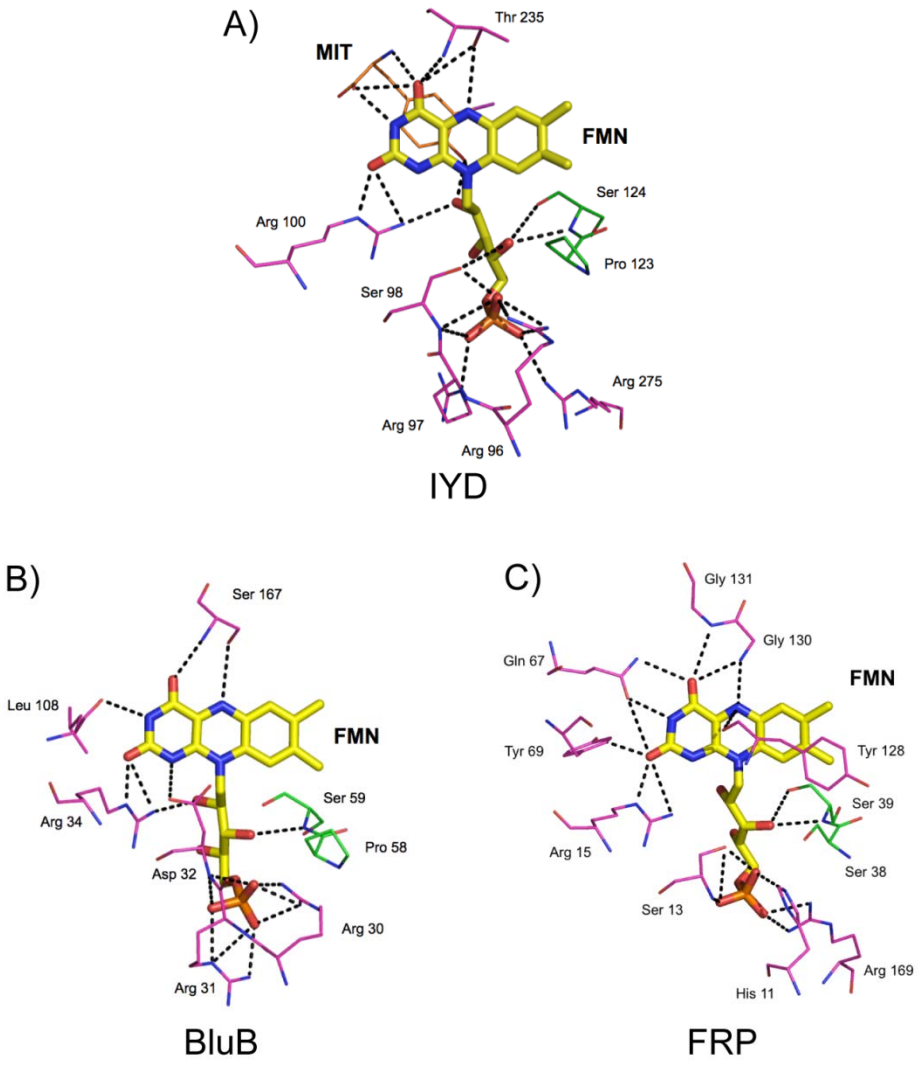

Figure 3-7. Polar contacts of A) IYD, B) BluB, and C) FRP to respective bound FMN cofactor. Residues making contacts are within 4 Å and correspond to structures 3GDF, 2ISJ, and 2BKJ, respectively. Figure was modified from Thomas et al. (*97*).

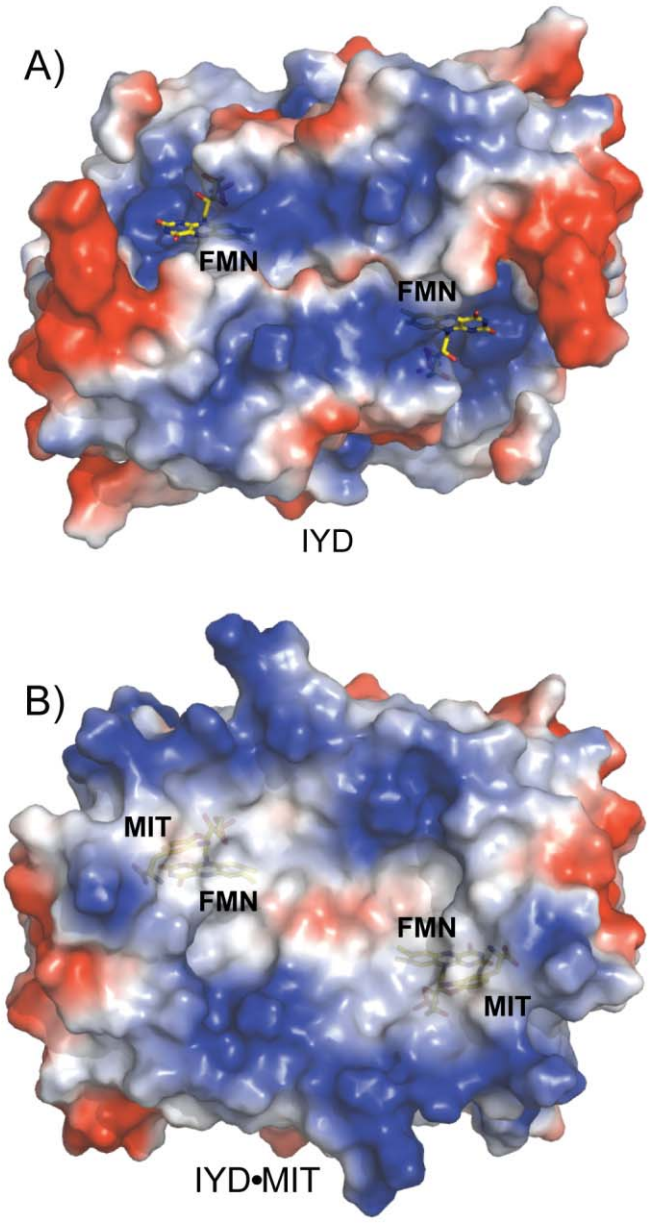

Figure 3-8. Surface properties of A) IYD and B) its complex with MIT. Surface properties were calculated in PyMOL using vacuum electrostatics (*110*). Blue indicates positive charge and red indicates negative charge. Figure is modified from Thomas et al. (*97*).

differentiates IYD and BluB from the two current NOX/FRase subfamilies which contain similar loops at the active site but on the opposite polypeptide chain (*107, 108*). This has led to the proposal of a new subfamily belonging to both IYD and BluB. IYD's induced structure acts as an active site lid, sequestering substrate from solvent. It is stabilized through polar interactions between Tyr 157, Glu 153, and Lys 178 and the zwitterion of the substrate, which is in turn anchored by interactions to the isoalloxazine of the FMN cofactor. These contacts to the zwitterion of substrate are unique in the NOX/FRase superfamily (*41, 42, 44, 80, 106-109*) and likely

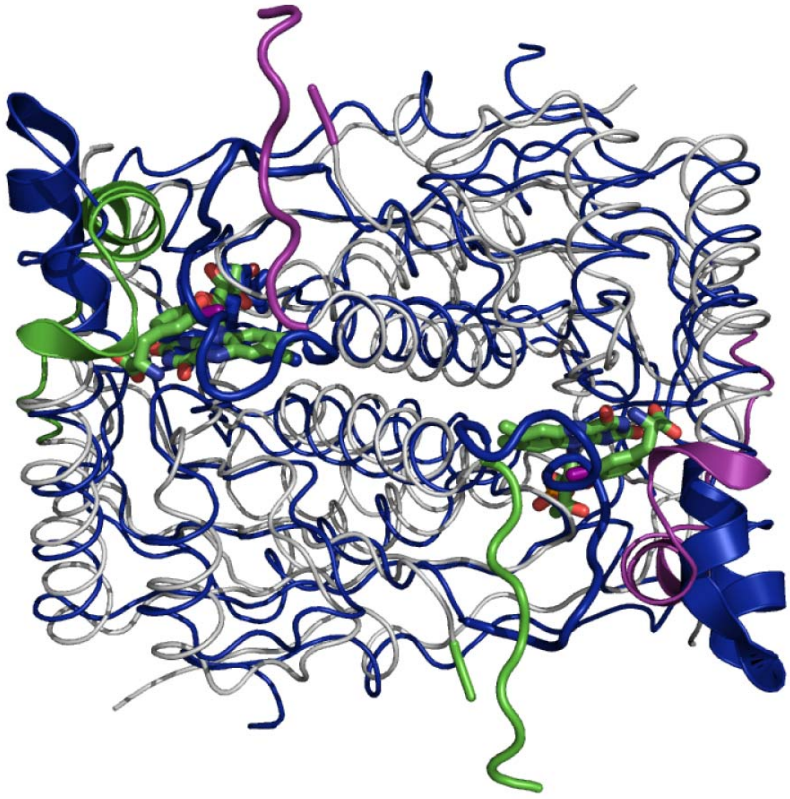

Figure 3-9. IYD structural overlay with BluB. Structural differences between IYD•MIT (grey) and BluB (blue) are highlighted with cartoon representation near the active sites. IYD induced structure is colored according to respective monomer units (green and purple). Figure modified from Thomas et al. (*97*).

influence the redox properties of the FMN cofactor. Additionally, the active site lid likely precludes thyroxine from binding in a productive orientation due to steric effects. IYD's ability to discern between substrate and T_4 is essential for iodide salvage as deiodination of T_4 is a futile process. The contacts made to the zwitterion of substrate, as well as contacts to the substrates' hydroxyl substituent from N10 of the isoalloxazine ring, the 2-hydroxy of the ribityl tail, and Ala 126 position the substrate almost parallel to the isoalloxazine ring of the FMN cofactor.

The *Mus musculus* and *Homo sapiens* IYD genes have high identity (91 %), and thus, the recently identified human IYD mutations (*28, 29*) can be rationalized with the reported structure (Figure 3-10). These congenital mutations were identified in patients deficient in retaining thyroidal iodide which resulted in goiter and in some cases, developmental impairment. Mutations equivalent to R97W and the combined I102L and F101 deletion in the *Mus musculus* gene affect the FMN binding. These mutations were the most severe of those identified as only minimal deiodinase activity was retained in each mutant (*28*). This was due in particular to disruption of FMN contacts. Arg 97 makes direct contact the phosphate of FMN and residues 101 and 102 are critical for properly orienting Arg 100 near the N1 position of the isoalloxazine ring. The human mutations corresponding to I112T and A216T were indicated to destabilize protein stability, leading to premature degradation (*28, 29*). These mutations appear to affect secondary structure and dimerization, respectively, based on the structure of IYD.

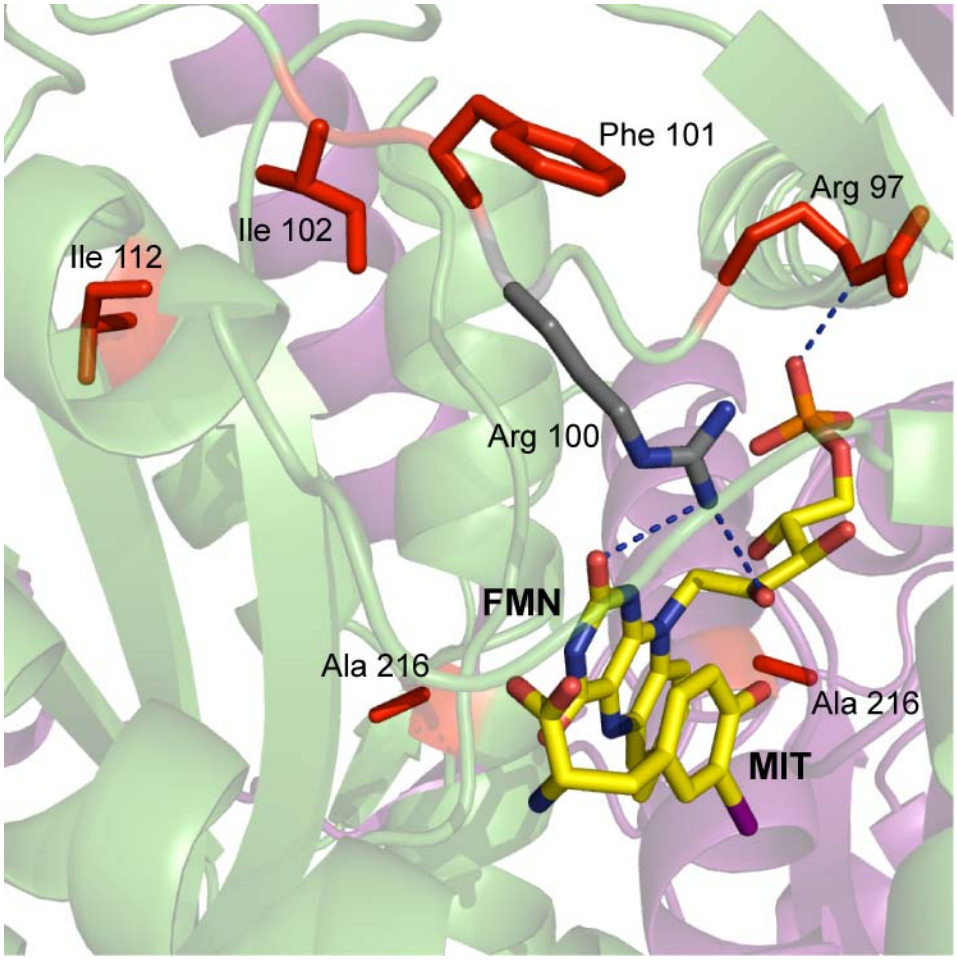

Figure 3-10. Mapping of IYD mutations. Residues of the *Mus musculus* gene corresponding to clinically identified IYD mutations in the *Homo sapiens* gene are shown in red. Residue Arg 100 highlighted in grey is not a site associated with direct mutation, but its polar interactions are affected by the combined I102L and F101 deletion mutation. IYD monomer units are colored accordingly. Figure modified from Thomas et al. (*97*).

The structure of IYD(ΔTM)His_6 provides a molecular basis for understanding mutations affecting the physiological capability of IYD to salvage iodide. The crystal structure along with additional characterization studies were enabled by heterologous expression and isolation of IYD(ΔTM)His_6. With initial characterization complete, the plentiful supply of protein now allows many new investigations of IYD.

Chapter 4: Ligand and substrate requirements for recognition and catalysis by IYD

4.1 Introduction

The co-crystal structure of IYD (*97*) and previous reversible inhibition experiments (*71, 72*) illustrate IYD's high turnover selectivity. This is evident as IYD seems unable to tolerate modifications at the zwitterion and phenolic functionalities of substrate (*71, 72*). The structure of IYD indicates that this is likely due to the polar contacts made by these functionalities to both protein residues and the FMN cofactor (Figure 4-1). In fact, these polar contacts orient the substrate's 3-position substituent directly above the FMN isoalloxazine (Figure 4-2) (*97*). In contrast to the zwitterion and phenolic functionalities of substrate, the role of the 3-position substituent in substrate specificity was ambiguous following reversible inhibition studies. This is because there was no clear correlation between IYD affinity and the electronics or sterics of 3-position substituents (*71, 72, 111, 112*). The reason for this is as much unknown as whether these tyrosine derivatives actually serve as substrates for IYD.

The structure of IYD with substrate indicates that the formation of IYD's active site lid confers the substrate specificity associated with the zwitterion of substrate (*97*). Seven residues (Glu 153, Tyr 167, Trp 166, Leu 169, Thr 174, Asn 175, and Lys 178) comprising the lid are in close proximity of the substrate (within 4 Å) with three (Glu 153, Tyr 167, and Lys 178) making direct polar contacts to the

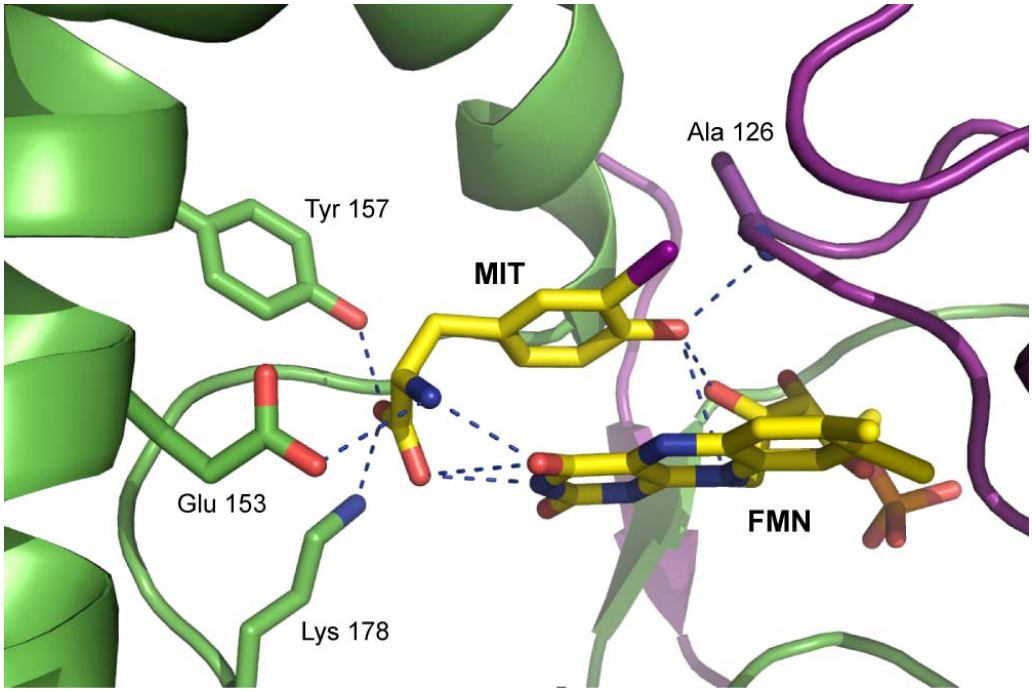

Figure 4-1. MIT substrate interactions with IYD and FMN. Polar contacts within 4 Å of MIT are indicated by dashed lines. Figure modified from Thomas et al. (*97*)

zwitterion (Figure 4-1). Additionally, the isoalloxazine of FMN makes polar contacts the zwitterion of substrate. These zwitterion contacts secure the active site lid once substrate is bound by acting as a bridge between the lid and the FMN cofactor. The loss of deiodinase inhibition upon modification to either the amine or carboxy of the zwitterion is consistent with the zwitterion contacts conferring specificity (*71*). The phenol displays similar specificity as methylation completely abolishes any deiodinase activity inhibition (*71*). This specificity likely results from polar contacts to the N10 of the isoalloxazine ring of FMN, the 2-hydroxy of the FMN ribityl tail, and the backbone nitrogen of Ala 126.

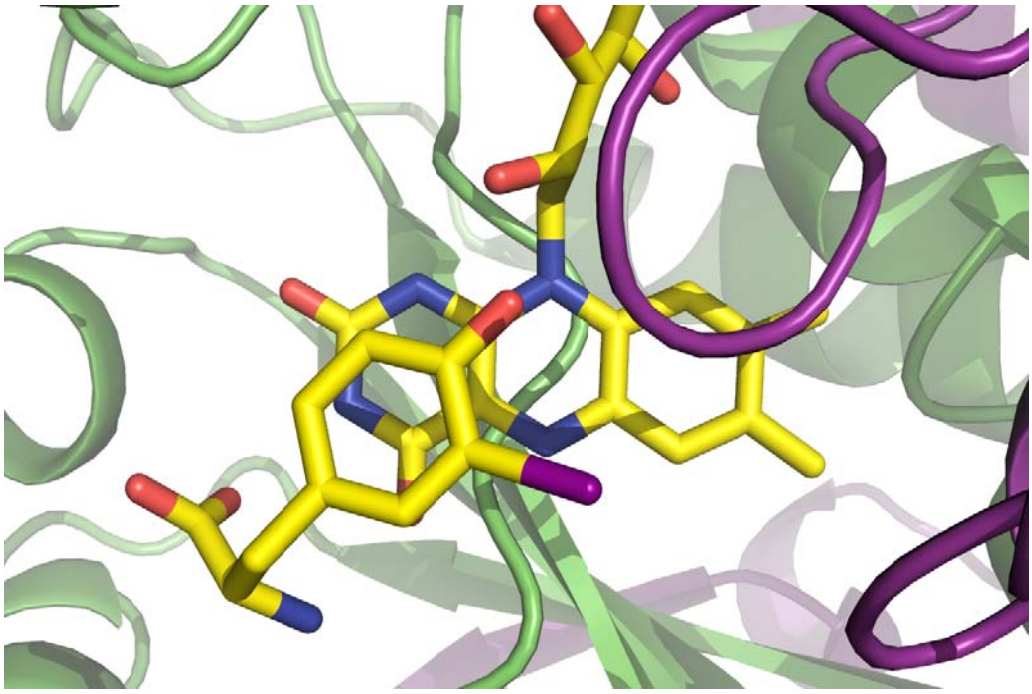

Figure 4-2. MIT substrate stacks above the isoalloxazine of FMN. The C-I bond of MIT is positioned directly above the C4a-N5 bond of FMN.

Despite having a structure for IYD, the substrate specificity requirements with regard to the 3-position substituent cannot be resolved. This is in part because the highly polarized iodine of MIT and DIT substrates makes no polar contacts (Figure 4-1) (*97*). In fact, the environment surrounding the iodine at the 3-position is primarily nonpolar despite iodine being relatively electronegative (Figure 4-3). The binding pocket of the 3-position substituent is quite large in order to accommodate the iodine and is composed of the β-carbon of Tyr 207, the α-carbon of Gly 125, two aromatic carbons of Tyr 208, and the π-system of the isoalloxazine ring. There are polar residues and atoms near the pocket, but the nitrogen of Ala 126 and the nitrogen of Trp 165 are greater than 3.5 Å from the iodine and are not oriented at an angle productive for halogen bonding (*113, 114*). The lack of polar contacts to the 3-

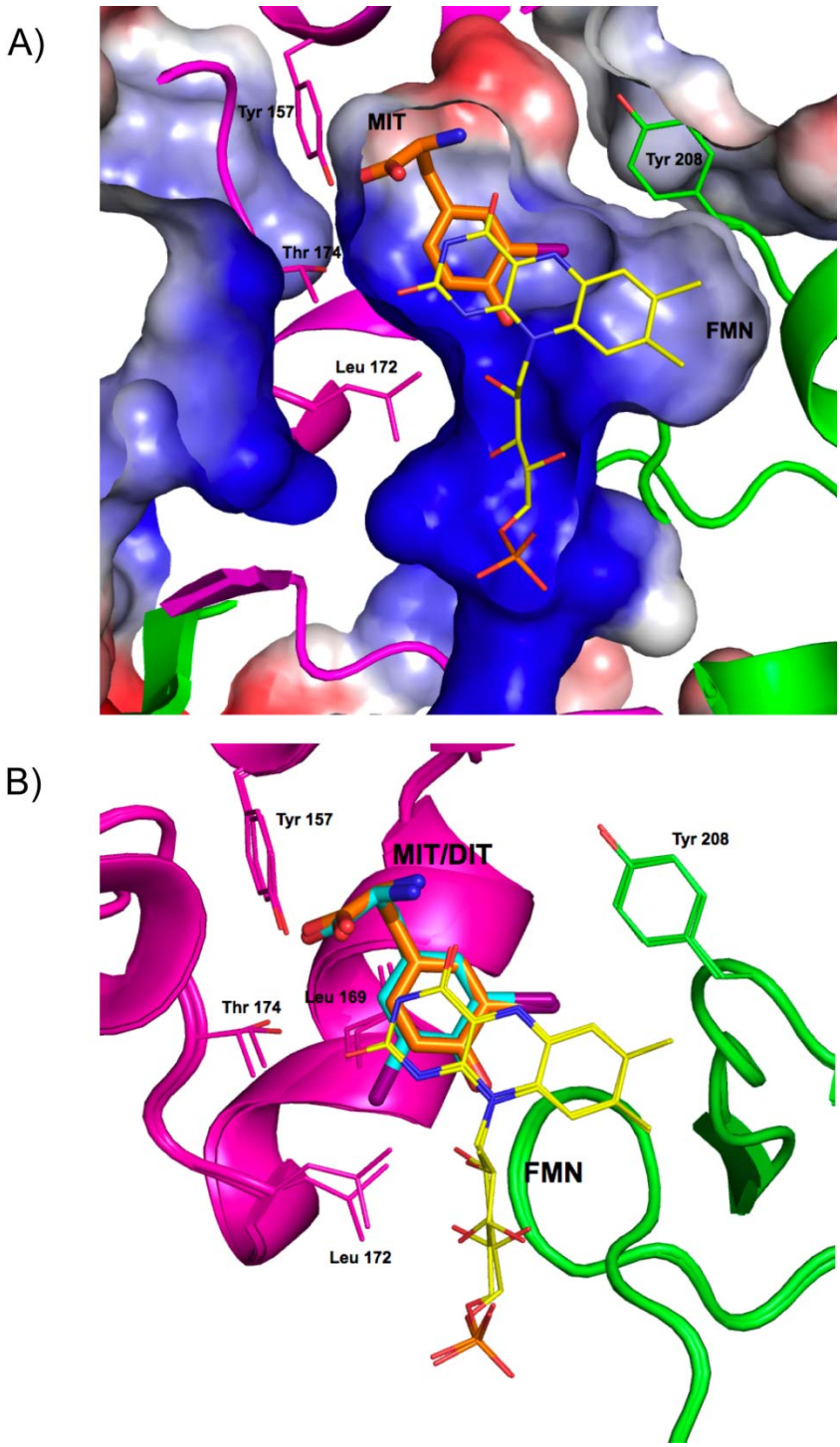

Figure 4-3. Active site binding pockets of IYD co-crystals. A) Surface properties for the IYD•MIT co-crystal active site as calculated using vacuum electrostatics in PyMOL (*110*). Blue indicates positive charge and red indicates negative charge. B) Active site alignment of IYD co-crsytal with MIT in orange and DIT in cyan. Figure is modified from Thomas et al. (*97*).

position substituent, as well as the relatively nonpolar pocket surrounding the 3-position supports the previous Tyr derivative inhibition data which indicates that IYD binds Tyr derivatives with varying electronic and steric characteristics. Although the role of the substituent at the 3-position is unclear, it is important to determine if IYD has substrate specificity associated with the 3-position substituent since it is directly involved in catalysis.

The only substituent requirements for IYD ligand recognition described to date were based upon inhibition of catalysis (*71, 72*). In fact, there is no ligand recognition data for MIT and DIT beyond their respective K_M values. This is because ligand binding has not been directly measured until now. A fluorescence quenching assay is reported here for investigating ligand specificity (*115*). The assay utilizes the intrinsic fluorescence of oxidized FMN and the quenching observed upon ligand binding. Since no reductant is present, reversible binding of MIT and DIT to IYD can be measured. This assay allowed the ligand requirements for substituents at the 3-position to be probed with a number of Tyr derivatives (Figure 4-4 and Table 4-1).

Additionally, ligands identified by the above fluorescence quenching assay have been probed as substrates for IYD catalysis. Previously, IYD activity assays were limited to the standard assay which detects dehalogenation via release of $^{125}I^-$. An anaerobic assay was developed to monitor single turnover of IYD by spectrophotometrically observing reduction of the protein's FMN by dithionite and subsequent discharge of those electrons from FMN_{red} to substrate (*115*). This assay alleviates the limitation of substrate ^{125}I radiolabeling, allowing compounds to be directly assayed in order to identify new IYD substrates. This assay has now

expanded the list of IYD substrates to include 3-bromo, and 3-chlorotyrosine (MBT and MCT, respectively).

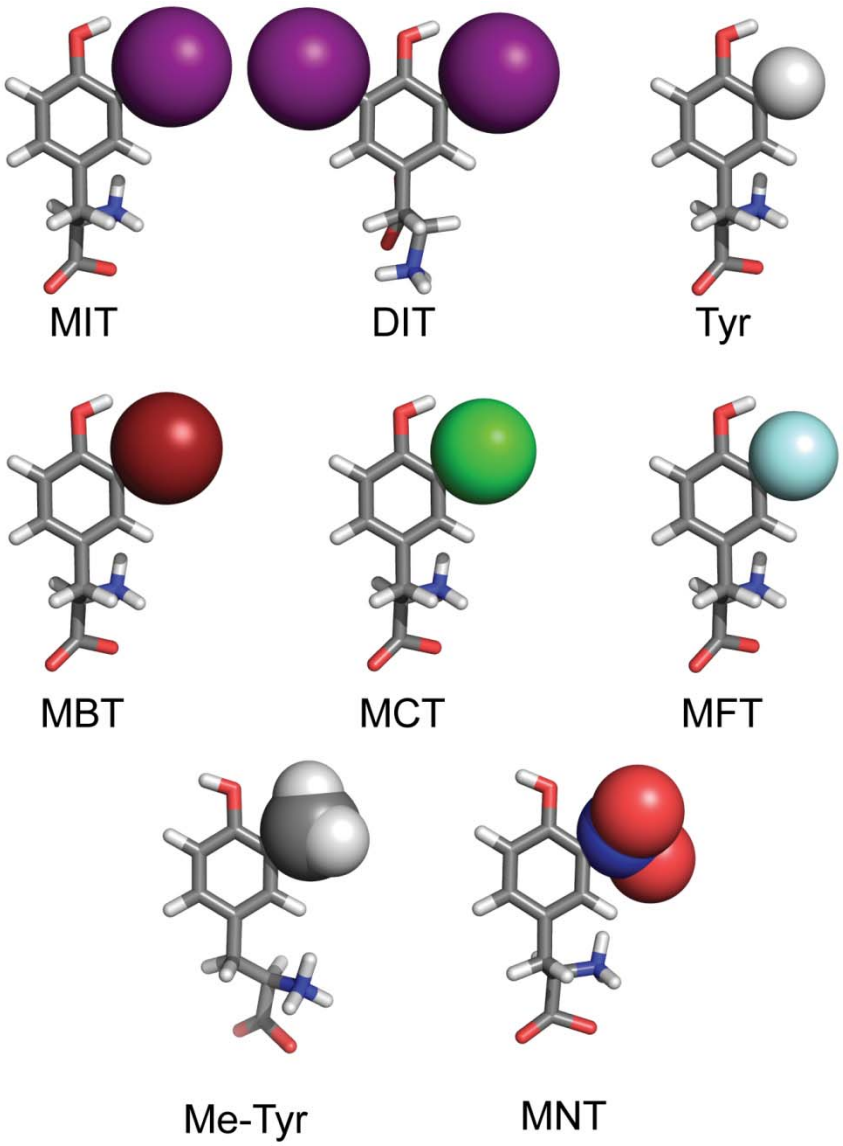

Figure 4-4. 3-Dimensional model of Tyr derivatives. Structures were generated in PyMOL (*110*) from coordinates of Tyr derivatives from Chem 3D 10.0. The Tyr derivative coordinates were energy minimums as determined by MM2 force feild calculations by Chem 3D 10.0. The spheres represents the Van der Waals radius of atoms.

4.2 Experimental Procedures

Materials. Methyl tyrosine (Me-Tyr) was obtained from Dr. Jessica Friedman (University of Maryland) and 3-(N-ethyl-2-pyridon-5-yl)alanine was obtained from Dr. Munetaka Kunishima (University of Maryland). All other reagents were obtained at the highest grade available and used without further purification.

General methods. IYD(ΔTM)His_6 was expressed and isolated from Sf9 cells according the method described in Chapter 3 (*97*). Protein concentration was determined using an ε_{280} of 57,600 M^{-1} cm^{-1} while an ε_{450} 12,500 M^{-1} cm^{-1} (*101*) was used to determine FMN concentration. IYD(ΔTM)His_6 isolated from Sf9 cells contained 2 bound FMN molecules per enzyme dimer. UV measurements were made with a Hewlett-Packard 8453 spectrophotometer (Palo Alto, CA) while fluorescence measurements were made with a Hitachi F-4500 fluorescence spectrophotometer (Tokyo, Japan). Analytical HPLC was performed on a JASCO PU-908/MD1510 diode array instrument (Tokyo, Japan).

Equilibrium binding measurements. Ligand binding assays were performed by monitoring IYD solutions (1.5 μM protein, 100 mM potassium phosphate, pH 7.4) for a change in FMN fluorescence using an excitation wavelength of 450 nm and an emission wavelength of 527 nm (25 °C with stirring). The enzyme solution was equilibrated 30 min prior to fluorescence analysis. Binding of Tyr derivatives was monitored over a range of 4 log units centered at the concentration which yields 50 % quenching of fluorescence (0.015 to 415 μM depending on the ligand). At least three individual measurements were performed for each ligand.

Fluorescence intensities were corrected for minimal dilution resulting from ligand addition and then normalized by dividing the observed fluorescence by the initial fluorescence (F_0) and plotted against ligand concentration [S]. Dissociation constants (K_D) were calculated according to literature and derive from best fit to Equation 4-1 (Tyr and Me-Tyr) and to Equation 4-2 (MIT, DIT, MBT, MCT, 3-fluoro and 3-nitrotyrosine (MFT and MNT, respectively)) (*61*) as calculated by Origin 7.0. Tyr and Me-Tyr were fit to Equation 4-1 because their calculated K_D was 5 fold greater than enzyme concentration used in the assay. The remaining Tyr derivatives were fit to the Equation 4-2, which is a quadratic binding equation that accounts for enzyme concentration. Fitting to this equation was required because the calculated K_D values for these Tyr derivatives were less than 5 times the enzyme concentration used in the assay. Fitting data to this equation, however, is associated with an increased error in the calculated K_D values because of the tight binding curves.

Equation 4-1.

$$F = F_0 + \Delta F[S]_0/([S]_0 + K_D)$$

Equation 4-2.

$$F = F_0 + \Delta F \times \left(\frac{(K_D + [E]_0 + [S]_0) - \sqrt{(K_D + [E]_0 + [S]_0)^2 - 4[E]_0[S]_0}}{2[E]_0} \right)$$

Single turnover of IYD under anaerobic conditions. The procedures for reduction and discharge of electrons from the FMN cofactor of IYD was adapted from Goswami and Rosenberg (*32*). IYD solutions (36 μM protein unless otherwise noted, 100 mM potassium phosphate, pH 7.4) made anaerobic by purging the head space of a sealed air tight cuvette using ultra-pure nitrogen at 4 °C for 6 hrs with stirring. The solution was purged an additional 1 hr at 25 °C with stirring, and these conditions were maintained throughout the rest of the assay. Reduction of IYD's FMN cofactor was performed by addition of anaerobic dithionite solution (~10 mM) until the A_{450} failed to decrease and the A_{317} (isobestic point of reduced and oxidized IYD) increased. A minimum of excess dithionite (5 %) was added to ensure complete reduction of the cofactor. Anaerobic solutions of Tyr derivatives (10 mM) were added to the reduced IYD solution in 0.333 molar equivalent additions. The assay mix was monitored spectrophotometrically for 15 min after each addition. A total of 2.0 molar equivalents of the respective Tyr derivative was added before the assay was stopped.

HPLC analysis of products formed by anaerobic single turnover of IYD. IYD was removed from anaerobic single turnover samples using a 10 kDa centrifugal membrane filter. These solutions were then run on a reverse phase C-18 analytical column (Varian, Microsorb-MV 300, 5 μm particle size, 250 mm, 4.6 mm) with a flow rate of 1 mL min^{-1} using the following method: 5 min 0 % B, 30 min linear gradient to 83 % B, and 10 min wash with 100 % B (Buffer A-10 mM TEAA pH 5.5/Buffer B-methanol with 10 mM TEAA pH 5.5). Aliquots (100 μL) of anaerobic single turnover samples obtained following IYD removal were analyzed 3 individual

times by HPLC. Solutions of Tyr standards (36 μM) were analyzed under identical conditions. The integrated signal of standards at 280 nm was used in order to quantitate the amount of Tyr product generated with each derivative.

4.3 Results and Discussion

Tyrosine substituent requirements for ligand binding to IYD. The binding of MIT and DIT substrates as well as Tyr was initially investigated using the newly developed fluorescence quenching assay. MIT and DIT both bind tightly to IYD, but there is an approximate 5 fold increase in K_D when DIT binding is compared to MIT (Table 4-1) (*115*). Clearly, the 5-position of Tyr affects binding of substrate, especially the addition of a large bulky group like iodine. This significant increase in K_D for DIT binding is likely because IYD must accommodate the bulky iodine, although this occurs with only slight perturbations of Leu 169, Thr 174 and Leu 172 in the active site according to the structure of IYD (*97*). This indicates that a substituent at the 5-position does not significantly impede ligand recognition.

The difference in binding between MIT and DIT is minor when MIT binding is compared Tyr, as the K_D of Tyr increases several orders of magnitude in comparison to MIT. This disparity in binding would likely be even greater except a full binding curve for Tyr could not be obtained due to its poor solubility (*115*). Thus, the reported K_D of Tyr is only a lower estimate. IYD's weak affinity for Tyr versus MIT suggests that the presence of the iodine substituent is important for ligand recognition. This is not surprising since Tyr is the product of MIT catalysis and tight

Table 4-1. Tyrosine derivative characteristics and IYD affinity.

Tyr Derivative	Molar Volume of Substituent[a] ($Å^3$)	Electronegativity of free atom (Pauling units)	pK_a of aryl-X phenol[c]	K_D[d] (μM)
Tyr	7.25	2.2	10.1	>1,400
DIT	41.6[b]	2.7	6.35	0.47 ± 0.06
MIT	41.6[b]	2.7	8.53	0.090 ± 0.40
MBT	34.3	3.0	8.35	0.11 ± 0.03
MCT	27.1	3.7	8.48	0.15 ± 0.02
MFT	13.2	4.0	8.86	1.3 ± 0.2
MNT			7.2	0.12 ± 0.05
Me-Tyr	32.3		10.4	>1,500

[a]See reference (*116*).
[b]Calculated from Van der Waals radius (*71*).
[c]See reference (*117*).
[d] Dissociation constants were calculated by line of best fit to data (See Appendix E). Uncertainties derive from the standard deviation from fitting three or more independent measurements. The large uncertainty is associated with tight ligand binding which requires data be fit with a quadratic binding equation, Equation 4-2.

binding would be catalytically unproductive. The only difference between the two compounds is the presence of the bulky iodide substituent of MIT. Addition of 1.5 mM free iodide which displays minor fluorescence quenching does not strengthen Tyr binding (Appendix E). This implies that certain steric or electronic characteristics of substituent at the 3-position may be necessary for tight binding to IYD.

Consequently, the role of the substituent at the 3-position of Tyr was investigated using the Tyr derivatives MBT, MCT, MFT, and MNT. These derivatives have a substituent at the 3-position with steric and electronic features that

range in size from 7.25 to 41.6 $Å^3$ and the halogen substituents range in electronics from 2.7 to 4.0 Pauling units (free halogen values) (Table 4-1). Of note, the steric requirements investigated here are only for substituents of similar or smaller size than the iodine. Despite their differences, MIT, MBT, MCT, and MNT all display similar binding to IYD while the K_D of MFT is an order of magnitude greater (Table 4-1) (*115*). This decreased affinity for MFT could not be directly correlated with fluorine's decreased sterics compared to the other halotyrosines or its altered electronics. Therefore, Me-Tyr was analyzed for binding since the methyl substituent of Me-Tyr is greater in size than the fluoro substituent of MFT, but lacks the electronic characteristics of halogens. Me-Tyr binding to IYD was poor, similar to Tyr (*115*). This result indicates that the sterics of the 3-position substituent do not govern ligand recognition, and instead, substituent electronics play a substantial role.

Interestingly, the phenolic pK_a's of the Tyr derivatives are all similar except for Tyr and Me-Tyr which are approximately 2 units higher. Tyr derivatives with lower pK_as were previously reported to display greater inhibition of IYD activity, resulting in the hypothesis by Green that Tyr derivatives with lower pK_a's bind more tightly to IYD (*72*). This hypothesis is consistent with Tyr and Me-Tyr having lower affinity than the other derivatives since their pK_as are much higher. The tight binding of MNT also supports this hypothesis because its pK_a is one unit below the halotyrosine derivative pK_as. This is significant because despite the bulky and highly charged nitro substituent of MNT, it still displays binding within experimental error of MIT. Therefore, a marked increase in the pK_a from 8 may cause a ligand to lose affinity since deprotonation is less favorable. Although the pK_a of Tyr derivatives

appear to influence ligand recognition, the importance of the pK_a in recognition is unclear.

The structure of IYD shows that the substrate phenol makes contacts with the protein and with FMN. These contacts could influence binding if they stabilize the deprotonated form of substrate. Similar polar contacts to substrate in the acylCoA dehydrogenases appear to stabilize the enolate form of substrates (*118, 119*), and thus, precedence supports the involvement of the polar contacts made by the phenol of Tyr derivatives for stabilizing the deprotonated form of substrate.

Ligand recognition by IYD appears to have distinct substituent requirements. First, the pK_a of ligands appears to influence binding as Tyr and Me-Tyr, which have the highest pK_as, bind poorly. The relative pK_a of Tyr derivatives is determined by the substituent at the 3-position. Thus, the substituent must have the proper electronic characteristics for binding since steric requirements appear superfluous. This was evidenced by Me-Tyr which has a substituent of greater size than MFT but binds orders of magnitude worse than MFT.

Zwitterion requirement for IYD substrate recognition. NADPH has been proposed not to be a substrate for IYD (*36*) although it is a common substrate of the NOX/FRase structural superfamily (*41-44*). This hypothesis is based on experiments in which solubilization of IYD removes NADPH–responsive activity yet dithionite activity remains (*35*) and the dithionite activity observed in CHO cells which lack NADPH activity (*38*). This has not been proven until now. The fluorescence quenching assay used to measure ligand binding to IYD was used to determine that NADPH does not function as a substrate for IYD. This conclusion results from the

lack of observed fluorescence quenching by NADPH over a range of concentrations (0.013-124 μM) since reduction of flavins results in loss of fluorescence (Appendix E). NADPH was not expected to quench fluorescence due to the likely involvement of a yet unidentified reductase proposed to mediate reduction of IYD by NADPH (*36*). Further, the absence of fluorescence quenching by NADPH likely results from the sterics of IYD's active site as IYD lacks the vestigial capacity to accommodate the full structure of NADPH beyond its nicotinic portion (*97*).

Nicotinic acid was then assayed since it lacks the additional functionalities of NADPH and has been shown to stack above the FMN in the co-crystal of another NOX/FRase protein (*44*). Nicotinic acid also failed to quench fluorescence (0.03-87 μM) (Appendix E). The lack of fluorescence quenching by nicotinic acid likely results from the absence of zwitterion and phenolic contacts which position ligands in the IYD active site. Interestingly, 2-iodophenol binds (K_D > 600 μM (Appendix E)) almost equivalently to Tyr and not MIT. These results are consistent with previous reports (*71, 72, 97*) which indicate that IYD has distinct substrate specificity with regard to the zwitterion functionality.

Substrate requirements for IYD catalysis. For IYD catalysis to occur, the FMN cofactor of IYD must first be reduced by electrons from its *in vivo* reductant NADPH (*23*) or its *in vitro* reductant dithionite (*36*). The FMN_{red} is then utilized to dehalogenate MIT and DIT (*31, 36*) by transferring those electrons to substrate. An anaerobic assay was developed to spectrophotometrically monitor both the reduction of FMN by dithionite and the discharge of those electrons to substrate. The

mechanistic implications of the assay will be discussed in greater detail in the following chapter.

The assay was first utilized to monitor single turnover catalysis with MIT, and as expected, addition of MIT caused FMN_{red} to reoxidize (Table 4-2, Figure 4-5, Appendix F). HPLC analysis of the resulting turnover confirmed that approximately 1 molar equivalent of Tyr is generated per mol of oxidation of FMN_{red} (Appendix G). The process of reducing the FMN cofactor and discharging those electrons is catalytic as the process was qualitatively repeated with an additional turnover. Ultimately, discharge of the reduced cofactor consistently yields an absorption spectrum with peaks similar to that of oxidized IYD except a new broad peak from 550 to 650 nm is also evident (*115*). The spectrum indicates the presence of two distinct FMN species and will also be discussed further in Chapter 5.

Table 4-2. Characteristics of 3-tyrosine derivatives and their turnover by IYD.

Sample	Bond Energy[a]		Discharge of Reduced IYD	Equivalents of[c] Tyr Product
	Phenyl-X (kcal/mol)	$H_2C{=}CHCH_2$-X (kcal/mol)		
MIT	65	41	Yes	0.96 ± 0.02
MBT	81	54	Yes	0.92 ± 0.01
MCT	96	68	Yes	0.94 ± 0.02
MFT	126	129[b]	No	0.02 ± 0.03
Tyr	111	86	No	

[a]Bond energies were obtained from from McMillan and Golden (*75*).
[b]Estimated using bond energy from McMillan and Golden (*75*) and Zavitsas et al. (*120*).
[c]Tyr product from anaerobic assays was quantified by HPLC for each respective Tyr derivative from three individual HPLC analyses per sample (See Appendix G for representative chromatograms).

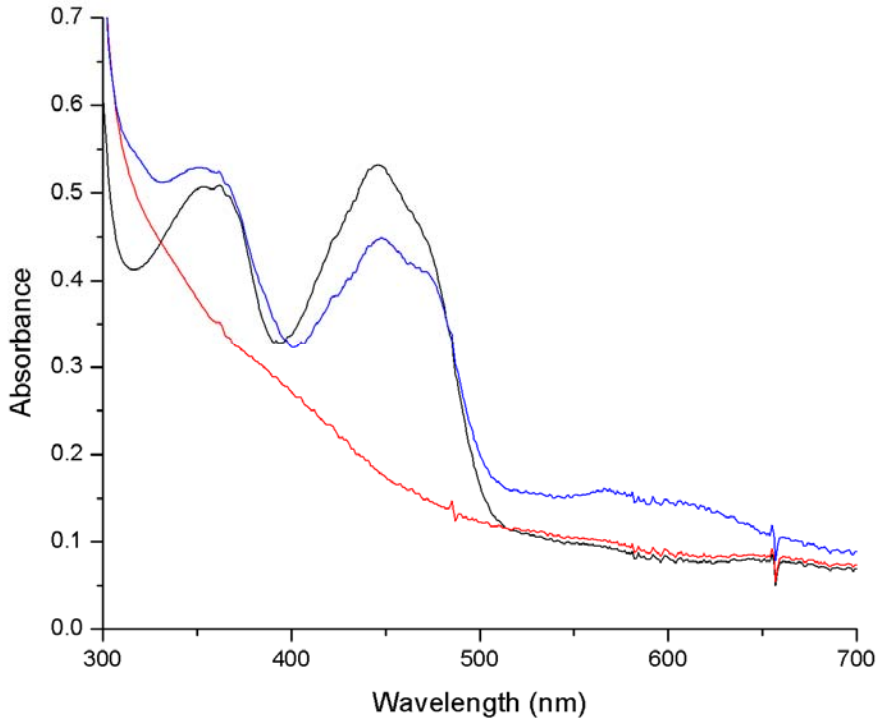

Figure 4-5. Absorbance spectra of the IYD anaerobic assay for reduction and discharge of electrons from its FMN cofactor. The oxidized FMN cofactor of IYD (—) was fully reduced by additions of dithionite (—) (See Appendix G for reduction titration). Electrons were discharged from the reduced FMN cofactor upon addition of 2 molar equivalents of I-Tyr substrate (—) (See Appendix F for oxidation titration). Figure was modified from McTamney et al. (*115*).

Since MBT, MCT, and MFT were all identified to be ligands for IYD, they were also tested as substrates for IYD catalysis. Both MBT and MCT discharged the reduced FMN cofactor alike to MIT (Table 4-2 and Figure 4-6). Both MBT and MCT were also dehalogenated by IYD with approximately 1 molar equivalent of Tyr product generated from each respective substrate. In contrast, MFT failed to discharge FMN_{red} similar to Tyr or be turned over to Tyr product.

MBT had previously been reported to be both a substrate (*112*) and inhibitor of IYD (*71*). In the report indicating MBT was a substrate for IYD, debromination of radiolabeled MBT was observed with thyroid homogenates (*112*). On the other hand, MBT was reported to be a competitive inhibitor of IYD catalysis (*71*). MCT was also previously reported to act as a reversible inhibitor of IYD (*71, 111*). The reason for these discrepancies is unclear, but this report shows that both MBT and MCT act as substrates for IYD.

IYD's ability to dehalogenate MIT, MBT, but not MFT indicates that IYD does have substrate specificity for 3-position substituents. In order to be

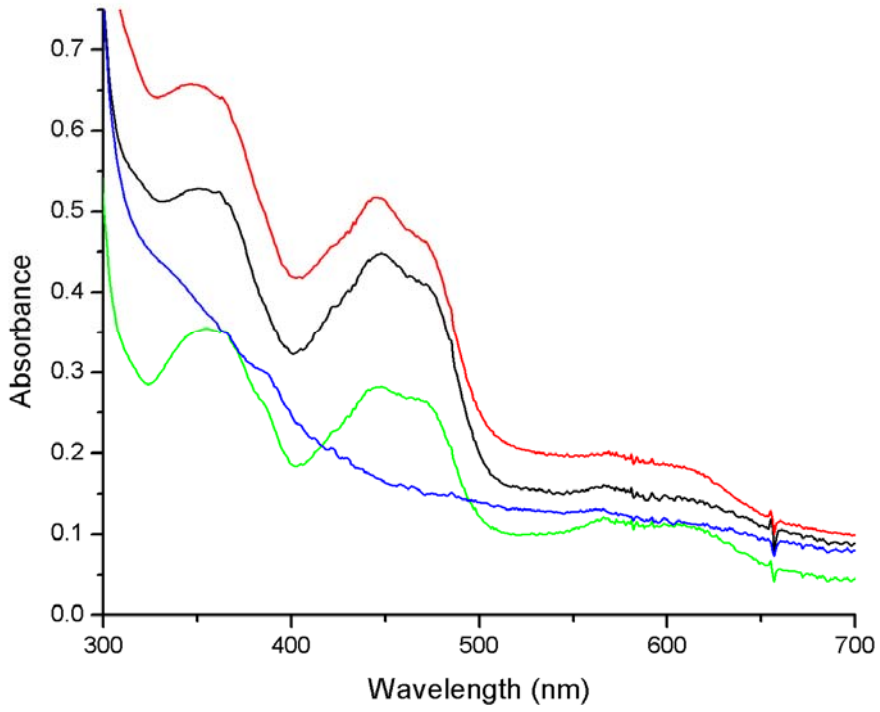

Figure 4-6. FMN absorbance spectra following oxidation of reduced FMN by addition of tyrosine derivatives. The fully reduced FMN cofactor of IYD was monitored for oxidation following addition of 2.0 molar equivalents of either **MIT**, **MBT**, **MCT**, or **MFT**. Figure was modified from McTamney et al. (*115*).

dehalogenated, these substituents must first be capable of being reductively cleaved and second be good leaving groups. This leaving group ability is evident in the initial discharge of electrons from FMN_{red} following substrate addition. Iodide, bromide, and chloride are all good leaving groups and MIT, MBT, and MCT all displayed similar rates in discharge (0.70, 0.33, 0.18 sec^{-1}, respectively) (Figure 4-7). Fluoride on the other hand, is not as good of a leaving group as the other halogens and FMN_{red} was not discharged by MFT. Although IYD does not possess enough reducing

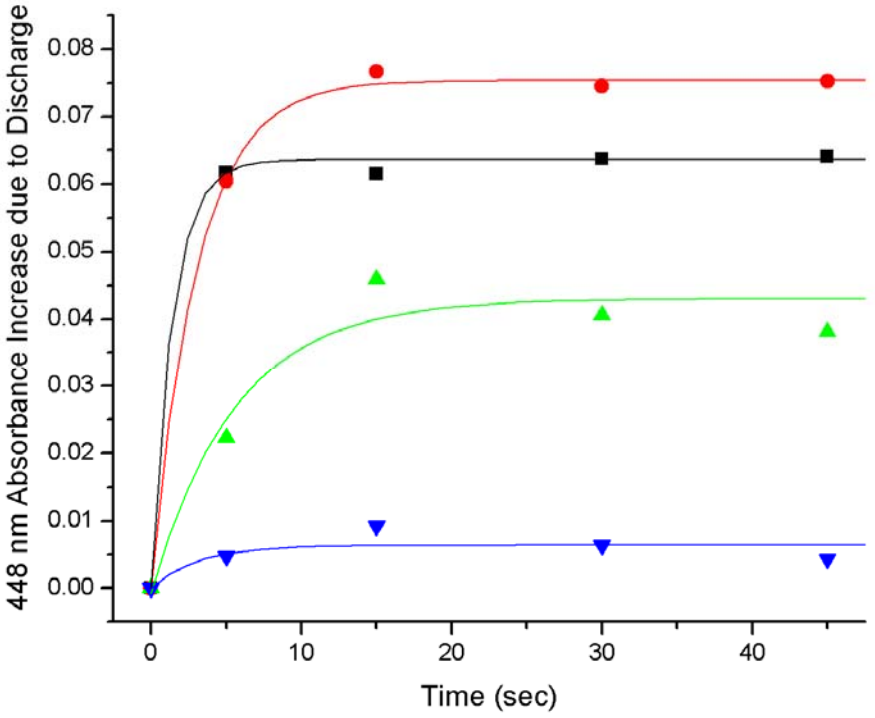

Figure 4-6. Absorbance measurements of the initial oxidation of the reduced FMN of IYD by addition of tyrosine derivatives. Time points for the initial oxidation of the reduced FMN were monitored at 448 nm under anaerobic conditions. Measurements were made following the initial addition of 0.333 molar equivalents of Tyr derivatives **MIT**, **MBT**, **MCT**, and **MFT**. The best fit (line) of data from a single trial with each Tyr derivative is to a first order process using Origin 8.0. Lines are colored accordingly to serve a guide for oxidation of the reduced FMN by the respective Tyr derivatives. Figure from McTamney et al. (*115*).

potential to facilitate dehalogenation of the C-F bond of MFT, clearly IYD has enough dehalogenating power to reductively dehalogenate both MBT and MCT.

Conclusion. This report definitively shows MBT and MCT serve as substrates for IYD. Biologically, MBT, MCT, and MNT serve as biomarkers for inflammatory diseases like asthma (*121*), rheumatoid arthritis (*122*), cystic fibrosis (*123*), and even arteriosclerosis (*124*). These Tyr derivatives are released upon proteolysis from proteins whose Tyr residues have been modified oxidatively. Upregulation of eosinophil peroxidase causes increased levels of hypobromous acid which ultimately leads to the generation of MBT (*125, 126*). Upregulation of myeloperoxidase causes increased hypochlorous acid and reactive nitrogen species production which results in the generation of MCT and MNT, respectively (*124, 127, 128*). These Tyr derivatives are liberated upon proteolysis and metabolized. However, not all of the enzymes involved in this metabolism have been identified (Figure 4-8). MNT is metabolized to 3-nitro-4-hydroxyphenylacetic acid and then excreted in urine (*129*). This contrasts MBT and MCT which are dehalogenated to Tyr before being metabolized to hydroxyphenlyacetic acid and excreted (*111*). The enzyme responsible for dehalogenating MBT and MCT is unknown. IYD localized to the thyroid is unlikely to be involved in MBT and MCT dehalogenation, but IYD's presence in the liver and the kidney would provide the means for such an involvement (*27, 30, 39, 111, 130*). Thus, further investigation into IYD's possible physiological role in metabolizing these derivatives is warranted.

Because IYD is able to dehalogenate both MBT and MCT in addition to its native iodinated substrates, IYD provides a valuable tool for future bioremediation.

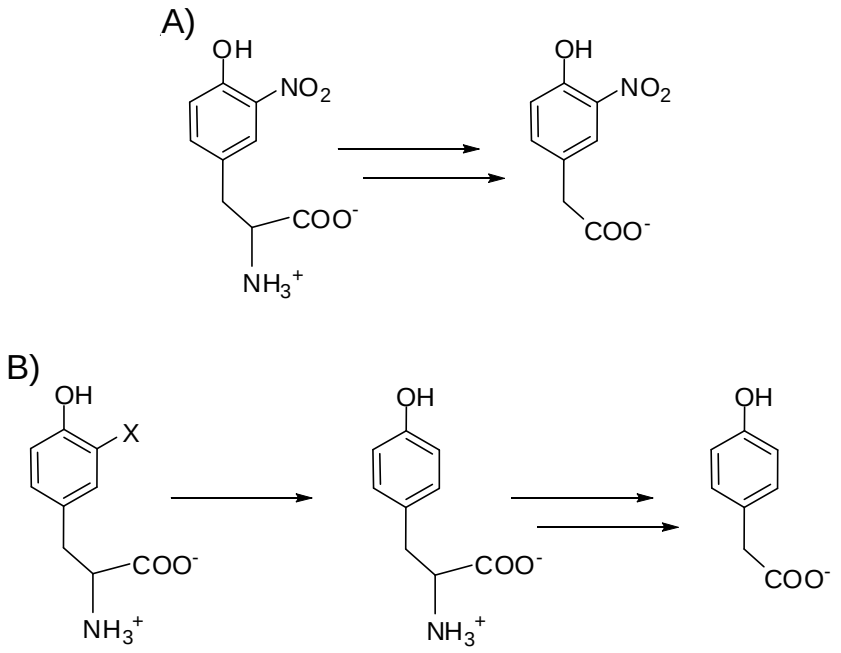

Figure 4-7. Metabolism of A) MNT and B) MBT and MCT. MBT and MCT are first dehalogenated by an unknown enzyme before being metabolized to 4-hydroxyphenylacetic acid derivitives similarly to MNT.

Halogenated compounds and solvents are valuable industrial components, but they persist in the environment long after their intended use as the strength of the C-X bond confers much of the natural stability of halocarbons. Although most microorganisms lack the enzymatic capacity to metabolize these recalcitrant pollutants, numerous organisms have evolved under selective pressure to degrade these halocarbons. This has resulted in enzymatic bioremediation of halocarbons receiving significant focus (*131-135*) as compounds like polychlorinated biphenyls continue to pose an environmental problem today (*136*) despite decades old manufacturing bans. Because IYD degrades C-Cl, C-Br, and C-I bonds, it presents a future bio-inspired method of degrading halogenated pollutants providing the dehalogenating power of IYD can be harnessed during protein engineering.

Chapter 5: Investigation of a 1 versus 2 electron mechanism of IYD catalysis

5.1 Introduction

The original mechanism proposed for IYD catalysis relied on a nucleophilic attack of an active site cysteine on the substrate's iodine (*67*). Despite the mechanistic precedence illustrated by TCHQ dehalogenase (*60*) and ID (Chapter 1) (*63, 64*), the Cys to Ala mutation variant enzymes presented in Chapter 2 maintained activity and proved this mechanism incorrect (*38*). The lack of Cys involvement was confirmed by the structure of IYD which located the Cys residues far from the active site of IYD (Figure 5-1) (*97*). Therefore, other 1 and 2 electron transfer mechanisms presented in Chapter 2 must be considered for IYD catalysis since IYD definitively breaks from mechanistic precedence. Although FMN supports both 1 and 2 electron processes, 5-deazaflavins are only capable of catalyzing 2 electron processes (*87, 88*). Consequently, reconstituting IYD with 5-deazaFMN can distinguish between possible 1 or 2 electron processes for IYD catalysis.

A 2 electron mechanism similar to the Cys-based proposed mechanism (*67*) could still be possible (Figure 2-6). This mechanism would require another residue replace the role of Cys as the nucleophile in the redox reaction. His and Lys are the most likely residues to act as the catalytic nucleophile in this mechanism since amines have been shown in the literature to promote reductive dehalogenation in a model

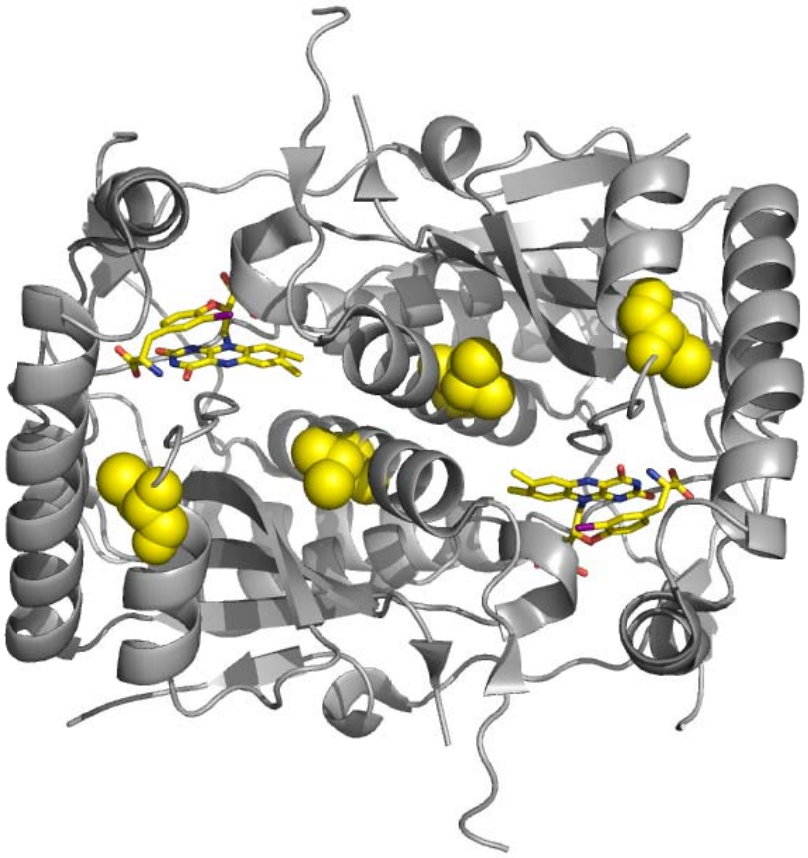

Figure 5-1. IYD cysteines are not located near the IYD active site. Cysteines are depicted as yellow spheres.

system (*81*). Further, an intermediate expected from the involvement of Lys in such a mechanism, Lys-εNH-Cl, has recently been proposed to occur during flavin dependent halogenations (*82*). The structure of IYD, however, shows that no His or Lys residues are located in the IYD active site (*97*). In fact, no obvious nucleophilic residues appear in the active site within the binding pocket surrounding the iodine. This region is composed only of the hydrocarbon regions of residues Tyr 207, Gly 125, and Tyr 208. The only polar atoms in proximity to this site are the nitrogens of Ala 126 and Trp 165 but are at a distance greater than 3.5 Å away.

Still, other 2 electron processes should also be considered. These mechanisms presented in Chapter 2 involve direct hydride transfer from FMN_{red} to substrate (Figure 2-7). The first of these possible mechanisms involves an S_NAr hydride reaction at the substrate's iodine bearing carbon. This mechanism is highly unlikely in the absence of electron withdrawing groups (*137*), which both MIT and DIT lack. Instead, an alternate 2 electron mechanism involving tautomerization of substrate prior to hydride transfer is more likely (Figure 5-2). This hydride transfer to an sp^3 hybridized carbon is similar to an S_N2 mechanism, and dehalogenation would be expected. Formation of the substrate tautomer is also consistent with the high affinity IYD has for *N*-pyridonal derivatives that mimic substrate tautomerization (*67*).

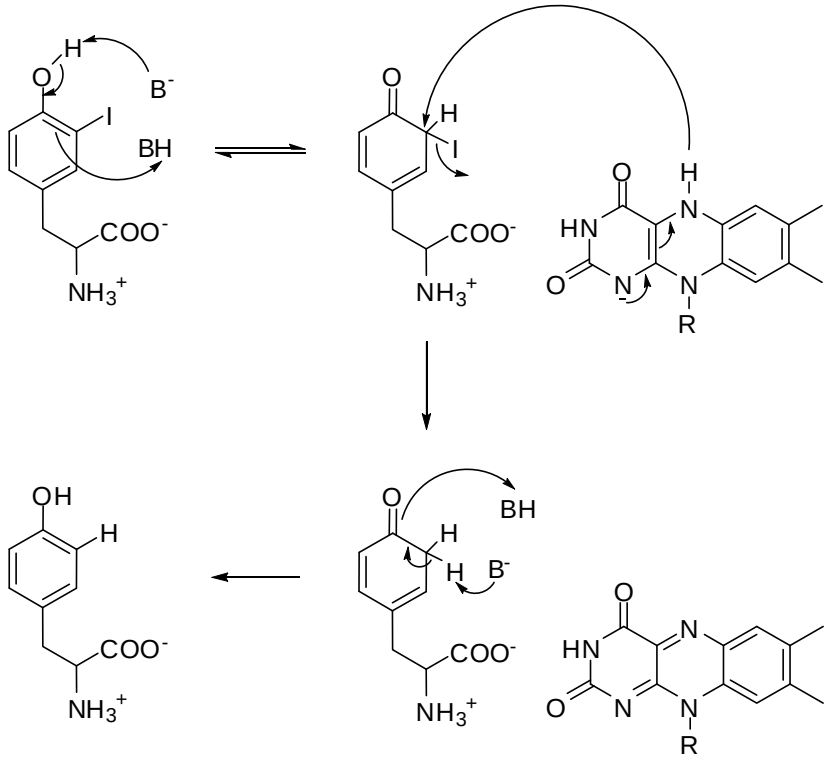

Figure 5-2. Possible 2 electron mechanism for IYD catalysis involving hydride transfer.

IYD catalysis via a 1 electron process should similarly be considered since few reductive dehalogenases being suggested to utilize 1 electron mechanisms (*68, 69*). Several IYD mechanisms involving 2 sequential 1 electron transfers to substrate which were presented in Chapter 2 are possible (Figure 2-8). The first plausible 1 electron transfer mechanism involves an $S_{RN}1$ reaction in which a single electron from FMN_{red} is injected into the aromatic system of substrate (Figure 5-3). This could occur by either injection into the aromatic π system of substrate to generate a radical anion intermediate, or by injection of an electron directly at the iodine bearing carbon (Figure 5-4). Both of these electron injections would lead to dehalogenation and generation of an intermediate with a radical in place of iodine. The second addition of an electron by FMN_{semi} and a proton to the radical intermediate would then complete catalysis to Tyr.

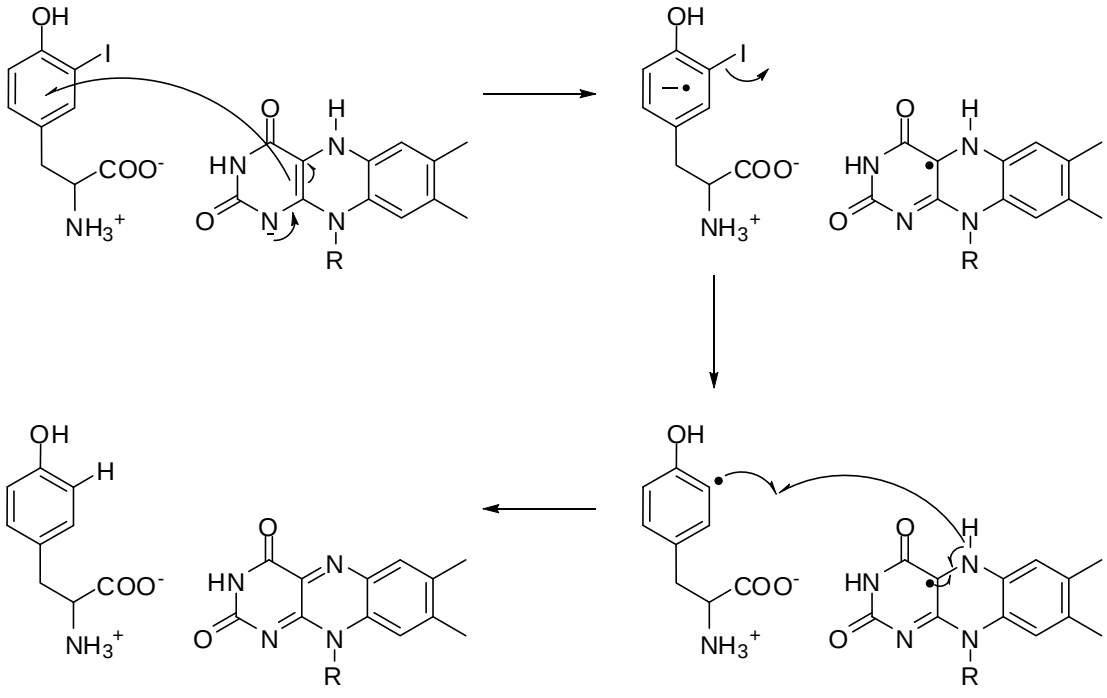

Figure 5-3. Possible $S_{RN}1$ electron mechanism for IYD catalysis involving electron transfer directly to substrate.

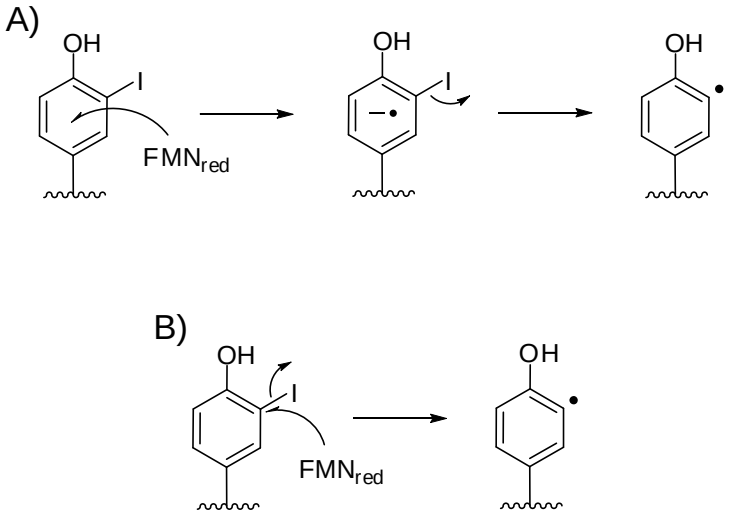

Figure 5-4. IYD aryl 1 electron mechanism could proceed by injection of an electron to the A) aromatic π system or to the B) iodine bearing carbon.

An alternative 1 electron mechanism involving injection of an electron into a substrate tautomer is also possible. This would occur by tautomerization of substrate to the proposed nonaromatic keto intermediate before an electron from FMN_{red} is injected into the system (Figure 5-5). The electron acceptor could be either the carbonyl to form a ketyl radical which labilizes the C-X, allowing for elimination of the halide, or the iodine bearing carbon which causes spontaneous iodide elimination (Figure 5-6). Of note, both possible tautomer mechanisms would yield the same stable tyrosyl radical. Catalysis would then be completed by transfer of a second electron from FMN_{semi} to the tyrosyl radical followed by reprotonation to the enol Tyr product.

IYD mechanisms involving either 1 or 2 processes can be differentiated by incorporating modified flavin analogues into IYD. The unnatural 5-deazaflavins are unable to promote radical transfer since they are unable to stabilize the FMN_{semi}

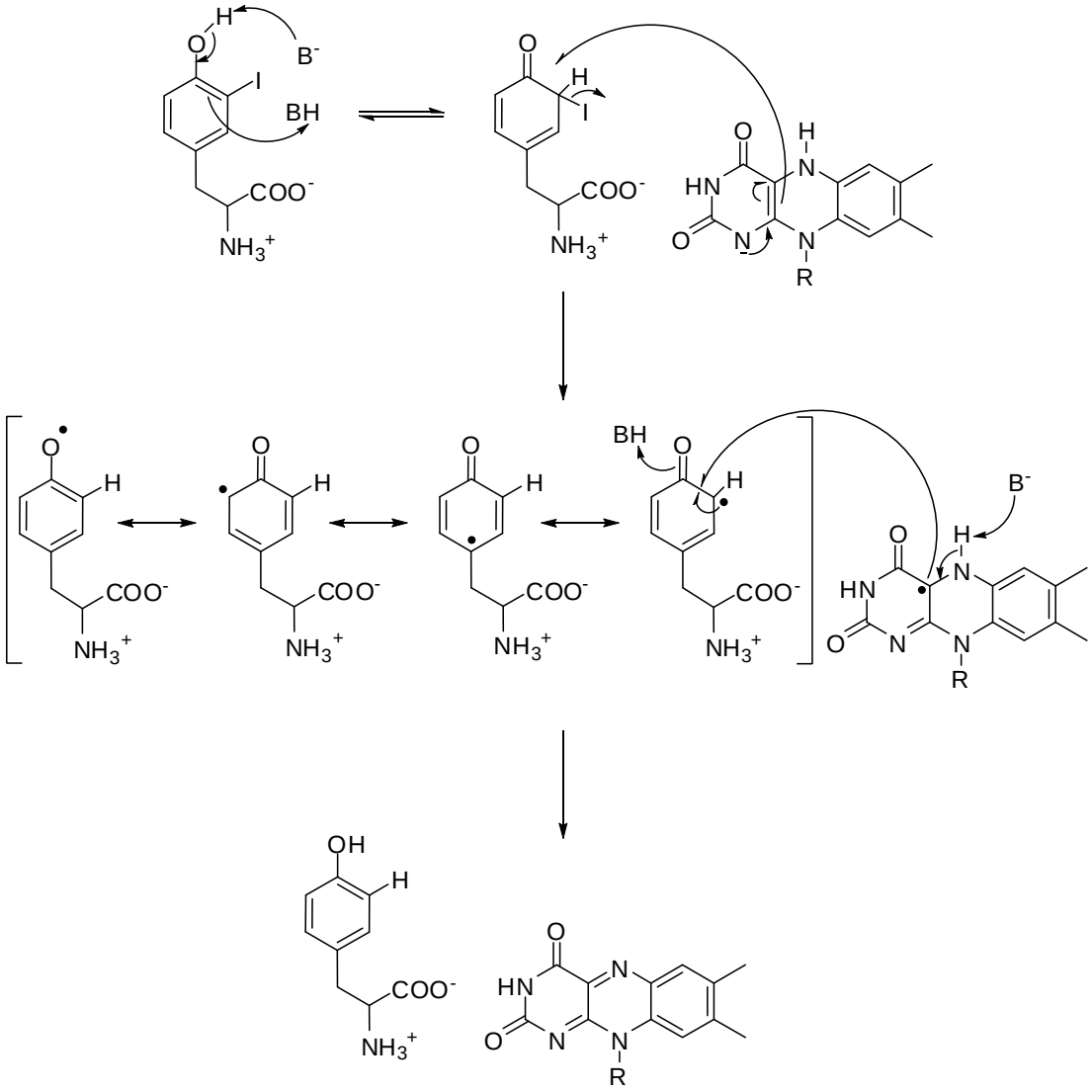

Figure 5-5. Possible 1 electron mechanism for IYD catalysis involving electron transfer directly to tautomerized substrate.

(*87, 88*) but are retain the capability of catalyzing 2 electron transfers. This is because the N5 position of the isoalloxazine is directly involved in stabilizing the FMN_{semi} (*88*). 5-deazaflavins are commonly thought to be catalytically similar to nicotinamides. Therefore, these deazaflavin derivatives have been utilized to differentiate whether an enzyme follows a 1 or 2 electron mechanism (*73, 83-86*). Enzymes which utilize a 1 electron process become inactive when its native flavin is

substituted with 5-deazaflavin, while enzymes which utilize a 2 electron process may retain catalytic activity with 5-deazaflavin.

Thus, the flavin derivative 5-deazaFMN can be used to distinguish between a 1 or 2 electron mechanism for IYD catalysis. Flavoproteins must first have their native flavin cofactor removed to generate apoprotein before 5-deazaflavins can be incorporated into the enzymes. Generally, the apoflavoproteins have been shown to readily recombine with flavin derivatives possessing modified isoalloxazine functionalities (*138-140*). IYD apoenzyme was therefore generated and reconstituted with 5-deazaFMN and a control deazaflavin, 1-deazaFMN, which can participate in both 1 and 2 electron processes (*87*). As described in this chapter, the IYD•5-deazaFMN reconstituted holoenzyme lacked appreciable deiodinase activity while IYD•FMN and IYD•1-deazaFMN reconstituted holoenzymes supported catalysis, indicating that IYD utilizes a 1 electron mechanism.

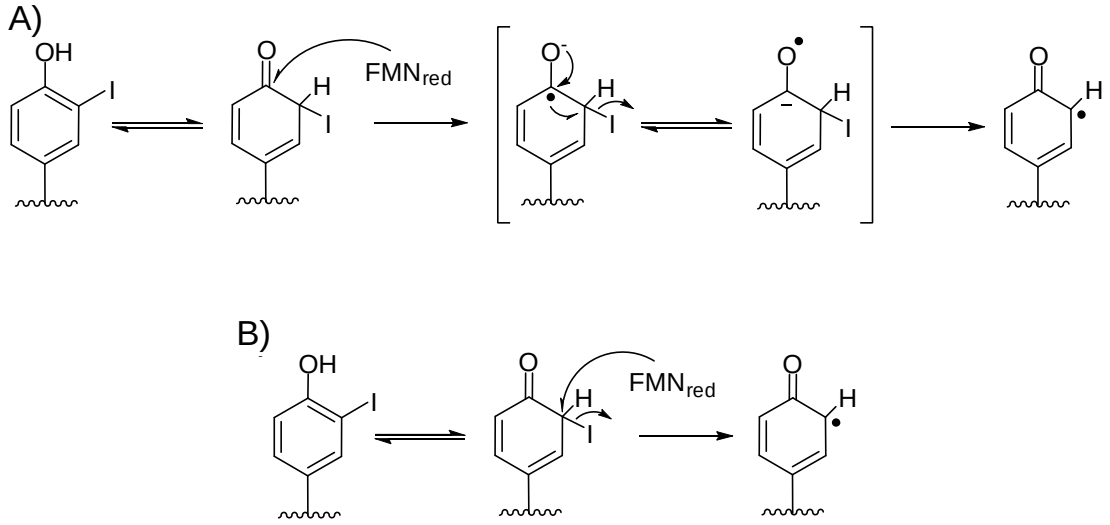

Figure 5-6. IYD tautomer 1 electron mechanism could proceed by injection of an electron to the A) carbonyl or to the B) iodine bearing carbon.

5.2 Experimental Procedures

Materials. 1-DeazaFAD and 5-deazaFAD were gifts from Dr. Dave Ballou and Dr. Bruce Palfey (University of Michigan). All other reagents were obtained at the highest grade available and used without further purification.

General methods. IYD(ΔTM)His_6 was expressed and isolated from Sf9 cells according the method described in Chapter 3 (*97*). The protein concentration of isolated IYD was determined using the ε_{280} of 57,600 M^{-1} cm^{-1} from Chapter 3. This value accounts for the A_{280} contribution of the 2.0 bound FMN cofactors of isolated IYD. This ε_{280} value can only be used for IYD samples containing two bound flavin cofactors. Protein concentration of reconstituted holoenzymes is described below in the next section. UV measurements were made with a Hewlett-Packard 8453 spectrophotometer (Palo Alto, CA) while fluorescence measurements were made with a Hitachi F-4500 fluorescence spectrophotometer (Tokyo, Japan). Analytical HPLC was performed on a JASCO PU-908/MD1510 diode array instrument (Tokyo, Japan).

Conversion of FAD analogues to FMN analogues. FMN, 1-deazaFMN and 5-deazaFMN were obtained from conversion of FAD, 1-deazaFAD, and 5-deazaFAD, respectively, using *Naja naja* snake venom (Sigma-Aldrich, St. Louis, MO) according to Chakraborty and Massey but on a 50 fold smaller scale (*106*). This phosphodiesterase reaction was run overnight at 25 ºC and monitored for completion by HPLC analysis using an isocratic elution containing 20 % methanol in 10 mM TEAA, pH 6.0. Upon full conversion to the respective FMN analogues, the reaction solution was boiled for 1-2 min to precipitate the venom and then centrifuged at

16,000 x g for 2 min. The supernatants containing the respective FMN derivatives were removed for reconstitution of IYD apoenzyme.

Generation of IYD apoenzyme. IYD(ΔTM)His_6 apoenzyme was generated using a procedure inspired by Rosenberg and Goswami (*31*). Purified IYD (1 mg) was applied to a 1 mL HisTrap HP column chelated with Ni^{2+} using an AKTA FPLC (GE Healthcare Bio-Sciences Corp.) and washed with 5 column volumes of wash buffer similar to the procedure described in Chapter 3. The FMN cofactor of isolated IYD(ΔTM)His_6 was then removed with wash buffer supplemented with guadinium hydrochloride (GdnHCl). This was performed with step washes increasing from 0.0, 0.6, 1.05, and finally 1.5 M GdnHCl followed by decreasing GdnHCl step washes from 1.5, 1.05, 0.6, and finally 0.0 M. The volume of each step wash was 3 column volumes except the 1.5 M GdnHCl wash which was 6 column volumes. The flow rate for the procedure was 1 mL/min, although the flow rate was altered to 0.05 mL/min for 1 min following the first and third column volume of the 1.5 M GdnHCl wash to remove the flavin cofactor. Upon completion of the step washes, IYD(ΔTM)His_6 apoenzyme was eluted from the column with wash buffer containing 300 mM imidazole. IYD(ΔTM)His_6 apoenzyme was analyzed by UV at 280 nm and 450 nm to determine the relative amount of generated apoenzyme and retained holoenzyme.

Reconstitution of IYD apoenzyme with flavin derivatives. IYD(ΔTM)His_6 apoenzyme was reconstituted with FMN, 1-deazaFMN, or 5-deazaFMN based on a procedure by Whitfield and Mayhew (*141*). These FMN analogues were obtained from their respective FAD derivatives following treatment with *Naja naja* snake

venom as described above. The respective FMN supernatants following the FAD digests were added directly to eluted IYD(ΔTM)His_6 apoenzyme (approximately 10 μM) for reconstitution by simply incubating with 2 eq. of the respective FMN derivatives at 4 ºC for 2 hrs. These solutions (approximately 10 mL) were then dialyzed overnight against 100 mM potassium phosphate buffer, pH 7.4 and analyzed spectrophotometrically to determine protein and cofactor concentrations as described. Protein concentration of IYD reconstituted holoenzymes were estimated using UV/Vis spectroscopy and the following steps. First, the bound cofactor concentration was determined using the FMN, 1-deazaFMN, and 5-deazaFMN extinction coefficients of ε_{450} 12,500 M^{-1} cm^{-1} (*101*), ε_{540} of 6,800 M^{-1} cm^{-1} (*87*), and ε_{396} of 12,000 M^{-1} cm^{-1}, respectively (*142*). Second, the A_{280} contribution of these FMN analogues was estimated based on the concentration of bound flavin. Next, the remaining A_{280} following correction from cofactor contribution was attributed to IYD protein. This absorbance was used to determine the IYD protein concentration with the ε_{280} of 45,100 M^{-1} cm^{-1} determined by the Edelhoch method (*102*) for IYD protein in the absence of cofactor. Now with both bound cofactor concentrations and IYD protein concentrations, the bound flavin ratio of cofactor molecules per IYD dimer was calculated. Lastly, enzyme concentrations used in experiments were normalized for IYD protein containing bound cofactor in the active site since only these active sites would be capable of performing catalysis.

Deiodinase activity. IYD turnover was measured according to the procedure described in Chapter 2 except the assay was performed in the absence of free FAD. Holoprotein concentrations were normalized for IYD active sites containing cofactor

as described above. The standard deiodinase assay was performed for IYD•FMN and IYD•1-deazaFMN to obtain kinetic parameters. Additionally, turnover was measured at 20 μM DIT for each of the respective IYD holoenzymes.

Equilibrium binding measurements with IYD•5-deazaFMN holoenzyme. Fluorescence quenching assays to measure MIT binding to IYD•5-deazaFMN holoenzyme were performed according the procedure described in Chapter 4. IYD•5-deazaFMN holoenzyme was excited at 399 nm and emission was monitored at 461 nm. Holoenzyme concentrations were normalized for IYD active sites containing cofactor as described above.

Single turnover of IYD•deaza holoenzymes under anaerobic conditions. Anaerobic assays of IYD cofactor reduction and discharge of electrons were performed similarly to the procedure described in Chapter 4. Holoenzyme concentrations were normalized for IYD active sites containing cofactor as described above. The deazaFMN cofactor of IYD•5-deazaFMN (7 μM) and IYD•1-deazaFMN (5 μM) was reduced by serial addition of anaerobic dithionite stock solution (~10 mM) until their oxidized cofactor absorbance maxima (540 nm and 396 nm for 1-deazaFMN and 5-deazaFMN, respectively) failed to decease. Anaerobic solutions of tyrosine derivatives (10 mM) were added to the reduced IYD solution in additions of 1 molar equivalent each. Additional equivalents were added simply to increase the rate of reaction and have little influence on the overall discharge as evidenced in Appendix F.

HPLC analysis of products formed by anaerobic single turnover of IYD•deaza holoenzymes. HPLC analysis of anaerobic assays was performed according to the procedure described in Chapter 4, except 500 μL rather than 100 μL aliquots of completed anaerobic assay solutions were analyzed.

X-band EPR measurements. Electron paramaganetic resonance (EPR) spectra were collected on a Bruker EMX 6/1 spectrometer equipped with a microwave frequency meter by Dr. Veronika Szalai (University of Maryland, Baltimore County). IYD sample spectra were collected with the following experimental parameters: microwave frequency, 9.415 GHz; microwave power, 0.054 mW; modulation amplitude, 10 G; time constant, 40.96 ms; conversion time, 81.92 ms; gain, 1×10^4; 16 scans; temperature, 77 K. Quantitative spectra were collected with the following changes in experimental parameters: microwave frequency, 9.41 GHz; gain, 5×10^4 and 5×10^3 for IYD and TEMPO, respectively; 4 scans. IYD sample was prepared by concentrating the anaerobic assay sample following completion to 500 μM using a 10 kDa centrifugal membrane filter and then diluting the concentrate with 50 % glycerol. The IYD sample was then stored 16 hrs at 4 °C prior to EPR measurements. Measurements of samples were scaled for any gain and volume differences. A calibration curve was generated using TEMPO (250, 100, 50, and 0 μM) where the double integral of sample intensity was plotted against concentration in order to determine the concentration of radical present in IYD.

5.3 Results and Discussion

Reconstitution of IYD apoenzyme with flavin derivatives. Before 1- and 5-deazaFMN could be utilized to probe IYD's mechanism, IYD's native FMN cofactor was removed. Generation of IYD apoenzyme requires strong denaturing conditions such as the presence of 1.5 M GdnHCl. IYD apoenzyme was ultimately obtained with no detectable bound FMN according to UV/Vis spectroscopy after washing several minutes under these denaturing conditions (Figure 5-7). Apoenzyme was then reconstituted with FMN, 1-deazaFMN, or 5-deazaFMN to yield an estimated 1.2, 0.9, and 1.2 cofactor molecules per IYD dimer, respectively (Figure 5-7). These ratios are

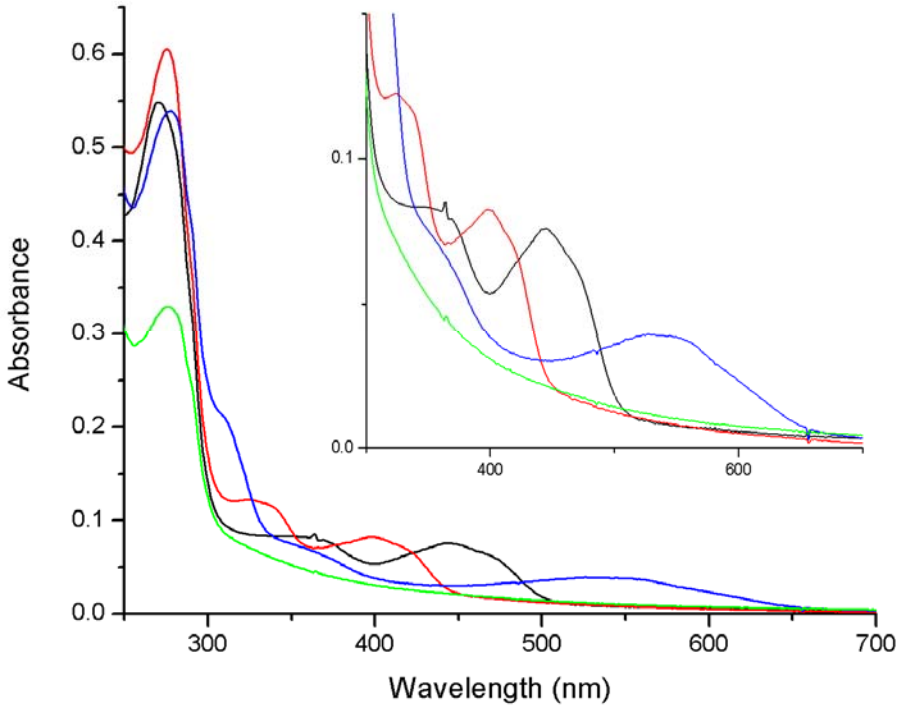

Figure 5-7. IYD holoenzymes reconstituted with flavin derivatives. IYD•**FMN**, **1-deazaFMN**, and **5-deazaFMN** holoenzymes were generated with the respective FMN derivatives and IYD **apoenzyme**. The inset graph shows the flavin absorbance of the respective IYD enzymes.

well below the 2.0 FMN cofactor molecules per IYD dimer for IYD isolated from Sf9 expression culture. The lack of full reconstitution in the generated holoenzymes may result from competition between phosphate from buffer and the flavin nucleotides since the site in which the phosphoester of FMN binds is critical to cofactor affinity (*28*). There is likely some irreversible denaturation occurring during the generation of IYD apoenzyme since approximately 70 % of the IYD was recovered following reconstitution according to absorption measurements. Nonetheless, the reconstituted holoenzymes allow the IYD mechanism to be probed.

Deiodinase activity of IYD•deazaFMN holoenzymes. Deiodinase activity of the reconstituted enzymes was analyzed using the standard iodide release assay. The resulting activity of the respective IYD holoenzymes was normalized for protein active sites containing flavin since only IYD active sites with bound cofactor are catalytically competent. When the activity of the respective holoenzymes at 20 μM substrate were compared, the IYD•5-deazaFMN holoenzyme was found to possess minimal deiodinase activity, while both IYD•FMN and IYD•1-deazaFMN holoenzymes support catalysis (Table 5-1). A difference between the deazaFMN holoenzymes is clearly evident as IYD•1-deazaFMN activity is 85 % of the IYD•FMN holoenzyme, while IYD•5-deazaFMN is only 10 % compared to IYD•FMN. The IYD "apoenzyme" also displayed deiodinase activity, although low. This minimal activity was attributed to the lack of complete removal of FMN cofactor from IYD. Interestingly, the IYD "apoenzyme" activity was greater than that of the IYD•5-deazaFMN holoenzyme. Therefore, the minimal IYD•5-deazaFMN activity

Table 5-1. Kinetics of reconstituted IYD flavin holoenzymes.[a]

IYD holoenzyme	Activity at 20 μM DIT (units μg^{-1})[b, c]	Kinetic parameters		
		K_M (μM)	k_{cat} (min^{-1})	k_{cat}/K_M (min^{-1} μM^{-1})
Isolated IYD[d]	Not determined	9.1 ± 1.4	4.5 ± 0.7	0.49
IYD•FMN	1.6 ± 0.2	52 ± 8	3.5 ± 0.4	0.07
IYD•1-deazaFMN	1.4 ± 0.2	25 ± 1	1.6 ± 0.1	0.06
IYD•5-deazaFMN	0.2 ± 0.01	Not determined		
IYD Apoenzyme	0.2 ± 0.02	Not determined		

[a]Measurements were performed in triplicate
[b]One unit μg^{-1} is defined as nmol of I^- released per hour per μg of IYD.
[c]Assays were performed with 9 μg of IYD•FMN, 11 μg of IYD•1-deazaFMN, 30 μg of IYD•5-deazaFMN, or 50 μg of IYD apoenzyme per 1 mL reaction.
[d]Kinetic values are from IYD isolated from Sf9 cells reported in Chapter 3.

likely results from residual apoenzyme activity and not from actual catalysis by the IYD•5-deazaFMN holoenzyme.

To verify that the IYD•5-deaza holoenzyme lacks catalytic ability and not just affinity for substrate, a fluorescence binding assay to measure MIT affinity was performed. The IYD•5-deazaFMN holoenzyme's affinity for MIT was 2 fold less than the isolated IYD enzyme (190 ± 20 nM for IYD•5-deazaFMN versus 90 ± 40 nM for MIT binding to isolated IYD (*115*), respectively (See Appendix E)). This showed that indeed incorporation of 5-deazaFMN does not significantly affect substrate binding.

Additionally, the 5-deazaFMN cofactor was also still capable of being reduced by dithionite because IYD activity requires a reduced cofactor. This was investigated using with the anaerobic single turnover assay. The holoenzyme's 5-

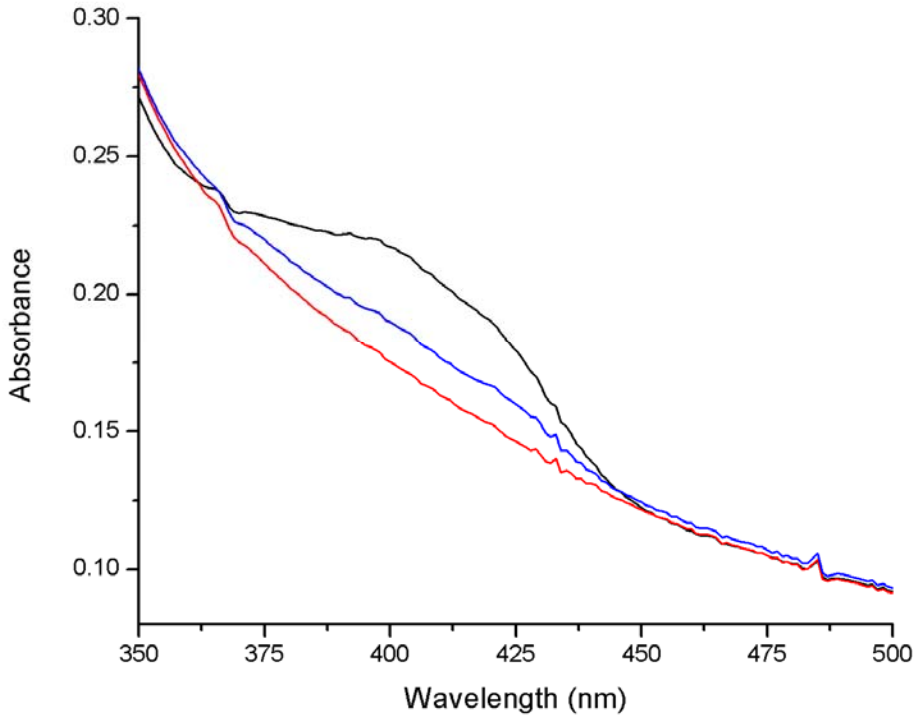

Figure 5-8. Absorbance spectra of the IYD•5-deazaFMN holoenzyme anaerobic assay for reduction and discharge of electrons from its cofactor with MIT. Additions of dithionite to the oxidized 5-deazaFMN (—) resulted in fully reduced 5-deazaFMN (—). Reoxidation of 5-deazaFMN (—) was monitored upon addition of 1 molar equivalent of MIT to the fully reduced cofactor.

deazaFMN cofactor was capable of being reduced anaerobically by dithionite since the λ_{max} of oxidized 5-deazaFMN (396 nm) clearly decreased upon addition of dithionite (Figure 5-8). Monitoring the reduction of the 5-deazaFMN cofactor was imperative since protein interactions or lack thereof can alter the redox properties of bound flavins. This is evident with IYD as FMN bound to IYD possess a significantly lower reduction potential than unbound FMN (-412 mV (*32*) versus -216 mV (*143*), respectively). Such a difference in 5-deazaFMN (-311 mV unbound)

(*143*) could prevent catalysis if when bound to IYD its reduction potential were lower than dithionite's (-660 mV).

In order to further validate that the IYD•5-deazaFMN holoenzyme lacks catalytic ability, MIT was added to the above reduced IYD•5-deazaFMN holoenzyme generated by the anaerobic single turnover assay and then analyzed for deiodination. Interestingly, MIT addition resulted in a 35 % increase in the λ_{max} absorbance compared with oxidized IYD•5-deazaFMN (Figure 5-8). Although this increase in absorbance might indicate that electrons from reduced 5-deazaFMN are discharged to MIT, resulting in deiodination, HPLC analysis of this assay detected less than 0.05 eq. of Tyr generated (Appendix G). This suggests that the increase in the cofactor absorbance must be caused by something other than catalysis. A change in cofactor absorbance could result from a change in the extinction coefficient possibly resulting from substrate binding since MIT stacks above the isoalloxazine of flavin, but this seems unlikely since the presence of MFT does not appear to affect the absorbance of FMN_{red} bound to IYD. The regain in A_{396} is more likely the result of slow reoxidation by trace molecular oxygen. Overall, IYD•5-deazaFMN is likely catalytically deficient because it is capable of undergoing the initial steps of IYD catalysis (binding of substrate and reduction of cofactor) but lacks the ability to catalyze substrate turnover.

Because IYD•5-deazaFMN holoenzyme appears catalytically deficient, the kinetic parameters of deiodination were calculated only for IYD•FMN and IYD•1-deazaFMN holoenzymes. The kinetics of these two holoenzymes differ as both the k_{cat} and K_M of reconstituted IYD•FMN are approximately 2 fold greater than the

IYD•1-deazaFMN holoenzyme (Table 5-1). The k_{cat} and K_M differences of the two holoenzymes are proportional to each other such that they yield an almost identical k_{cat}/K_M for each. Compared to isolated IYD, IYD•FMN retains a similar k_{cat}, but its K_M is increased by over 5 fold. The IYD•1-deazaFMN holoenzyme's k_{cat} is almost 3 fold lower and the K_M is 2.5 fold greater compared to isolated IYD. Also, the overall k_{cat}/K_M of the two reconstituted holoenzymes is several fold lower than the protein directly isolate form Sf9 cells. These kinetic results for the IYD•FMN and IYD•1-deazaFMN holoenzymes present a more accurate depiction of the activity differences between the two holoenzymes than the measurements at the single substrate concentration of 20 μM described previously. This is because their activities at 20 μM are not at their respective maximum catalytic rates, and hence, their activities appear far more similar at 20 μM substrate.

The reason for the 2 fold difference in kinetic parameters of IYD•FMN and IYD•1-deazaFMN is unclear since both likely perform catalysis in a 1 electron fashion. IYD's reduction potential is approximately 200 mV lower than free FMN (-216 mV (*143*)). Although free 1-deazaFMN has a lower redox potential (-280 mV (*143*)) than free FMN, its unknown whether binding to IYD would cause a similar decrease in the reduction potential for bound 1-deazaFMN. It is possible that 1-deazaFMN could disrupt the involvement of Arg 100 in catalysis since Arg 100 is positioned at the N1 of the isoalloxazine and likely stabilizes the reduced flavin (Figure 5-9). The use of 1-deazaFMN with a carbon at the N1 position could obstruct the reduction of the cofactor and alter the reduction potential of the holenzyme.

IYD•1-deazaFMN is catalytically less efficient than IYD•FMN and may result from a loss of IYD's reducing power. This possibility was investigated with the turnover of MCT since its aryl C-X bond strength is approximately 30 kcal/mol greater than MIT (Table 4-2). IYD•1-deazaFMN holoenzyme did have enough reducing power to discharge electrons from the reduced cofactor to MCT (Figure 5-10). Also, HPLC analysis of the assay confirmed dehalogenation of MCT as 0.75 eq. of Tyr were generated (Appendix G). This process was lengthy as addition of 6 equivalents of MCT over 1.5 hrs still did not fully discharge the reduced cofactor. In fact, full oxidation of the cofactor required the system be aerobic for almost 1.5 additional hrs. This contrasts IYD•FMN which undergoes complete oxidation

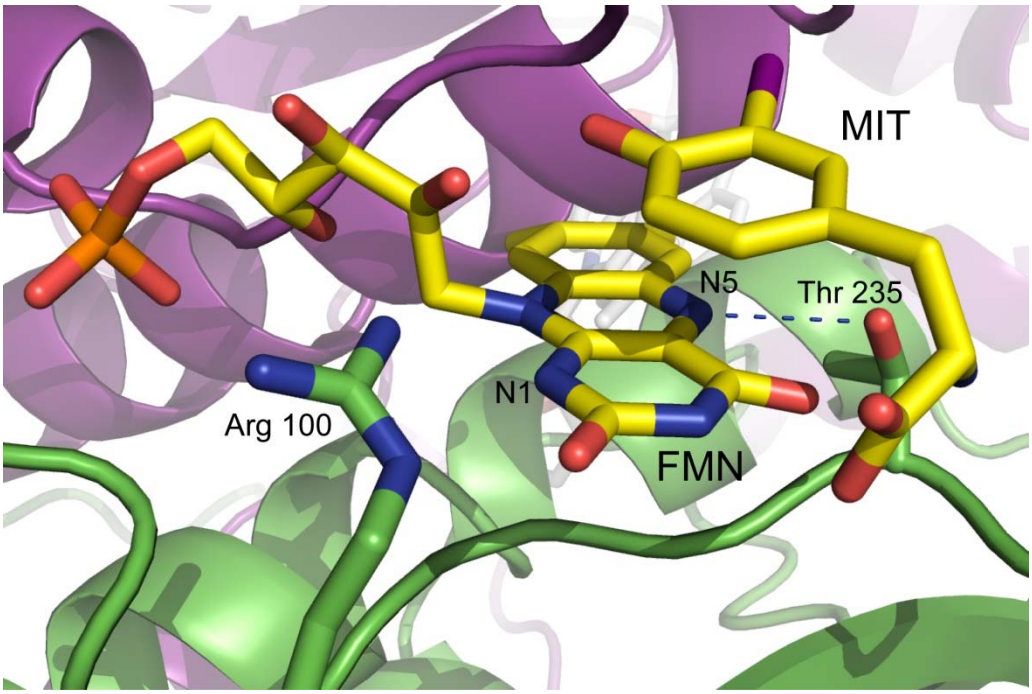

Figure 5-9. The N1 and N5 of the isoalloxazine of FMN are positioned for catalytic involvement of residues. Thr 235 makes a polar contact (represented by the blue dash) to the N5 of the isoalloxazine of FMN. Arg 100 is positioned to stabilize the N1 position of reduced FMN.

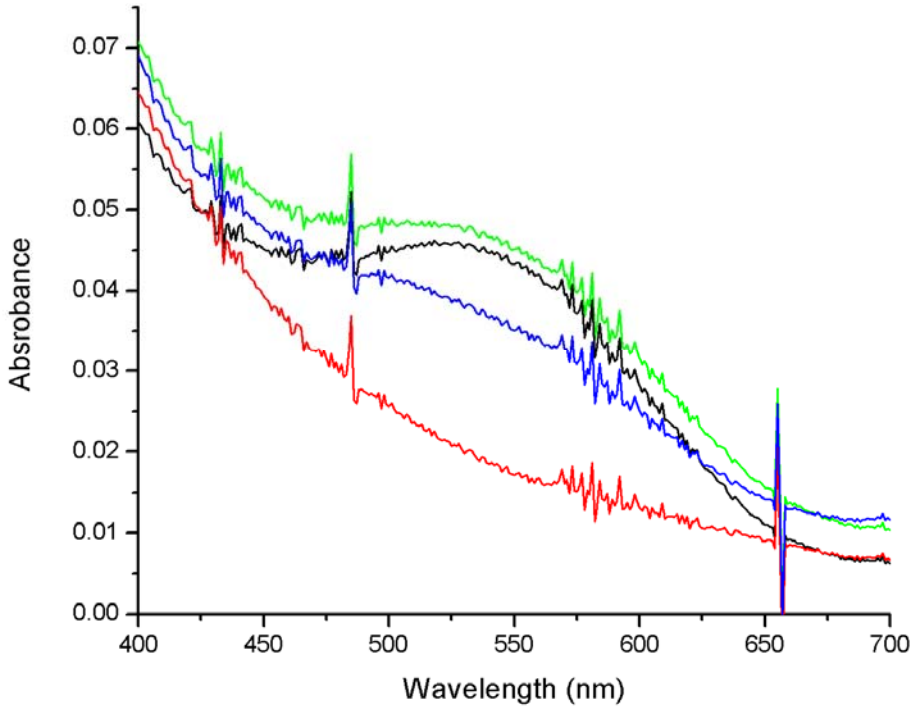

Figure 5-10. Absorbance spectra of the IYD•1-deazaFMN holoenzyme anaerobic assay for reduction and discharge of electrons from its cofactor with MCT. Additions of dithionite to the oxidized 1-deazaFMN (—) resulted in fully reduced 1-deazaFMN (—). Reoxidation of 1-deazaFMN by MCT (—) (6 molar equivalents) was monitored for 1.5 hrs. Complete reoxidation of 1-deazaFMN (—) by aerobic conditions was monitored over an additional 1.5 hours.

approximately 6 fold faster. Because IYD•1-deazaFMN holoenzyme does possess enough reducing power to dehalogenate MCT, the basis for the kinetic discrepancy between the IYD•FMN and IYD•1-deazaFMN holoenzymes remains unclear.

IYD catalysis likely follows a 1 electron mechanism of dehalogenation. The activity of the 1- and 5-deazaflavin holoenzymes indicate that IYD performs catalysis using a 1 electron mechanism. If this indication is accurate, IYD likely stabilizes an FMN_{semi}. Goswami and Rosenberg reported the generation of a broad absorbance with a maximum of 585 nm during the reduction of IYD with 0.5

equivalents of dithionite (*32*). This absorbance then decreased as the enzyme approached full reduction and was attributed to a neutral FMN_{semi} radical because these flavin species generally have a broad absorbance from 500-700 nm (*46*). Interestingly, this species was never observed in the reduction of isolated IYD reported here despite the use of identical conditions (Appendix F). However, a similar species was observed during the anaerobic discharge of electrons from FMN_{red} by MIT, MBT, MCT, and MNT.

Two distinct FMN species appear within IYD after single turnover (Appendix F). The characteristic FMN_{ox} species is not fully regenerated during the discharge and an additional broad absorbance similar to that observed by Goswami and Rosenberg (*32*) is generated around 600 nm. Because the FMN species' broad absorbance spans the same wavelengths (500-700 nm) as characteristic neutral FMN_{semi} radicals, a discharged IYD sample was analyzed by EPR. X-band EPR measurements confirmed the presence of a radical with a g-factor of 2.0027 and a line width of 20.3 G (Figure 5-11). These EPR features indicate that the radical is likely a neutral flavin semiquinone since these radicals have a line width of 20 G and anionic flavin radicals have a characteristic line width of 15 G (*144*). It was considered that the broad 600 nm peak and radical could result from the presence of either an active site Trp or catalytic intermediate tyrosyl radical, but neither of these possibilities seem likely as tyrosyl radicals have a g-factor of 2.004 and a λ_{max} at 412 nm (*145-147*), while Trp radicals have a line width of 18 G and λ_{max} at 512 nm and 536 (*145, 148, 149*).

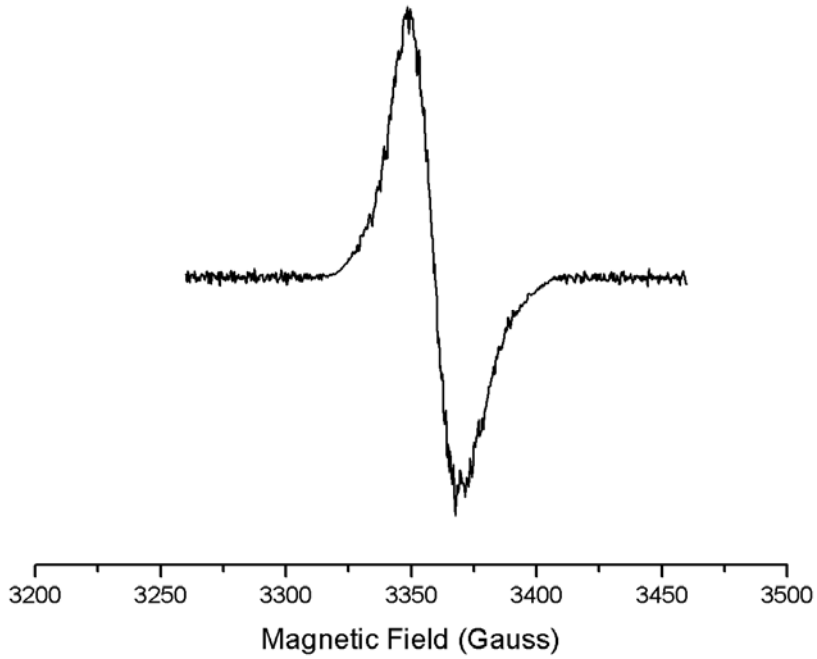

Figure 5-11. EPR spectrum of IYD following anaerobic assay for reduction and discharge electrons from FMN. X-band EPR measurements were made with an IYD sample (250 μM) stored 16 hours at 4 °C under aerobic conditions following completion of the anaerobic assay with MIT substrate.

The radical species of IYD possesses unusual stability. When stored under aerobic conditions at 4 ºC following completion of the anaerobic single turnover assay, the broad 600 nm absorbance peak associated with the radical is stable for several days. Interestingly, this neutral semiquinone radical comprises only 8 % of the total FMN. The reason for this low concentration is unclear, but this species appears to be a catalytically unproductive trap. Anaerobic reduction of the FMN_{semi} species which is generated following a single turnover with MIT only occurs after the FMN_{ox} species is fully reduced.

This radical species is evident after discharge of electrons from FMN_{red} by addition of MIT, MBT, MCT, and MNT. However, discharge by MNT generates approximately 2 fold more of the radical species than the other derivatives based on their absorbencies at 585 nm (Figure 5-12). The 448 nm peak associated with FMN_{ox} could not be used to confirm the difference in the amount of FMN_{semi} generated between MNT and the halotyrosines because of the A_{448} contribution of MNT. Unlike the halotyrosines which discharged the FMN_{red}, there was a lack of reactivity with MNT. HPLC analysis of the completed MNT assay yielded a single peak with a retention time identical to MNT standard and less than 0.05 eq. of Tyr generated. It is

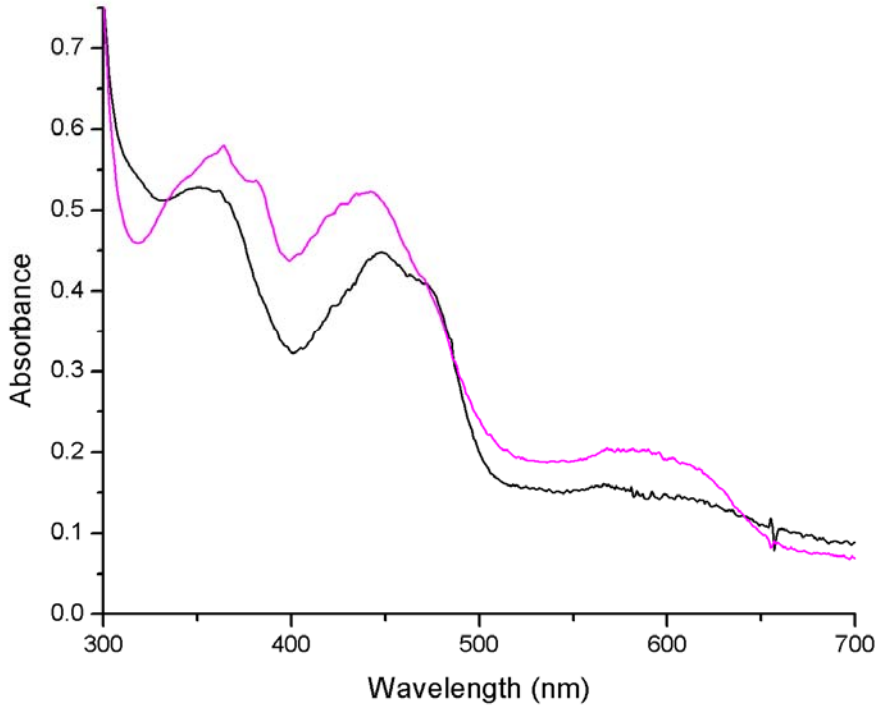

Figure 5-12. FMN absorbance spectra following oxidation of reduced FMN by addition of **MIT** or **MNT** derivatives. The fully reduced FMN cofactor of IYD was monitored for oxidation following addition of 2.0 molar equivalents of MIT or MNT.

possible that discharge of electrons from the FMN_{red} to MNT could occur in a radical fashion without elimination of the nitro substituent. This would result in an MNT anion radical species which could be readily reoxidized by oxygen when the solution became aerobic following the assay. A similar process occurs in the reduction of nitroaromatic compounds by a number of oxygen sensitive nitroreductases (*150-155*). Ironically, nitroreductases from the NOX/FRase superfamily are all oxygen insensitive and perform catalysis in an obligate 2 electron fashion (*80, 109*).

The contrasting ability of IYD to promote 1 electron chemistry is also supported by the hydrogen bond interaction between the side chain-OH of Thr 235 and the N5 position of isoalloxazine (Figure 5-9) (*97*). This is unusual for flavoproteins as hydrogen bond contacts to the N5 position usually consist of backbone or side chain-NH interactions (*47*), as seen with backbone interactions of the NOX/FRase superfamily proteins. Side chain contacts to the N5 similar to IYD are predicted to aid stabilization of anionic semiquinone radicals in a family of electron transfer flavoproteins (*156*). Additionally, BluB, which is the only other protein in the same subclass as IYD within the NOX/FRase superfamily, contains a similar contact between the side chain-OH of a Ser residue and the N5 of the isoalloxazine. Further, this enzyme is believed to perform catalysis utilizing a 1 electron mechanism as described in Chapter 3.

Distinguishing between the possible 1 electron mechanisms of IYD catalysis. Even if the possible IYD mechanisms have been narrowed to only include 1 electron processes, there are still a number of possibilities. Distinguishing between the four possible 1 electron mechanisms introduced in the beginning of the chapter is

difficult. If IYD were to follow a 1 electron mechanism involving injection of an electron into the substrate's aryl system (Figure 5-3), there would be two possibilities (Figure 5-4). If the electron were injected directly into the aryl carbon with bound iodine, dehalogenation would be concerted and the rate of catalysis should be dependent upon the aryl C-X bond strength (Table 4-2). The initial discharge of electrons from FMN_{red} monitored during the single turnover assays with the halotyrosines presented in Chapter 4 were all similar despite the approximate 31 kcal/mol span in energy from C-I to C-Cl (Figure 4-7). These results do not support the rate of IYD catalysis being dependent upon the C-X bond energy since they do not appear to notably influence catalysis. Hence, IYD likely does not utilize a 1 electron process where the electron is injected directly to the iodine bearing aryl carbon.

Alternatively, if the electron were injected into the aromatic π system of substrate, a radical anion intermediate would be generated (Figure 5-4). In this case, dehalogenation would correlate to the electron-withdrawing ability of the substituent if the electron transfer is the rate determining step. Because fluorine is the most electron-withdrawing of the halogens, the rate of halotyrosine dehalogenation would likely be fastest for MFT. IYD likely does not utilize this 1 electron process since the trend for dehalogenation is opposite and MFT does not discharge electrons from FMN_{red}.

The two possible mechanisms remaining both involve dehalogenation of nonaromatic keto intermediates formed by tautomerization of substrate (Figure 5-5). The rate of dehalogenation for the 1 electron mechanism in which an electron is

injected from FMN_{red} to the sp^3 hybridized carbon with the bound halide would be dependent upon the allylic C-X bond strength which spans 27 kcal/mol in energy from C-I to C-Cl (Table 4-2 and Figure 5-6). Because dehalogenation following injection of an electron to the sp^3 hybridized carbon with iodine is dependent upon the C-X bond strength like the aryl mechanism involving the similar injection of an electron to the iodine bearing carbon, the single turnover assay does not support this keto intermediate mechanism (Figure 4-7).

An alternative 1 electron mechanism involving injection of an electron into the carbonyl of the keto intermediate (Figure 5-6) would likely correlate the rate of dehalogenation to the injection of the electron. This aspect is unique to the 1 electron mechanism presented since the rate limiting step in dehalogenation would likely involve the formation of the ketyl radical. The rate of subsequent elimination of halide resulting from ketyl radical formation would not be significantly altered by the halide substituent. The single turnover assay is consistent with this mechanism since the initial rate of discharge by the halotyrosines is not considerably different.

Therefore, dehalogenation by the ketyl radical mechanism seems the most likely of the possible 1 electron mechanisms. Further, the inhibition observed by the *N*-pyridonal compounds which mimic a nonaromatic keto intermediate indicate that IYD stabilizes a ketyl intermediate (*67*). This is because the *N*-pyridonal derivatives display orders of magnitude tighter apparent binding than Me-Tyr.

Lastly, there is mechanistic precedence to support ketyl radical 1 electron mechanism for IYD dehalogenation. The catalytic mechanism utilized by TCE reductive dehalogenase presented in Chapter 1 (Figure 1-10) involves a radical

transfer to a substrate which could be envisioned for IYD (Figure 5-13). Structurally, IYD's tautomer intermediate is similar to the TCE reductive dehalogenase substrate 2,3-dichloropropene (*70*). Both the IYD keto intermediate and 2,3-dichloropropene have a halogen in an allylic position which is removed following electron injection. Further, dehalogenation of allylic halide by electron injection is supported by the dehalogenation precedence of α-haloacetophenones by the reducing agent 1,3-dimethyl-2-phenylbenzimidazoline in organic solvent (Figure 5-14). These compounds rely on the generation of a ketyl radical before dehalogenation occurs (*108*).

Conclusion. Overall, the 1 electron ketyl radical mechanism for IYD catalysis is supported by most data and precedence. This mechanism involves tautomerization of substrate to a nonaromatic keto intermediate followed by injection of single electron from FMN_{red} into the carbonyl of the intermediate which then facilitates dehalogenation. The IYD•5-deazaFMN holoenzyme's lack of observable

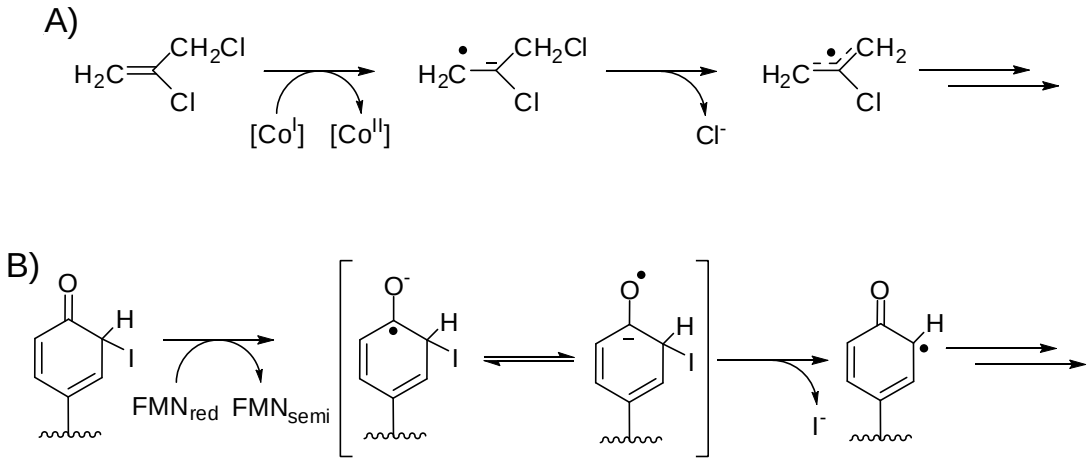

Figure 5-13. Possible 1-electron mechanistic similarities of A) TCE dehalogenase (*70*) and B) IYD ketyl radical mechanism.

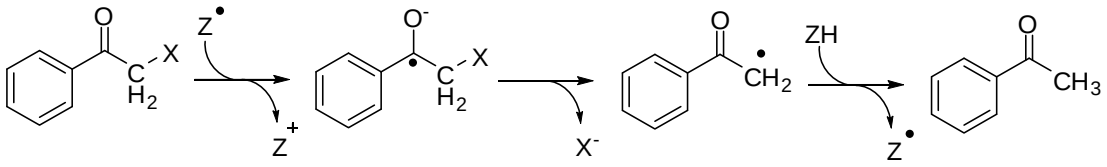

Figure 5-14. Mechanistic precedence of dehalogenation by ketyl radical of α-haloacetophenone (*108*). *Z* is reducing agent 1,3-dimethyl-2-phenylbenzimidazoline.

deiodinase activity (Table 5-1) is consistent with a 1 electron mechanism since 5-deazaflavins are unable to catalyze 2 electron processes. Differentiating between the four possible 1 electron mechanisms is less direct. The single turnover assay with halotyrosine does not support either of the aryl 1 electron mechanisms. It also does not support the keto intermediate 1 electron mechanism involving direct injection into the sp^3 hybridized carbon with the bound halide. This is because the initial discharge of electrons from FMN_{red} by the halotyrosines was not notably influenced by the halide substituent. The lack of an appreciable halogen affect on the rate of discharge, however, does support the ketyl radical mechanism which is likely rate dependent on generation of the ketyl radical. The formation of a nonaromatic keto intermediate is supported by the reversible inhibition of the *N*-pyridonal derivatives which mimic the keto tautomer (*67*). Lastly, mechanistic precedence by TCE dehalogenase (*70*) and dehalogenation of α-haloacetophenones (*108*) supports IYD catalysis through a ketyl radical.

Chapter 6: Conclusions

IYD remained poorly characterized for almost 50 years despite its physiological importance for iodide homeostasis. The work described in this dissertation has provided the first molecular insights into IYD catalysis. Prior discovery of the gene encoding IYD (*37, 40*) allowed for limited expression in mammalian culture, and subsequently site-directed mutagenesis to initiate mechanistic studies. Despite the precedence (*60, 65, 66*) used for IYD catalysis involving nucleophilic attack of the substrate iodine by cysteine, this mechanism has been proven incorrect as Cys to Ala mutation variants retained deiodinase activity (*38*). These results established IYD as a novel enzyme since no mechanistic precedent for flavin promoting reductive dehalogenation is available. Because flavin is capable of performing both 1 and 2 electron processes, mechanisms of catalysis involving a single 2 electron transfer or 2 sequential 1 electron transfer had to be reconsidered.

However, further investigation of these mechanisms was plagued by a lack of a convenient source of active and soluble protein. This was overcome by expressing a synthetic *Mus musculus* IYD gene designed for expression in *Pichia pastoris*, as well as by expressing the truncated *Mus musculus* IYD gene in Sf9 insect cells. Large scale expression and isolation of soluble IYD from Sf9 cells provided an abundant supply (43 ± 8 mg of isolated IYD per L of expression culture) of highly pure enzyme (99 ± 0.1 %).

Subsequent crystallographic studies yielded a structure of IYD at 2.0 Å (*97*). This structure confirmed IYD's placement in the NOX/FRase structural superfamily and provided an understanding of congenital mutations in the IYD human gene (*28, 29*). Further, the structure showed that Cys residues are not located near the active site. Additional structures with MIT and DIT substrates bound to IYD were also obtained and indicate that substrate binding induces the formation of an active site lid. This lid sequesters substrate from solvent and confers IYD's substrate specificity for amino acids. Several polar contacts from the substrate to the active site lid and the FMN cofactor orient the substrate parallel to the isoalloxazine of FMN with the substrate C-X bond directly above the C4a and N5 positions of FMN.

IYD's substrate recognition appears to be governed by the 3-position substituent as indicated by its nM binding affinity for Tyr derivatives with optimal electronics. Single turnover experiments with these derivatives identified MBT and MCT in addition to MIT and DIT as substrates of IYD. IYD clearly has significant dehalogenating power due to its ability to dehalogenate both MBT and MCT which have C-X bond energies significantly greater than MIT.

The absence of observable dehalogenase activity in the IYD•5-deazaFMN holoenzyme indicates that IYD utilizes a catalytic mechanism involving two sequential electron transfers to substrate because 5-deazaflavins are incapable of performing 1 electron processes (*87, 88*). Two 1 electron mechanisms involving a nonaromatic keto intermediate are consistent with the reversible inhibition observed with *N*-pyridonal compounds which mimic keto intermediate. Single turnover assays performed with halotyrosine derivatives indicate that the halogen substituent does not

have an appreciable effect on the rate of catalysis. This supports an IYD mechanism involving injection of a single electron into the carbonyl of a keto intermediate which then facilitates dehalogenation because the rate determining step in the mechanism is likely the electron injection into the carbonyl. This ketyl radical mechanism is also supported by the mechanistic precedence of TCE dehalogenase (*70*) and dehalogenation of α-haloacetophenones (*108*).

These mechanistic studies presented were preliminary in nature and further investigation of the mechanism is needed. Synthesis of substrate derivatives capable of trapping a 1 electron intermediate would provide additional mechanistic information. Also, stopped flow kinetics experiments with a wide range of Tyr derivatives would aid in further distinguishing between the possible 1 electron mechanisms.

Appendices

A. Densitometry estimate of IYD concentrations in HEK293 cell lysates.

HEK 293 cells expressing wild-type IYD and IYD Cys to Ala mutation variants were harvested following transformation. These cells were lysed and analyzed by SDS-PAGE, Coomassie staining, and densitometry to determine the concentration of the protein. A-1) A representative SDS-PAGE analysis is presented here with IYD expression lysates (lane 1), a control lane of HEK293 cells lacking IYD expression (lane 2) and molecular weight markers (lane M). Densitometry was performed with the full lane length and width in order to calculate the amount of the respective IYD proteins in the lysates. A-2) A representative densitometry analysis is shown for the determination of IYD relative to the cell lysates where it is calculated from the difference in "c" between lane 1 and lane 2. Cellular proteins "a" and "b" were used as controls in the calculations and varied by less than 3 % in each of the lysates. Modified from Watson et al. (*38*).

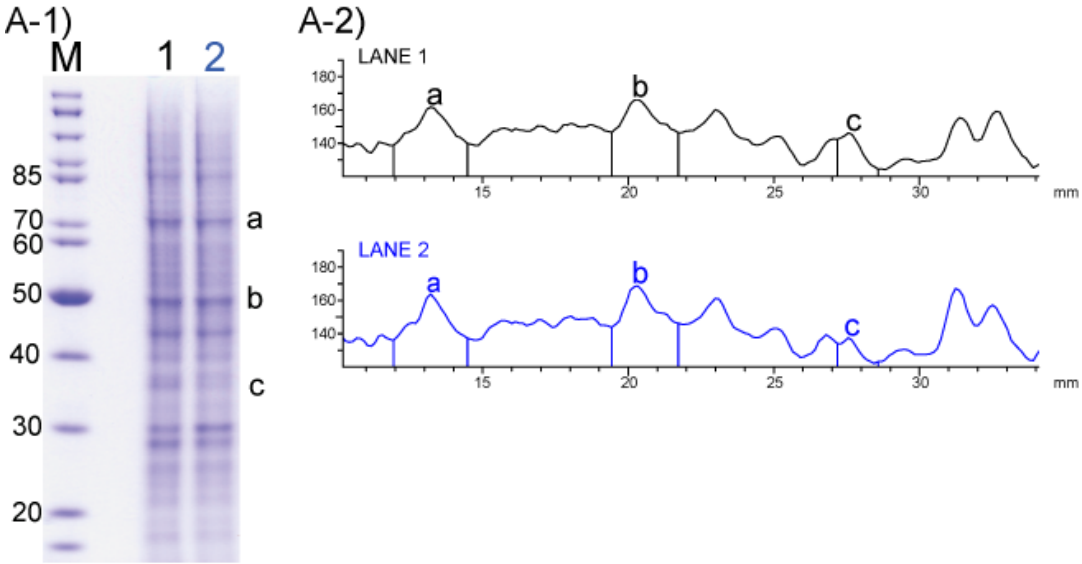

B. Rate of DIT deiodination by IYD and IYD Cys to Ala mutation variants.

Deiodinase activity of B-1) IYD, B-2) IYD C217A, B-3) IYD C239A, and B-4) IYD C217A C239A from HEK293 expression lysates was determined using standard dithionite kinetic assays. The data, colored according to individual assay data sets, was fit to the Michaelis-Menten equation using Origin 7.0. The fit and standard deviation error bars from the overall data points is shown in black. Modified from Watson et al. (*38*).

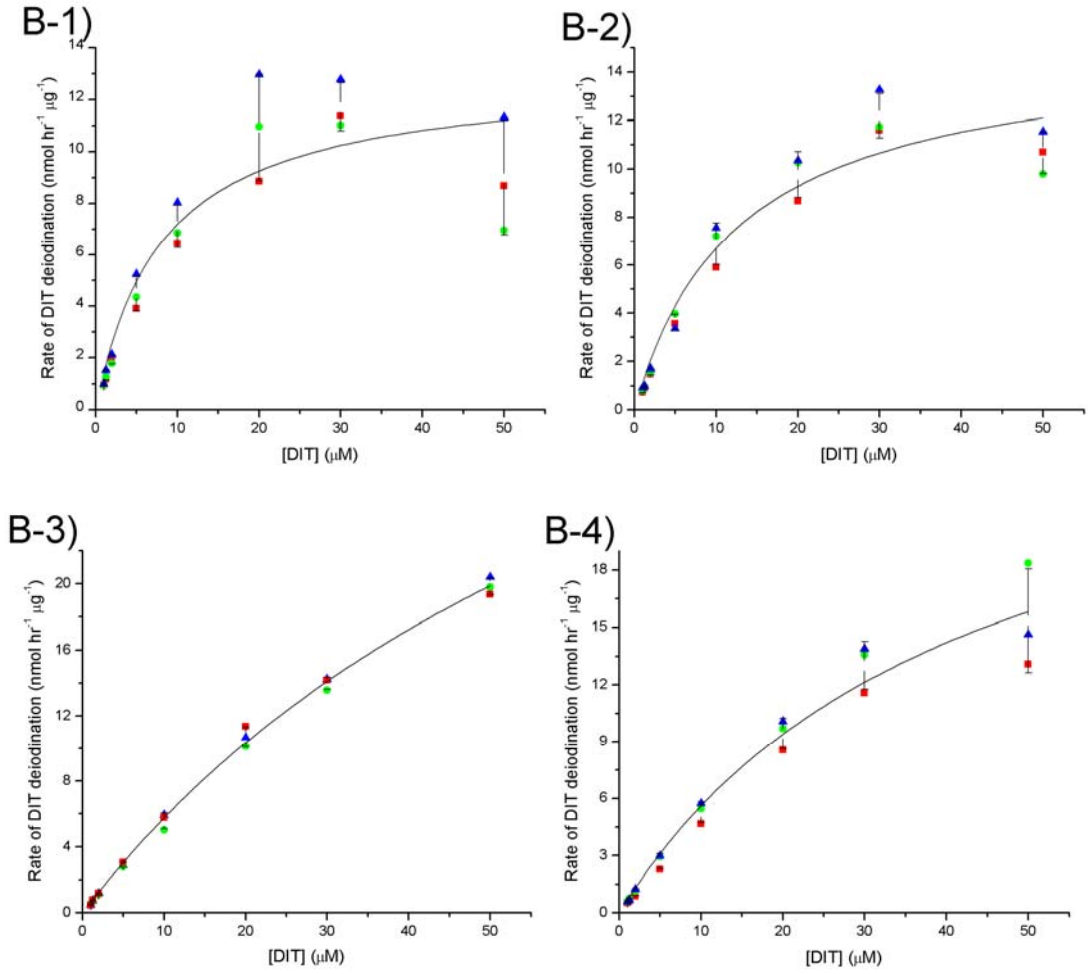

C. Representative determination of isolated IYD purity.

The purity of isolated IYD was analyzed by SDS-PAGE, Coomassie staining and densitometry. C-1) A representative SDS-PAGE analysis is presented here with IYD isolated from Sf9 cells after purification (lane 1) and molecular weight markers (lane M). The gel was imaged using an HP Scanjet 4050. Densitometry was then performed on the entire protein isolate lane (length and width). The percent of the area under the peak associated with IYD was used to calculate the purity. C-2) A representative densitometry analysis is shown for the determination of purity for IYD isolated from Sf9 cells (99 %).

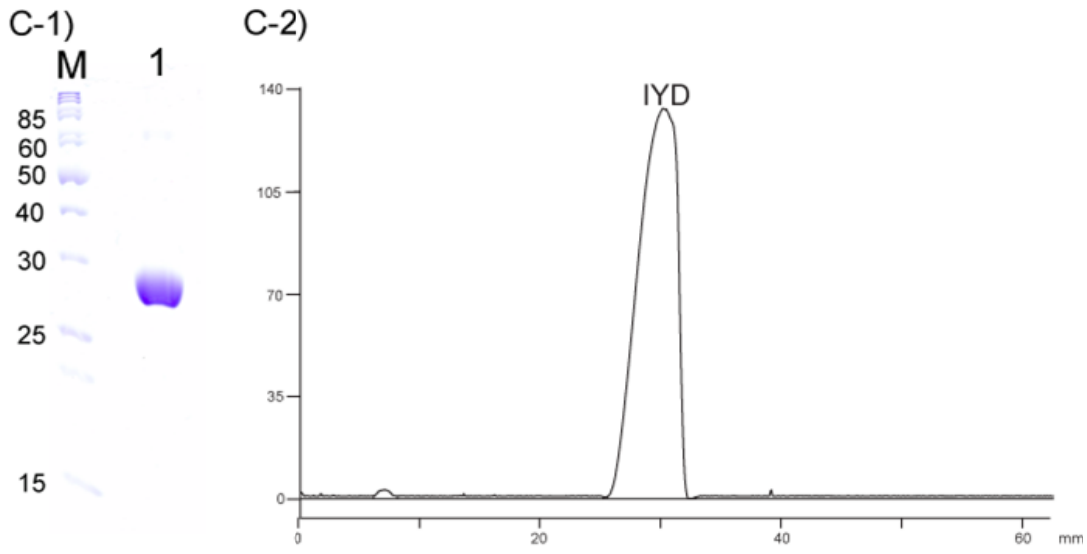

D. Rate of DIT deiodination by isolated IYD(ΔTM)His_6.

Deiodinase activity of IYD isolated from D-1) *Pichia* and D-2) Sf9 cells was determined using the standard steady state assays. The data, colored according to individual assay data sets, was fit to the Michaelis-Menten equation using Origin 7.0. The fit and standard deviation error bars from the overall data points are shown in black. The kinetics obtained from fitting for protein isolated from A) Pichia was a K_M of 19 ± 3 μM and a k_{cat} of 6.9 ± 1.3 min^{-1} and from B) Sf9 cells was a K_M of 9 ± 1 μM and a k_{cat} of 4.5 ± 0.7 min^{-1}.

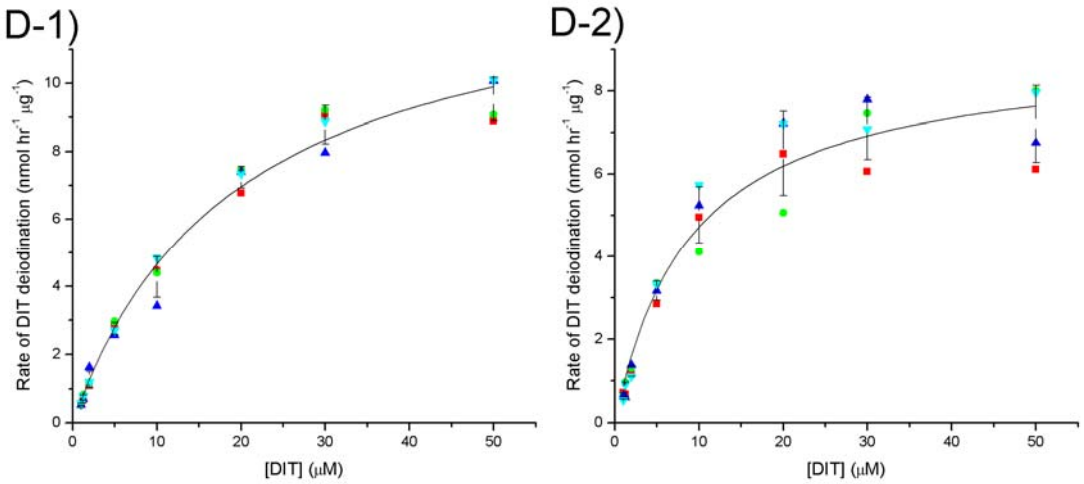

E. Fluorescence quenching assay to measure IYD affinity for Tyr derivatives.

Fluorescence emission was monitored upon titration with tyrosine derivatives. Binding (λ_{ex} 450 and λ_{em} 527 nm) of E-1) Tyr derivatives and E-2) halotyrosine derivatives to IYD isolated from Sf9 cells was measured was calculated from fluorescence quenching by **MIT**, **DIT**, **MNT**, **Me-Tyr**, **Tyr**, **MBT**, **MCT**, and **MFT**. Data points are an average of 3 or more independent sets of measurements, and indicated error represents standard deviation at each ligand concentration. Dissociation constants derive from best fit (line) to either Eq. 4-1 (Tyr and Me-Tyr) or Eq. 4-2 (MIT, MBT, MCT, MFT, DIT) according to Origin 7.0. See Table 4-2 for K_D values. Modified from McTamney and Rokita (*115*). E-3) Binding of **Tyr**, **Tyr in the presence of 1.5 mM free iodide**, **2-iodophenol**, **NADPH**, and **nicotinic acid** was performed with isolated IYD. Dissociation constants were estimated as a lower limit from best fit (line) to either Eq. 4-1 because full binding curves could not be obtained due to poor solubility. E-4) Binding of **MIT to IYD•5-deazaFMN** was calculated from fluorescence quenching (λ_{ex} 399 and λ_{em} 461 nm). Data points are an average of 3 or more independent sets of measurements, and indicated error represents standard deviation at each ligand concentration. The K_D derives from best fit (line) to Equation 5-1 because fitting to Equation 5-2 gave an error 2.5 fold more than the K_D value. MIT binding to IYD isolated from Sf9 is shown for binding comparison.

E-1)

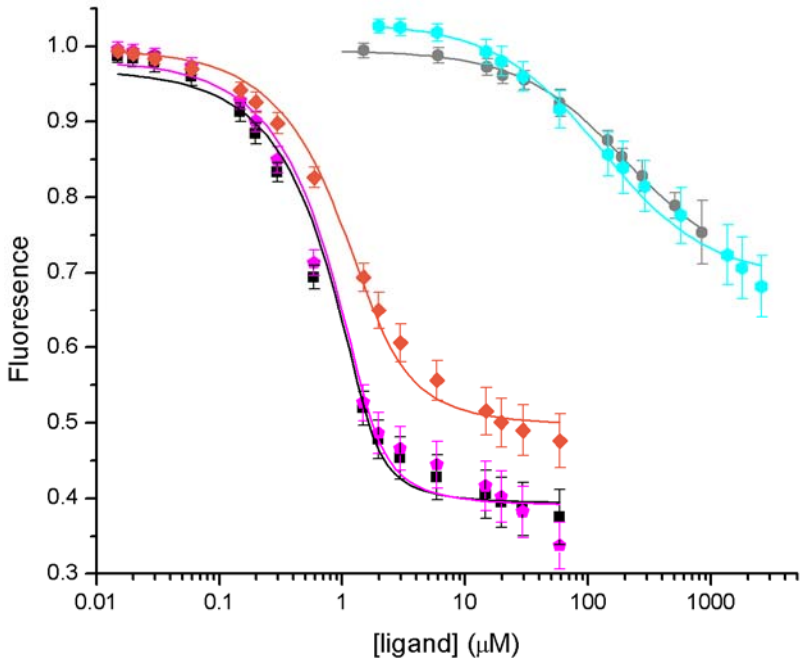
Fluoresence
1.0
0.9
0.8
0.7
0.6
0.5
0.4
0.3
0.01
0.1
1
10
100
1000
[ligand] (μM)

E-2)

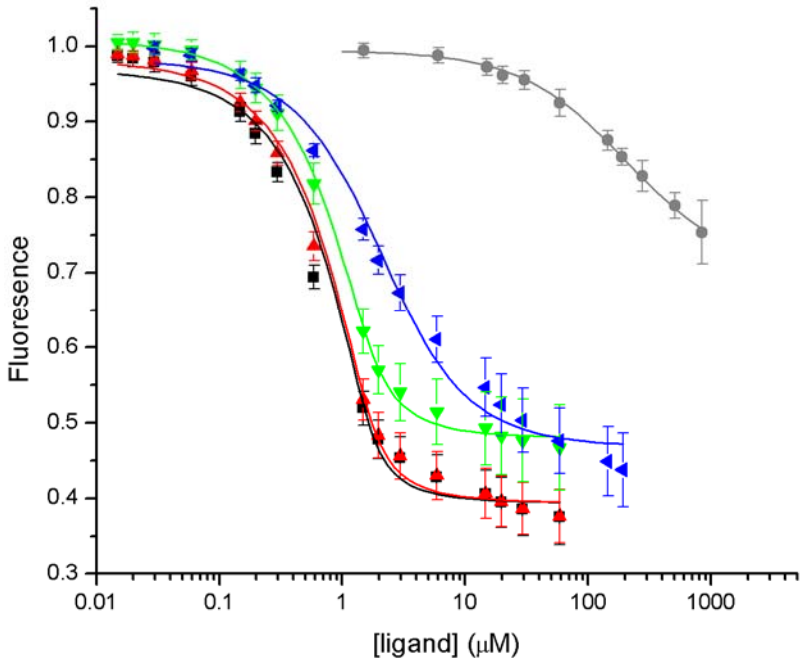
Fluoresence
1.0
0.9
0.8
0.7
0.6
0.5
0.4
0.3
0.01
0.1
1
10
100
1000
[ligand] (μM)

E-3)

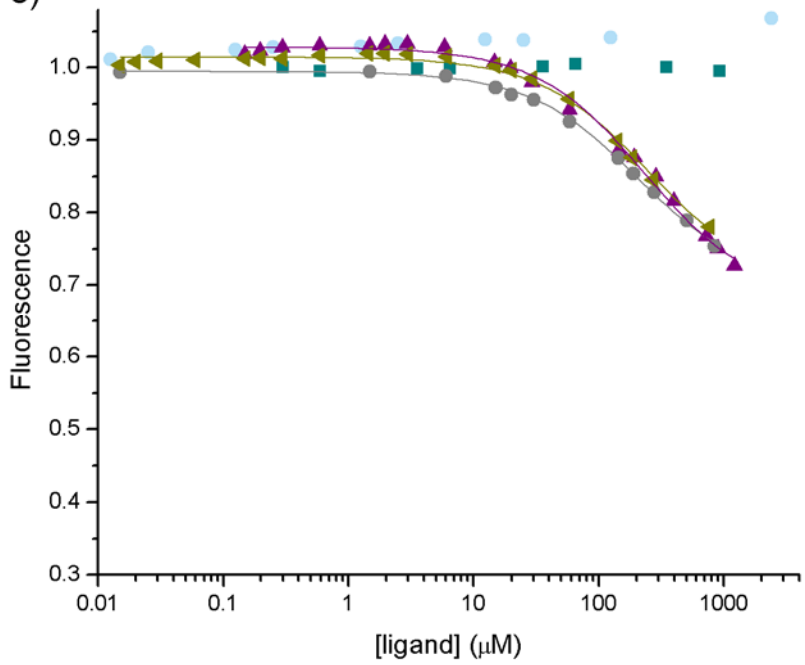
Fluorescence
1.0
0.9
0.8
0.7
0.6
0.5
0.4
0.3
0.01
0.1
1
10
100
1000
[ligand] (μM)

E-4)

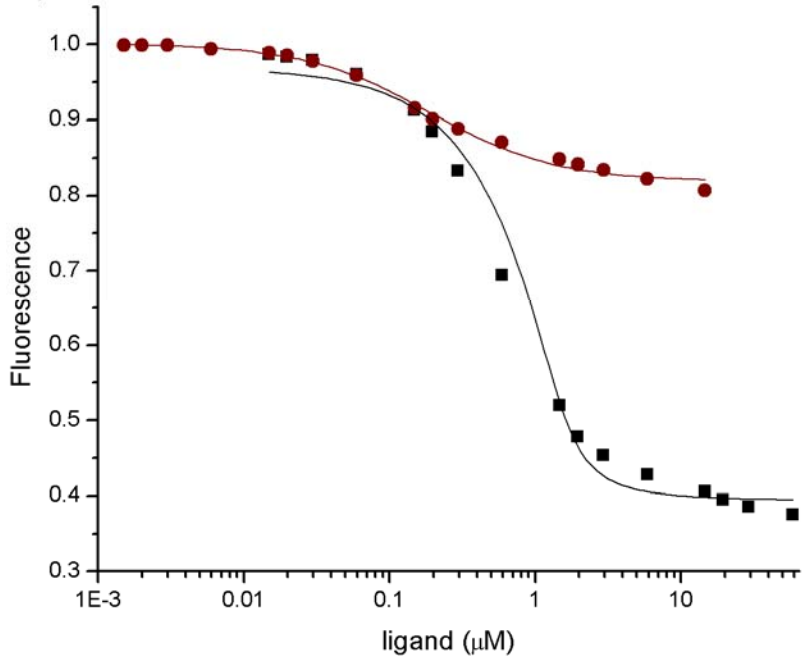
Fluorescence
1.0
0.9
0.8
0.7
0.6
0.5
0.4
0.3
1E-3
0.01
0.1
1
10
ligand (μM)

F. Anaerobic reduction and discharge of electrons from IYD's FMN cofactor by MIT.

Single turnover assays were monitored spectrophotometrically for F-1) reduction and F-2) discharge of electrons from IYD's FMN cofactor. F-1) Anaerobic reduction of IYD's active site FMN (50 μM) (—) was performed by addition of anaerobic dithionite (0.075 molar equivalents). The inset graph illustrates that 1 molar equivalent of dithionite is sufficient for full reduction of IYD's FMN cofactor (—). F-2) Reoxidation of IYD's fully reduced FMN occurred following serial additions of anaerobic MIT, which yielded the final spectrum of oxidized IYD (—). Modified from McTamney and Rokita (*115*).

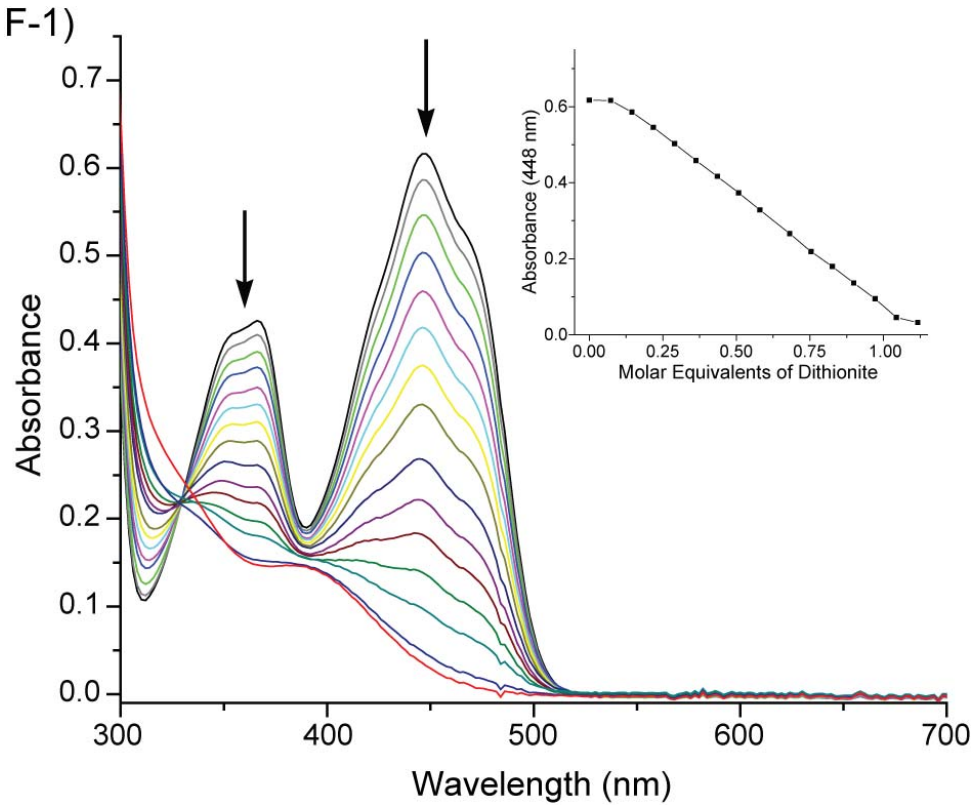

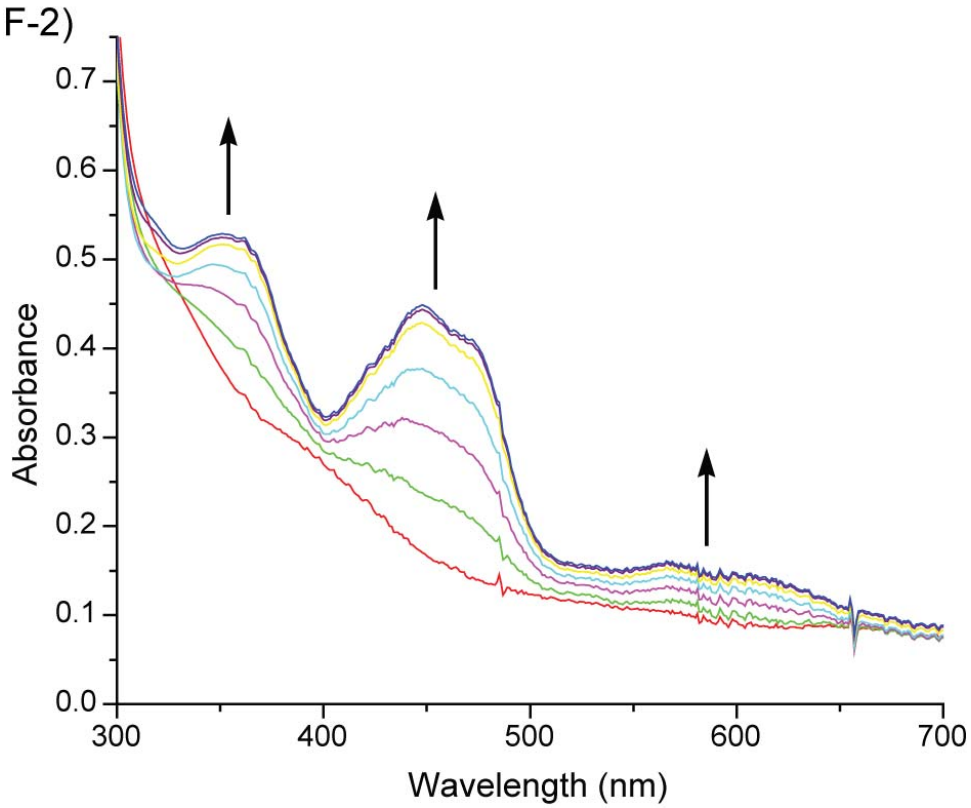
F-2)
Absorbance
0.0
0.1
0.2
0.3
0.4
0.5
0.6
0.7
300
400
500
600
700
Wavelength (nm)

G. HPLC analysis of substrate catalysis by reduced IYD under anaerobic conditions.

Completed anaerobic assays for oxidation of G-1) FMN_{red} or G-2) deazaFMN derivatives by respective Tyr derivatives were analyzed by reverse phase (C-18) HPLC with a methanol elution gradient 0-83 % in 10 mM TEAA, pH 5.5. G-1) Completed assays were analyzed with 100 μL aliquots (2 molar equivalents of respective Tyr derivative added during assay) and were compared to appropriate standards (1 molar equivalent). MFT and MNT assays samples were spiked with Tyr standard as a control for Tyr generation. Modified from McTamney and Rokita (*115*). G-2) Completed deazaFMN assays were analyzed with 500 μL aliquots containing 1 molar equivalent of MIT added to the 5-deazaFMN assay and 6 molar equivalents of MCT added to the 1-deazaFMN assay.

G-1)

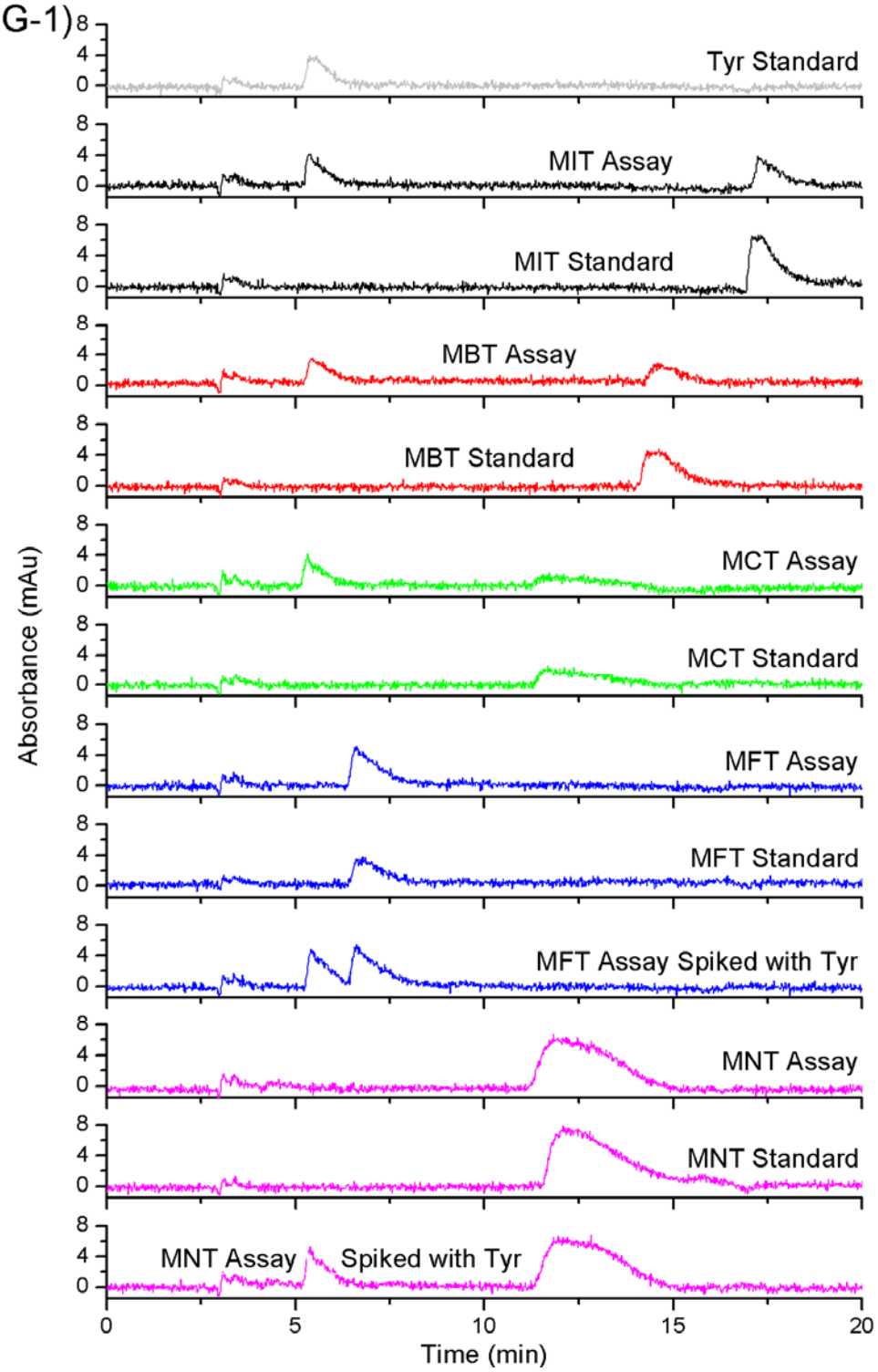
Tyr Standard
MIT Assay
MIT Standard
MBT Assay
MBT Standard
MCT Assay
MCT Standard
MFT Assay
MFT Standard
MFT Assay Spiked with Tyr
MNT Assay
MNT Standard
MNT Assay
Spiked with Tyr
Absorbance (mAu)
Time (min)
0
4
8
0
5
10
15
20

G-2)

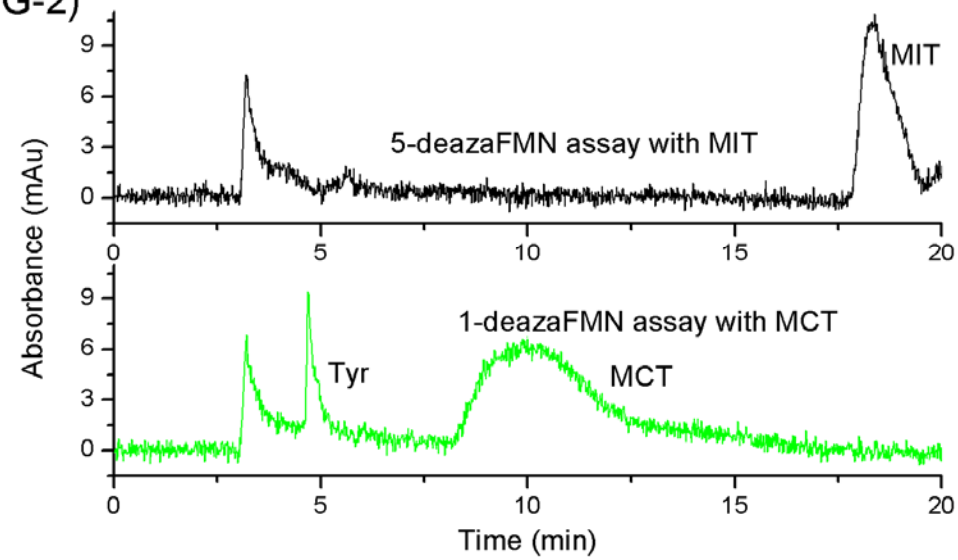
Absorbance (mAu)
9
6
3
0
0
5
10
15
20
5-deazaFMN assay with MIT
MIT
1-deazaFMN assay with MCT
Tyr
MCT
Time (min)

Bibliography

(1) Coindet, J.-F. (1820) Decouverte d'um nouveau remede contre le goitre. *Ann. Chim. Phys. 21*, 319-330.

(2) Kendall, E. C. (1915) The isolation in crystalline form of the compound which occurs in the thyroid: its chemical nature and physiologic activity. *JAMA 64*, 2042-2-43.

(3) McNabb, F. M. (1992) Physiological actions of thyroid hormones, in *Thyroid hormones* pp 165-196, Prentice-Hall, Englewood, NJ.

(4) Cavalieri, R. R. (1997) Iodine metabolism and thyroid physiology: current concepts. *Thyroid 7*, 177-81.

(5) Kohrle, J. (2000) The deiodinase family: selenoenzymes regulating thyroid hormone availability and action. *Cell. Mol. Life Sci. 57*, 1853-63.

(6) Leonard, J. L., and Visser, T. J. (1986) Biochemistry of deiodination, in *Thyroid hormone metabolism* (Hennemann, G., Ed.) pp 189-220, Marcel Dekker, Inc., New York, New York.

(7) McNabb, F. M. (1992) Mechanism of action of thyroid hormones, in *Thyroid hormones* pp 135-164, Prentice-Hall, Englewood Cliffs, NJ.

(8) Hands, E. (2000) *Nutrients in food*, Vol. 59, Lippincott, Williams, & Wilkins, Philadelphia.

(9) McNabb, F. M. (1992) Thyroid hormones: Production, storage, and release by the thyroid gland, in *Thyroid hormones* pp 21-48, Prentice-Hall, Englewood, NJ.

(10) Nunez, J., and Pommier, J. (1982) Formation of thyroid hormones. *Vitam. Horm. 39*, 175-229.

(11) McNabb, F. M. (1992) Control of thyroid gland function, in *Thyroid hormones* pp 49-73, Prentice-Hall, Englewood, NJ.

(12) Dai, G., Levy, O., and Carrasco, N. (1996) Cloning and characterization of the thyroid iodide transporter. *Nature 379*, 458-60.

(13) Andros, G., and Wollman, S. H. (1967) Autoradiographic localization of radioiodide in the thyroid gland of the mouse. *Am. J. Physiol. 213*, 198-208.

(14) Dunn, J. T., Dunn, A. D., Heppner, D. G., Jr., and Kim, P. S. (1981) A discrete thyroxine-rich iodopeptide of 20,000 daltons from rabbit thyroglobulin. *J. Biol. Chem. 256*, 942-947.

(15) Dunn, J. T., and Dunn, A. D. (1999) The importance of thyroglobulin structure for thyroid hormone biosynthesis. *Biochimie 81*, 505-9.

(16) Taurog, A., Dorris, M. L., and Doerge, D. R. (1996) Mechanism of simultaneous iodination and coupling catalyzed by thyroid peroxidase. *Arch. Biochem. Biophys. 330*, 24-32.

(17) Robbins, J., and Bartalena, L. (1986) Plasma transport of thyroid hormones, in *Thyroid hormone metabolism* (Hennemann, G., Ed.) pp 3-38, Marcel Dekker, Inc., New York, New york.

(18) Kohrle, J. (1999) Local activation and inactivation of thyroid hormones: the deiodinase family. *Mol. Cell. Endocrinol. 151*, 103-19.

(19) Lever, E. G., Medeiros-Neto, G. A., and DeGroot, L. J. (1983) Inherited disorders of thyroid metabolism. *Endocr. Rev. 4*, 213-39.

(20) Delange, F. (1994) The disorders induced by iodine deficiency. *Thyroid 4*, 107-28.

(21) de Benoist, B., McLean, E., Andersson, M., and Rogers, L. (2008) Iodine deficiency in 2007: global progress since 2003. *Food Nutr. Bull. 29*, 195-202.

(22) (2004) (de Benoist, B., Andersson, M., Egli, I., Takkouche, B., and Allen, H., Eds.) pp 1-58, World Health Organization, Geneva.

(23) Stanbury, J. B. (1960) Deiodination of the iodinated amino acids. *Ann. N. Y. Acad. Sci. 86*, 417-39.

(24) Solis-S, J. C., Villalobos, P., Orozco, A., and Valverde, R. C. (2004) Comparative kinetic characterization of rat thyroid iodotyrosine dehalogenase and iodothyronine deiodinase type 1. *J. Endocrinol. 181*, 385-92.

(25) Stanbury, J. B., Kassenaar, A. A., and Meijer, J. W. (1956) The metabolism of iodotyrosines. I. The fate of mono- and di-iodotyrosine in normal subjects and in patients with various diseases. *J. Clin. Endocrinol. Metab. 16*, 735-46.

(26) Stanbury, J. B., Meijer, J. W., and Kassenaar, A. A. (1956) The metabolism of iodotyrosines. II. The metabolism of mono- and diiodotyrosine in certain patients with familial goiter. *J. Clin. Endocrinol. Metab. 16*, 848-68.

(27) Querido, A., Stanbury, J. B., Kassenaar, A. A., and Meijer, J. W. (1956) The metabolism of iodotyrosines. III. Di-iodotyrosine deshalogenating activity of human thyroid tissue. *J. Clin. Endocrinol. Metab. 16*, 1096-101.

(28) Moreno, J. C., Klootwijk, W., van Toor, H., Pinto, G., D'Alessandro, M., Leger, A., Goudie, D., Polak, M., Gruters, A., and Visser, T. J. (2008) Mutations in the iodotyrosine deiodinase gene and hypothyroidism. *N. Engl. J. Med. 358*, 1811-8.

(29) Afink, G., Kulik, W., Overmars, H., de Randamie, J., Veenboer, T., van Cruchten, A., Craen, M., and Ris-Stalpers, C. (2008) Molecular characterization of iodotyrosine dehalogenase deficiency in patients with hypothyroidism. *J. Clin. Endocrinol. Metab. 93*, 4894-901.

(30) Roche, J., Michel, R., Michel, O., and Lissitzky, S. (1952) Enzymatic dehalogenation of iodotyrosine by thyroid tissue; on its physiological role. *Biochim. Biophys. Acta. 9*, 161-9.

(31) Rosenberg, I. N., and Goswami, A. (1979) Purification and characterization of a flavoprotein from bovine thyroid with iodotyrosine deiodinase activity. *J. Biol. Chem. 254*, 12318-25.

(32) Goswami, A., and Rosenberg, I. N. (1979) Characterization of a flavoprotein iodotyrosine deiodinase from bovine thyroid. Flavin nucleotide binding and oxidation-reduction properties. *J. Biol. Chem. 254*, 12326-30.

(33) Rodkey, F. L., and Donovan, J. A., Jr. (1959) Oxidation-reduction potentials of the triphosphopyridine nucleotide system. *J. Biol. Chem. 234*, 677-80.

(34) Stanbury, J. B. (1957) The requirement of monoiodotyrosine deiodinase for triphosphopyridine nucleotide. *J. Biol. Chem. 228*, 801-11.

(35) Rosenberg, I. N. (1970) Purification of iodotyrosine deiodinase from bovine thyroid. *Metabolism 19*, 785-98.

(36) Goswami, A., and Rosenberg, I. N. (1977) Studies on a soluble thyroid iodotyrosine deiodinase: activation by NADPH and electron carriers. *Endocrinology 101*, 331-41.

(37) Gnidehou, S., Caillou, B., Talbot, M., Ohayon, R., Kaniewski, J., Noel-Hudson, M. S., Morand, S., Agnangji, D., Sezan, A., Courtin, F., Virion, A., and Dupuy, C. (2004) Iodotyrosine dehalogenase 1 (DEHAL1) is a transmembrane protein involved in the recycling of iodide close to the thyroglobulin iodination site. *Faseb. J. 18*, 1574-6.

(38) Watson, J. A., Jr., McTamney, P. M., Adler, J. M., and Rokita, S. E. (2008) Flavoprotein iodotyrosine deiodinase functions without cysteine residues. *ChemBioChem 9*, 504-6.

(39) Moreno, J. C. (2003) Identification of novel genes involved in congenital hypothyroidism using serial analysis of gene expression. *Horm. Res. 60 Suppl 3*, 96-102.

(40) Friedman, J. E., Watson, J. A., Jr., Lam, D. W., and Rokita, S. E. (2006) Iodotyrosine deiodinase is the first mammalian member of the NADH oxidase/flavin reductase superfamily. *J. Biol. Chem. 281*, 2812-9.

(41) Kobori, T., Sasaki, H., Lee, W. C., Zenno, S., Saigo, K., Murphy, M. E., and Tanokura, M. (2001) Structure and site-directed mutagenesis of a flavoprotein from *Escherichia coli* that reduces nitrocompounds: alteration of pyridine nucleotide binding by a single amino acid substitution. *J. Biol. Chem. 276*, 2816-23.

(42) Koike, H., Sasaki, H., Kobori, T., Zenno, S., Saigo, K., Murphy, M. E., Adman, E. T., and Tanokura, M. (1998) 1.8 Å crystal structure of the major NAD(P)H:FMN oxidoreductase of a bioluminescent bacterium, *Vibrio fischeri*: overall structure, cofactor and substrate-analog binding, and comparison with related flavoproteins. *J. Mol. Biol. 280*, 259-73.

(43) Lei, B., Liu, M., Huang, S., and Tu, S. C. (1994) *Vibrio harveyi* NADPH-flavin oxidoreductase: cloning, sequencing and overexpression of the gene and purification and characterization of the cloned enzyme. *J. Bacteriol. 176*, 3552-8.

(44) Lovering, A. L., Hyde, E. I., Searle, P. F., and White, S. A. (2001) The structure of *Escherichia coli* nitroreductase complexed with nicotinic acid: three crystal forms at 1.7 Å, 1.8 Å and 2.4 Å resolution. *J. Mol. Biol. 309*, 203-13.

(45) Häggblom, M. M., and Bossert, I. D. (2003) *Dehalogenation: Microbial processes and environmental applications*, Kluwer Academic Publishers, Boston, MA.

(46) Massey, V. (2000) The chemical and biological versatility of riboflavin. *Biochem. Soc. Trans. 28*, 283-96.

(47) Fraaije, M. W., and Mattevi, A. (2000) Flavoenzymes: diverse catalysts with recurrent features. *Trends Biochem. Sci. 25*, 126-32.

(48) Heuts, D. P., Scrutton, N. S., McIntire, W. S., and Fraaije, M. W. (2009) What's in a covalent bond? On the role and formation of covalently bound flavin cofactors. *Febs J. 276*, 3405-27.

(49) Belas, R., Mileham, A., Cohn, D., Hilman, M., Simon, M., and Silverman, M. (1982) Bacterial bioluminescence: isolation and expression of the luciferase genes from *Vibrio harveyi*. *Science 218*, 791-3.

(50) Zanetti, G., and Aliverti, A. (1991) *Chemistry and Biochemistry of Flavoenzymes*, Vol. II, CRC Press, Boca Raton, FL.

(51) Susin, S. A., Lorenzo, H. K., Zamzami, N., Marzo, I., Snow, B. E., Brothers, G. M., Mangion, J., Jacotot, E., Costantini, P., Loeffler, M., Larochette, N., Goodlett, D. R., Aebersold, R., Siderovski, D. P., Penninger, J. M., and Kroemer, G. (1999) Molecular characterization of mitochondrial apoptosis-inducing factor. *Nature 397*, 441-6.

(52) Jorns, M. S., Wang, B., and Jordan, S. P. (1987) DNA repair catalyzed by *Escherichia coli* DNA photolyase containing only reduced flavin: elimination of the enzyme's second chromophore by reduction with sodium borohydride. *Biochemistry 26*, 6810-6.

(53) Xun, L., and Orser, C. S. (1991) Purification and properties of pentachlorophenol hydroxylase, a flavoprotein from Flavobacterium sp. strain ATCC 39723. *J. Bacteriol. 173*, 4447-53.

(54) Boersma, M. G., Cnubben, N. H., van Berkel, W. J., Blom, M., Vervoort, J., and Rietjens, I. M. (1993) Role of cytochromes P-450 and flavin-containing monooxygenase in the biotransformation of 4-fluoro-N-methylaniline. *Drug Metab. Dispos. 21*, 218-30.

(55) Wieser, M., Wagner, B., Eberspacher, J., and Lingens, F. (1997) Purification and characterization of 2,4,6-trichlorophenol-4-monooxygenase, a dehalogenating enzyme from Azotobacter sp. strain GP1. *J. Bacteriol. 179*, 202-8.

(56) Esaac, E. G., and Matsumura, F. (1978) A novel reductive system involving flavoprotein in the rat intestine. *Bull. Environ. Contam. Toxicol. 19*, 15-22.

(57) Suzuki, T., and Kasai, N. (2003) Generation of optically active glycerol derivatives by microbial resolution for development of useful synthetic units for pharmaceuticals. *Trends Glycosci. Glycotechn. 15*, 329-349.

(58) Fetzner, S. (1998) Bacterial dehalogenation. *Appl. Microbiol. Biotechnol. 50*, 633-57.

(59) Copley, S. D. (2003) Aromatic dehalogenases: insight into structures, mechanisms, and evolutionary origins in *Dehalogenation: microbial*

processes and environmental applications (Häggblom, M. M., and Bossert, I. D., Eds.) pp 227-259, Kluwer Academic Publishing, Boston, MA.

(60) Warner, J. R., Behlen, L. S., and Copley, S. D. (2008) A trade-off between catalytic power and substrate inhibition in TCHQ dehalogenase. *Biochemistry 47*, 3258-65.

(61) Warner, J. R., and Copley, S. D. (2007) Pre-steady-state kinetic studies of the reductive dehalogenation catalyzed by tetrachlorohydroquinone dehalogenase. *Biochemistry 46*, 13211-22.

(62) Warner, J. R., and Copley, S. D. (2007) Mechanism of the severe inhibition of tetrachlorohydroquinone dehalogenase by its aromatic substrates. *Biochemistry 46*, 4438-47.

(63) Visser, T. J. (1979) Mechanism of action of iodothyronine-5'-deiodinase. *Biochim. Biophys. Acta 569*, 302-8.

(64) Larsen, P. R., and Berry, M. J. (1995) Nutritional and hormonal regulation of thyroid hormone deiodinases. *Annu. Rev. Nutr. 15*, 323-52.

(65) Berry, M. J., Banu, L., and Larsen, P. R. (1991) Type I iodothyronine deiodinase is a selenocysteine-containing enzyme. *Nature 349*, 438-40.

(66) Berry, M. J., Kieffer, J. D., Harney, J. W., and Larsen, P. R. (1991) Selenocysteine confers the biochemical properties characteristic of the type I iodothyronine deiodinase. *J. Biol. Chem. 266*, 14155-8.

(67) Kunishima, M., Freidman, J. E., and Rokita, S. E. (1999) Transition-state stabilization by a mammalian reductive dehalogenase. *J. Am. Chem. Soc. 121*, 4722-4723.

(68) van de Pas, B. A., Smidt, H., Hagen, W. R., van der Oost, J., Schraa, G., Stams, A. J., and de Vos, W. M. (1999) Purification and molecular characterization of *o*-chlorophenol reductive dehalogenase, a key enzyme of halorespiration in *Desulfitobacterium dehalogenans*. *J. Biol. Chem. 274*, 20287-92.

(69) Krone, U. E., Thauer, R. K., and Hogenkamp, H. P. (1989) Reductive dehalogenation of chlorinated C1-hydrocarbons mediated by corrinoids. *Biochemistry 28*, 4908-4914.

(70) Schmitz, R. P., Wolf, J., Habel, A., Neumann, A., Ploss, K., Svatos, A., Boland, W., and Diekert, G. (2007) Evidence for a radical mechanism of the dechlorination of chlorinated propenes mediated by the tetrachloroethene reductive dehalogenase of *Sulfurospirillum muftivorans*. *Environ. Sci. Technol. 41*, 7370-7375.

(71) Friedman, J. E. Purification and characterization of iodotyrosine deiodinase. Ph. D. Dissertation, University of Maryland, College Park, College Park, MD. 2001.

(72) Green, W. L. (1968) Inhibition of thyroidal iodotyrosine deiodination by tyrosine analogues. *Endocrinology 83*, 336-47.

(73) Callebaut, I., Curcio-Morelli, C., Mornon, J. P., Gereben, B., Buettner, C., Huang, S., Castro, B., Fonseca, T. L., Harney, J. W., Larsen, P. R., and Bianco, A. C. (2003) The iodothyronine selenodeiodinases are thioredoxin-fold family proteins containing a glycoside hydrolase clan GH-A-like structure. *J. Biol. Chem. 278*, 36887-96.

(74) Hartmann, K., and Hartmann, N. (1971) Untersuchungen zum reaktionsablauf der dejodierung von 3,-5-dijod-tyrosin durch cystein. *Z. Chem. 11*, 344-345.

(75) McMillen, D. F., and Golden, D. M. (1982) Hydrocarbon bond dissociation energies. *Ann. Rev. Phys. Chem. 33*, 493-592.

(76) Hoffmann, H., and Michael, D. (1962) Phosphororganische Verbindungen, XXXIII. Zum Mechanismus der Phosphinimid- bildung aus Brom-arylaminen und Triphenylphosphin. *Chem. Ber. 95*, 528-535.

(77) Brown, D. D. (1997) The role of thyroid hormone in zebrafish and axolotl development. *Proc. Natl. Acad. Sci. USA 94*, 13011-6.

(78) Rosenberg, I. N., and Goswami, A. (1984) Iodotyrosine deiodinase from bovine thyroid. *Methods Enzymol. 107*, 488-500.

(79) Ausubel, F. M., Brent, R., Kingston, R. E., Moore, D. D., Seidman, J. G., Smith, J. A., and Struhl, K., *Short protocols in molecular biology* Vol. 1 and 2, 5th ed., John Wiley & Sons, Inc., 2002, pp.1512.

(80) Haynes, C. A., Koder, R. L., Miller, A. F., and Rodgers, D. W. (2002) Structures of nitroreductase in three states: effects of inhibitor binding and reduction. *J. Biol. Chem. 277*, 11513-20.

(81) Talekar, R. S., Chen, G. S., Lai, S. Y., and Chern, J. W. (2005) Nonreductive deiodination of o-iodo-hydroxylated arenes using tertiary amines. *J. Org. Chem. 70*, 8590-3.

(82) Yeh, E., Blasiak, L. C., Koglin, A., Drennan, C. L., and Walsh, C. T. (2007) Chlorination by a long-lived intermediate in the mechanism of flavin-dependent halogenases. *Biochemistry 46*, 1284-92.

(83) Hemmi, H., Ikeda, Y., Yamashita, S., Nakayama, T., and Nishino, T. (2004) Catalytic mechanism of type 2 isopentenyl diphosphate:dimethylallyl diphosphate isomerase: verification of a redox role of the flavin cofactor in a reaction with no net redox change. *Biochem. Biophys. Res. Commun. 322*, 905-10.

(84) Kittleman, W., Thibodeaux, C. J., Liu, Y. N., Zhang, H., and Liu, H. W. (2007) Characterization and mechanistic studies of type II isopentenyl diphosphate:dimethylallyl diphosphate isomerase from *Staphylococcus aureus*. *Biochemistry 46*, 8401-13.

(85) Averill, B. A., Schonbrunn, A., and Abeles, R. H. (1975) Studies on the mechanism of *Mycobacterium smegmatis* L-lactate oxidase. 5-Deazaflavin mononucleotide as a coenzyme analogue. *J. Biol. Chem. 250*, 1603-5.

(86) Sherry, B., and Abeles, R. H. (1985) Mechanism of action of methanol oxidase, reconstitution of methanol oxidase with 5-deazaflavin, and inactivation of methanol oxidase by cyclopropanol. *Biochemistry 24*, 2594-605.

(87) Hersh, L. B., and Walsh, C. (1980) Preparation, characterization, and coenzymic properties of 5-carba-5-deaza and 1-carba-1-deaza analogs of riboflavin, FMN, and FAD. *Methods Enzymol. 66*, 277-87.

(88) Edmondson, D. E., Barman, B., and Tollin, G. (1972) On the importance of the N-5 position in flavin coenzymes. Properties of free and protein-bound 5-deaza analogs. *Biochemistry 11*, 1133-8.

(89) Watson, J. A., Jr. Insight into the structure and mechanism of iodotyrosine deiodinase, the first mammalian member of the NADH oxidase/flavin reductase superfamily. Ph.D. Dissertation, University of Maryland, College Park, College Park, MD.

(90) Solís-S, J. C., and Rokita, S. E. Unpublished work.

(91) Nakamura, Y. Codon Usage Database. http://www.kazusa.or.jp/codon/

(92) Adler, J. M., and Rokita, S. E. Unpublished work.

(93) Gehret, J., and Rokita, S. E. Unpublished work.

(94) Cereghino, J. L., and Cregg, J. M. (2000) Heterologous protein expression in the methylotrophic yeast *Pichia pastoris*. *FEMS Microbiol. Rev. 24*, 45-66.

(95) Fraser, M. J. (1992) The baculovirus-infected insect cell as a eukaryotic gene expression system. *Curr. Top. Microbiol. Immunol. 158*, 131-72.

(96) Hollenberg, C. P., and Gellissen, G. (1997) Production of recombinant proteins by methylotrophic yeasts. *Curr. Opin. Biotechnol. 8*, 554-60.

(97) Thomas, S. R., McTamney, P. M., Adler, J. M., LaRonde-LeBlanc, N., and Rokita, S. E. (2009) Crystal structure of iodotyrosine deiodinase, a novel flavoprotein responsible for iodide salvage in thyroid glands. *J. Biol. Chem. 284*, 19659-19667.

(98) Roskams, J., and Rogers, L. 2002. *Lab Ref: A Handbook of Recipes, Reagents, and Other Reference Tools for Use at the Bench* Cold Spring Laboratory Press, Cold Spring Harbor, NY.

(99) Cregg, J. M., and Russell, K. A. (1998) Transformation. *Methods Mol. Biol. 103*, 27-39.

(100) O'Reilly, D. R., Miller, L. K., and Luckow, V. A. (1994) *Baculovirus Expression Vectors: A Laboratory Manual*, pp. l30-134, Oxford University Press, Inc., New York, New York.

(101) Koziol, J. (1971) Fluoromitric analyses of riboflavin and ites coenzymes. *Methods Enzymol. 18*, 253-285.

(102) Edelhoch, H. (1967) Spectroscopic determination of tryptophan and tyrosine in proteins. *Biochemistry 6*, 1948-54.

(103) Zuker, M. (2003) Mfold web server for nucleic acid folding and hybridization prediction. *Nucleic Acids Res. 31*, 3406-15.

(104) Kudla, G., Murray, A. W., Tollervey, D., and Plotkin, J. B. (2009) Coding-sequence determinants of gene expression in *Escherichia coli*. *Science 324*, 255-8.

(105) Pace, C. N., Vajdos, F., Fee, L., Grimsley, G., and Gray, T. (1995) How to measure and predict the molar absorption coefficient of a protein. *Protein Sci. 4*, 2411-23.

(106) Ryan, K. S., Chakraborty, S., Howard-Jones, A. R., Walsh, C. T., Ballou, D. P., and Drennan, C. L. (2008) The FAD cofactor of RebC shifts to an IN conformation upon flavin reduction. *Biochemistry 47*, 13506-13.

(107) Hecht, H. J., Erdmann, H., Park, H. J., Sprinzl, M., and Schmid, R. D. (1995) Crystal structure of NADH oxidase from *Thermus thermophilus*. *Nat. Struct. Biol. 2*, 1109-14.

(108) Tanner, D. D., Chen, J. J., Chen, L., and Luelo, C. (1991) Fragmentation of substituted acetophenone and halobenzophenone ketyls. Calibration of a mechanistic probe. *J. Am. Chem. Soc. 113*, 8074-8081.

(109) Parkinson, G. N., Skelly, J. V., and Neidle, S. (2000) Crystal structure of FMN-dependent nitroreductase from *Escherichia coli* B: a prodrug-activating enzyme. *J. Med. Chem. 43*, 3624-31.

(110) Delano, W. (2002), *PyMOL,* Delano Scientific, *San* Carlos, CA.

(111) Mani, A. R., Ippolito, S., Moreno, J. C., Visser, T. J., and Moore, K. P. (2007) The metabolism and dechlorination of chlorotyrosine *in vivo*. *J. Biol. Chem. 282*, 29114-21.

(112) Roche, J., Michel, O., Michel, R., Gorbman, A., and Lissitzky, S. (1953) The enzymatic dehalogenation of halogenated tyrosine derivatives by the thyroid gland and its physiological role. *Biochim. Biophys. Acta. 12*, 570-6.

(113) Auffinger, P., Hays, F. A., Westhof, E., and Ho, P. S. (2004) Halogen bonds in biological molecules. *Proc. Natl. Acad. Sci. USA 101*, 16789-94.

(114) Gales, L., Macedo-Ribeiro, S., Arsequell, G., Valencia, G., Saraiva, M. J., and Damas, A. M. (2005) Human transthyretin in complex with iododiflunisal: structural features associated with a potent amyloid inhibitor. *Biochem. J. 388*, 615-21.

(115) McTamney, P. M., and Rokita, S. E. (2009) A mammalian reductive deiodinase has broad power to dehalogenate chlorinated and brominated substrates. *J. Am. Chem. Soc.* (Submitted).

(116) Ammon, H. L. (2001) New atom/functional group volume additivity data bases for the calculation of the crystal densities of C, H, N, O, F, S, P, Cl and Br-containing compounds. *Struct. Chem. 12*, 205-212.

(117) Stradins, J., and Hansanli, B. (1993) Anodic voltammetry of phenol and benzenthiol derivatives.1. Influence of pH on electrooxidation potentials of substitutes phenols and evaluation of pKa from anodic voltammetry data. *J. Electroanal. Chem. 353*, 57-69.

(118) Thorpe, C., and Kim, J. J. (1995) Structure and mechanism of action of the acyl-CoA dehydrogenases. *FASEB J. 9*, 718-25.

(119) Vock, P., Engst, S., Eder, M., and Ghisla, S. (1998) Substrate activation by acyl-CoA dehydrogenases: transition-state stabilization and pKs of involved functional groups. *Biochemistry 37*, 1848-60.

(120) Zavitsas, A. A., Rogers, D. W., and Matsunaga, N. (2007) Remote substituent effects on allylic and benzylic bond dissociation energies: Effects on stabilization of parent molecules and radicals. *J. Org. Chem. 72*, 7091-7101.

(121) Mita, H., Higashi, N., Taniguchi, M., Higashi, A., Kawagishi, Y., and Akiyama, K. (2004) Urinary 3-bromotyrosine and 3-chlorotyrosine concentrations in asthmatic patients: lack of increase in 3-bromotyrosine concentration in urine and plasma proteins in aspirin-induced asthma after intravenous aspirin challenge. *Clin. Exp. Allergy 34*, 931-8.

(122) Kaur, H., and Halliwell, B. (1994) Evidence for nitric oxide-mediated oxidative damage in chronic inflammation. Nitrotyrosine in serum and synovial fluid from rheumatoid patients. *FEBS Lett. 350*, 9-12.

(123) Saude, E. J., Lacy, P., Musat-Marcu, S., Mayes, D. C., Bagu, J., Man, S. F., Sykes, B. D., and Moqbel, R. (2004) NMR analysis of neutrophil activation in sputum samples from patients with cystic fibrosis. *Magn. Reson. Med. 52*, 807-14.

(124) Mohiuddin, I., Chai, H., Lin, P. H., Lumsden, A. B., Yao, Q., and Chen, C. (2006) Nitrotyrosine and chlorotyrosine: clinical significance and biological functions in the vascular system. *J. Surg. Res. 133*, 143-9.

(125) Wu, W., Samoszuk, M. K., Comhair, S. A., Thomassen, M. J., Farver, C. F., Dweik, R. A., Kavuru, M. S., Erzurum, S. C., and Hazen, S. L. (2000) Eosinophils generate brominating oxidants in allergen-induced asthma. *J. Clin. Invest. 105*, 1455-63.

(126) Weiss, S. J., Test, S. T., Eckmann, C. M., Roos, D., and Regiani, S. (1986) Brominating oxidants generated by human eosinophils. *Science 234*, 200-3.

(127) Weiss, S. J., Klein, R., Slivka, A., and Wei, M. (1982) Chlorination of taurine by human neutrophils. Evidence for hypochlorous acid generation. *J. Clin. Invest. 70*, 598-607.

(128) Foote, C. S., Goyne, T. E., and Lehrer, R. I. (1983) Assessment of chlorination by human neutrophils. *Nature 301*, 715-6.

(129) Mani, A. R., Pannala, A. S., Orie, N. N., Ollosson, R., Harry, D., Rice-Evans, C. A., and Moore, K. P. (2003) Nitration of endogenous para-hydroxyphenylacetic acid and the metabolism of nitrotyrosine. *Biochem. J. 374*, 521-7.

(130) Stanbury, J. B., and Morris, M. L. (1958) Deiodination of diiodotyrosine by cell-free systems. *J. Biol. Chem. 233*, 106-8.

(131) Singh, A., and Ward, O. P. (2004) in *Soil Biology* pp 305, Springer, Verlag.

(132) Solyanikova, I. P., and Golovleva, L. A. (2004) Bacterial degradation of chlorophenols: pathways, biochemica, and genetic aspects. *J. Environ. Sci. Health B. 39*, 333-51.

(133) Parales, R. E., and Haddock, J. D. (2004) Biocatalytic degradation of pollutants. *Curr. Opin. Biotechnol. 15*, 374-9.

(134) Furukawa, K., and Fujihara, H. (2008) Microbial degradation of polychlorinated biphenyls: biochemical and molecular features. *J. Biosci. Bioeng. 105*, 433-49.

(135) Chaudhry, G. R., and Chapalamadugu, S. (1991) Biodegradation of halogenated organic compounds. *Microbiol. Rev. 55*, 59-79.

(136) DePalma, A. (2007) in *The New York Times*, New York.

(137) Hepworth, J. D., Waring, D. R., and Waring, M. J. (2002) Aromatic substitution, in *Aromatic chemistry* pp 15-35, Wiley-The Royal Society of Chemistry, Cambridge, UK.

(138) Abramovitz, A. S., and Massey, V. (1976) Interaction of phenols with old yellow enzyme. Physical evidence for charge-transfer complexes. *J. Biol. Chem. 251*, 5327-36.

(139) Barman, B. G., and Tollin, G. (1972) Flavine-protein interactions in flavoenzymes. Temperature-jump and stopped-flow studies of flavine analog binding to the apoprotein of *Azotobacter flavodoxin*. *Biochemistry 11*, 4746-54.

(140) Tsibris, J. C., McCormick, D. B., and Wright, L. D. (1966) Studies on the binding and function of flavin phosphates with flavin mononucleotide-dependent enzymes. *J. Biol. Chem. 241*, 1138-43.

(141) Whitfield, C. D., and Mayhew, S. G. (1974) Purification and properties of electron-transferring flavoprotein from *Peptostreptococcus elsdenii*. *J. Biol. Chem. 249*, 2801-10.

(142) Spencer, R., Fisher, J., and Walsh, C. (1976) Preparation, characterization, and chemical properties of the flavin coenzyme analogues 5-deazariboflavin, 5-deazariboflavin 5'-phosphate, and 5-deazariboflavin 5'-diphosphate, 5'leads to5'-adenosine ester. *Biochemistry 15*, 1043-53.

(143) Walsh, C., Fisher, J., Spencer, R., Graham, D. W., Ashton, W. T., Brown, J. E., Brown, R. D., and Rogers, E. F. (1978) Chemical and enzymatic properties of riboflavin analogues. *Biochemistry 17*, 1942-51.

(144) Palmer, G., Muller, F., and Massey, V. (1971) in *Flavins and Flavoproteins, 3rd International Symposium* (Karmin, H., Ed.) pp 123-140, University Park Press, Baltimore.

(145) Bleifuss, G., Kolberg, M., Potsch, S., Hofbauer, W., Bittl, R., Lubitz, W., Graslund, A., Lassmann, G., and Lendzian, F. (2001) Tryptophan and tyrosine radicals in ribonucleotide reductase: a comparative high-field EPR study at 94 GHz. *Biochemistry 40*, 15362-8.

(146) Rigby, S. E., Hynson, R. M., Ramsay, R. R., Munro, A. W., and Scrutton, N. S. (2005) A stable tyrosyl radical in monoamine oxidase A. *J. Biol. Chem. 280*, 4627-31.

(147) Mezzetti, A., Maniero, A. L., Brustolon, M., Giacometti, G., and Brunel, L. C. (1999) A tyrosyl radical in an irradiated single crystal of N-acetyl-L-tyrosine studied by X-band cw-EPR, high-frequency EPR, and ENDOR spectroscopies. *J. Phys. Chem. 103*, 9636-9643.

(148) Miller, J. E., Gradinaru, C., Crane, B. R., Di Bilio, A. J., Wehbi, W. A., Un, S., Winkler, J. R., and Gray, H. B. (2003) Spectroscopy and reactivity of a photogenerated tryptophan radical in a structurally defined protein environment. *J. Am. Chem. Soc. 125*, 14220-1.

(149) Solar, S., Getoff, N., Surhdar, P. S., Armstrong, D. A., and Singh, A. (1991) Oxidation of tryptophan and N-methylindole by $N_3^{\cdot-}$, $Br_2^{\cdot-}$, and $(SCN)_2^{\cdot-}$ radicals in light and heavy-water solutions: A pulse radiolysis study. *J. Phys. Chem. 95*, 3639-3643.

(150) Wolpert, M. K., Althaus, J. R., and Johns, D. G. (1973) Nitroreductase activity of mammalian liver aldehyde oxidase. *J. Pharmacol. Exp. Ther. 185*, 202-13.

(151) Moreno, S. N., Mason, R. P., and Docampo, R. (1984) Reduction of nifurtimox and nitrofurantoin to free radical metabolites by rat liver mitochondria. Evidence of an outer membrane-located nitroreductase. *J. Biol. Chem. 259*, 6298-305.

(152) Fann, Y. C., Metosh-Dickey, C. A., Winston, G. W., Sygula, A., Rao, D. N., Kadiiska, M. B., and Mason, R. P. (1999) Enzymatic and nonenzymatic production of free radicals from the carcinogens 4-nitroquinoline N-oxide and 4-hydroxylaminoquinoline N-oxide. *Chem. Res. Toxicol. 12*, 450-8.

(153) Carlberg, I., and Mannervik, B. (1986) Reduction of 2,4,6-trinitrobenzenesulfonate by glutathione reductase and the effect of NADP+ on the electron transfer. *J. Biol. Chem. 261*, 1629-35.

(154) Miskiniene, V., Sarlauskas, J., Jacquot, J. P., and Cenas, N. (1998) Nitroreductase reactions of *Arabidopsis thaliana* thioredoxin reductase. *Biochim. Biophys. Acta. 1366*, 275-83.

(155) Adams, P. C., and Rickert, D. E. (1995) Metabolism of [^{14}C] 1,3-dinitrobenzene by rat small intestinal mucosa in vitro. *Drug Metab. Dispos. 23*, 982-7.

(156) Yang, K. Y., and Swenson, R. P. (2006) Modulation of the redox properties of the flavin cofactor through hydrogen-bonding interactions with the N(5) atom: Role of αSer254 in the electron-transfer flavoprotein from the methylotrophic bacterium W3A1. *Biochemistry 46*, 2289-2297.